Investigating oxidative stress and large-scale genomic reduction in *Vibrio natriegens* through the development and application of new genetic techniques

A Dissertation Presented for the

Doctor of Philosophy

Degree

The University of Tennessee, Knoxville

Elizabeth Dawn Glasgo

August 2024

ACKNOWLEDGEMENTS

Thank you to my parents: Tim and Suzette, my siblings: Ivan and Victor, and all friends and family who shaped me and gave me the opportunities to succeed. Thank you to my aunts, Jeanette and Elcira, who encouraged my interests in science and urged me to pursue a graduate degree.

I would not be the scientist I am today without my many lab mates, colleagues, and mentors from over the years. I want to thank Geroge Bullerjahn and Mike McKay for giving me my first research opportunity and continuing to be wonderful mentors.

Thank you to the graduate students and postdocs in the Department of Microbiology for providing friendship, mentorship, and lots of borrowed equipment and reagents. I want to specially acknowledge my cohort (2018), and the past and present members of the Zinser, Wilhelm, and Buchan labs. My six years here would not have been as much fun without this group of people. Finally, thank you to my brilliant committee members: Steve, Liz, Mike, and Erik. The patience, kindness, priceless advice, and unwavering support was needed and appreciated more than I can explain in this paragraph. Special thanks to Erik for his daily guidance and support, and for building a fun work environment and arranging even more fun lab outings.

Lastly, I want to thank Nick and Pepperoni for bringing joy to my everyday life. Thank you to Nick for the endless support and encouragement, for listening to me, caring for me, and being with me every day of this journey.

ABSTRACT

Vibrio natriegens is the fastest replicating bacterium and recent work has demonstrated its potential for biotechnology and synthetic biology applications. While these industries have been the focus of *V. natriegens* research, it offers a promising system for diverse laboratory studies. However, currently a complete understanding of *V. natriegens* biology is lacking. As such, there is a need to advance genetic techniques and physiological understanding to better inform all aforementioned applications. Here we describe our contributions to the growing field of *V. natriegens* genetics and the application of these new techniques to study physiological processes and themes in genome evolution. Briefly, we performed a case study on a set of physiologically important genes natively found in *V. natriegens* genome, called *katG1, katG2,* and *katG3,* whose function is to protect the cell from oxidative stress. We report functional and phylogenetic analyses that inform the evolutionary and ecological basis for *katG* multiplicity in *V. natriegens*. We next expand our analysis to investigate generalized genome reduction as a simulation of genome streamlining. Genome streamlining theory posits that reduction of DNA content is selectively advantageous under persistent nutrient limitation. *V. natriegens* has an expansive genome and we leverage this characteristic and apply our new genetic techniques to investigate the physiological impacts of large-scale genomic reductions under theoretically relevant conditions. Together the work presented here expands the capabilities and understanding of *V. natriegens* has a host for molecular biology.

TABLE OF CONTENTS

LIST OF TABLES

LIST OF FIGURES

LIST OF ATTACHMENTS

CHAPTER ONE

Vibrio natriegens : A New Frontier

Disclosure statement

This document was written by Liz Glasgo. Erik Zinser helped edit and refine the contents.

Abstract

Though it has existed in culture for over 60 years, *Vibrio natriegens* has gained substantial attention in the past decade as an ideal system for molecular and biotechnological research. Well renowned for its fast replication time, metabolic versatility, and efficiency for genetic manipulation, it has been fast-tracked as a host for synthetic biology. However, a comprehensive understanding of its ecology and physiology is currently lacking. Here we review *V. natriegens'* discovery, characterization, and rapid emergence as a host for genetic engineering. We focus on current gaps in the field of *V. natriegens* research and discuss its potential as a model organism to transition into the chapters of this dissertation.

Discovery and early findings

Vibrio natriegens was first isolated from salt marsh mud taken from Sapelo Island, Georgia in 1958 [1]. Initial characterization classified it as a member of the *Pseudomonas* genus [2], until a decade later when it was re-categorized as *Beneckea natriegens* [3], and then terminally recognized as a member of the *Vibrio* genus in 1978 [4]. Along with taxonomic identity, *V. natriegens* was characterized as a Gram-negative, rod-shaped, facultative anaerobe, with a polar flagellum, and a requirement for Na^+. Notably, *V. natriegens'* fast generation time, < 10 minutes, was documented early on [5]. But despite these early investigations, little attention was given to *V. natriegens* until roughly the past decade. Now a renaissance in *V. natriegens* research has emerged, leading to rapid development of new genetic tools and synthetic biology applications.

Genomic features and gene essentiality

Multiple strains of *V. natriegens* have been isolated and investigated in efforts to characterize the species [6, 7]. While different strains varied slightly in genomic properties, they also highlight several shared characteristics. *V. natriegens'* genome consists of two chromosomes (Chr 1. ~ 3.5 Mbp, Chr. 2 ~ 1.9 Mbp), totaling 5.1 – 5.7

Mb, with 4,493 – 5,040 coding genes, 11-12 rRNA operons, and a GC content of 44-45% [6-10]. Lastly, various strains of *V. natriegens* have demonstrated different specific growth rates, yet all share the ability for rapid growth [6, 7]. It is noteworthy, however, that some isolation methods for *V. natriegens* select for fast growth, thus fast growers may be overrepresented in laboratory isolates [7]. Notably, *Vibrio natriegens* strain ATCC 14048 is the commonly used type-strain and often regarded as "wildtype."

Regarding genome organization, most putative essential genes are located on Chromosome 1 (272 / 278). Additionally, of core genes, required for rapid growth in rich media, 14.3% have duplicate copies (84/587), and 60.3% of the duplicates (53/84), are located on Chr. 2 [11]. It is noteworthy that essentiality was assayed under nutrient replete conditions. With an increasing interest in *V. natriegens* for diverse research and industrial applications including plastic degradation, wastewater treatment, and production of renewable feedstocks, a deeper understanding of gene functions under a wide range of nutrient landscapes will be required [12-15].

Culturing

Routine culturing conditions established for *V. natriegens* generally utilize a nutrient rich, high salt (1.5 – 3%) medium. Variations of temperature, pH, and % NaCl have been explored to optimize for fast growth rate and high biomass yield [9, 16]. Notably, the fastest growth rate reported, $\mu = 4.43\ hr^{-1}$ (doubling time of 9.4 minutes), was obtained under aerobic conditions, in Brain and Heart Infusion Medium with 1.5% NaCl (BHIN), at pH 7.5 and 37° C. However, even in minimal medium supplemented with glucose as the sole carbon source, *V. natriegens* achieved a growth rate of $\mu = 1.48\ hr^{-1}$ (doubling time of 28.1 minutes), still faster than other model systems under comparable conditions [17]. Importantly, *V. natriegens* has demonstrated an incredibly versatile metabolism, shown to utilize over 60 different carbon substrates for energy under aerobic conditions, and can ferment D-ribose, D-glucose, D-gluconate, and D-mannitol under anaerobic conditions [3, 14].

A limited number of recent studies have investigated *V. natriegens* during nutrient limitation. Glucose limitation has been investigated for optimized growth in

bioreactors. These studies focused on achieving high cell density and controlling production of exopolysaccharides (EPS) under these conditions [18, 19]. This is an important endeavor considering the bioengineering and industrial potential of *V. natriegens.* Still, a comprehensive understanding of *V. natriegens* physiology under nutrient limitation is lacking. A few earlier studies explored nitrogen- or phosphate-limitation with speculations on the ecological relevance of *V. natriegens* under these conditions. Under anaerobic nitrogen-deplete conditions, *V. natriegens* was found to fix atmospheric N_2. This may implicate *V. natriegens* as an important supplier of nitrogen to the ecosystem [20]. Lastly, a phosphate-limited and phosphate-pulsed chemostat experiment demonstrated the rapid nutrient acquisition ability of *V. natriegens* and found formation of polyphosphate bodies, suggested to aid in phosphate uptake by reducing the concentration gradient across the cell membrane. This adaptation holds important ecological advantages in environments with fluctuating nutrients where competition inevitably ensues [21].

In conclusion, *V. natriegens* has been thoroughly investigated in rich, complex medium, particularly for the achievement of fast growth. However, understanding *V. natriegens'* physiology, metabolism, and gene functions, under a variety of conditions requires more attention. As mentioned previously, this is crucial as *V. natriegens* is being used for diverse applications, conditions, and nutrient regimes. Improving understanding of *V. natriegens* under a variety of conditions will contribute to a greater comprehension of this organism as is needed to become an effective model organism.

Metabolism

The fast growth rate of *V. natriegens* has generated significant interest and considerable effort has been put forth to elucidate the metabolic underpinnings for this record setting characteristic. Some considerations include resource uptake, metabolic flux, and protein synthesis allocation. Comparative analysis with model systems have shed light on divergent features of *V. natriegens.* However, a singular or collective attribute(s) responsible for fast growth remains to be discerned.

V. natriegens central metabolic pathway has been extensively compared to *E. coli* [17, 22, 23]. One of the main distinctions is a higher consumption rate of carbon sources by *V. natriegens* [17, 22]. Due to higher uptake, total carbon flux through *V. natriegens* is expected to be higher than for *E. coli* [22]. However, discrete carbon flow through *V. natriegens* is fairly similar to *E. coli*, the main difference being a 33% reduction in flux through the Pentose Phosphate Pathway (PPP) [22]. Notably, another shared characteristic between *V. natriegens* and *E. coli* is the production of pyruvate and acid by-products even under aerobic conditions, during growth on glucose [2, 24]. These indicate a high oxygen demand that is not being met with typically culturing systems, leading overflow metabolism to occur. Overall, *V. natriegens* has many shared qualities with *E.*coli and no obvious difference gives *V. natriegens* a metabolic advantage that would explain its fast growth rate.

In contrast, obvious distinctions from *E. coli* exist for the translational machinery of *V. natriegens*. As stated previously, *V. natriegens* contains 11-12 rRNA operons, whereas *E.coli* has seven [25]. Likewise, *V. natriegens* is estimated to produce about 115,000 ribosomes / cell (at 4 doublings/ hr), this is estimated to be about 25,000 more ribosomes than *E. coli* normalized to the same doubling time [26]. Additionally, *V. natriegens* encodes 124 – 129 genes for tRNAs, roughly 30 more than *E. coli* [9, 10]. Notably, these features are implicated in *V. natriegens* fast growth rate though causation has not yet been demonstrated.

Genetic tools and applications

The extraordinarily fast growth rate and metabolic versatility of *V. natriegens* has sparked interest as a promising new host for molecular and biotechnology applications. Beginning in roughly 2016, a wealth of genetic manipulation techniques have been implemented and innovated for application in *V. natriegens*. This has allowed a boom in synthetic applications for bioremediation and heterologous protein expression.

Early success with classical techniques such as heat-shock transformation, electroporation, and conjugation were instrumental for genetic development in *V. natriegens.* Ultimately these allowed the execution of functional genomics studies with

TN-Seq and CRISPRi which utilized plasmids to induce transposon mutagenesis or guide RNA (gRNA) and dCas9 (nuclease-deficient Cas9) mediated gene interruptions [6, 9, 11]. Additionally, a number of commercially available plasmids with various origins of replication and antibiotic resistance cassettes have been shown to function in *V. natriegens* [9, 27]. Importantly, differences in plasmid transformability and retention have been noted [27]. Likewise, working concentrations for antibiotics and suitable inducible promoters have recently been reviewed [28, 29]. Finally, suicide-plasmid and counter-selection based mutagenesis techniques have also been developed [9, 17, 24].

Importantly, *V. natriegens* is capable of taking up linear DNA fragments through natural competency and incorporating this DNA via homologous recombination. This ability is shared by *V. cholerae,* and indeed they appear to share mechanisms of induction. In *V. cholerae,* environmental signals such as carbon starvation, high cell density, and chitin induce the competence regulator *tfoX,* and *tfoX* begins a signaling cascade that results in type IV pili assembly, activation of a second major competence regulator *qstR,* and DNA translocation by *comEA* and *comF* [30, 31]. Unfortunately, studies with the lab strain of *V. natriegens* indicate competence is poorly expressed even under inducing conditions. However, a high rate of natural competency can be obtained if *tfoX* from *V. natriegens* or *V. cholerae* is ectopically expressed on a plasmid source or integrated into the chromosome (Figure 1.1) [32, 33]. Notably, inducing competence in *V. natriegens* revealed significant overlap of gene regulation with *V. cholerae* during competency, demonstrating key competence genes that are shared between both systems [31]. Establishment of natural competency in *V. natriegens*, has allowed the development of a high-efficiency mutagenesis protocol, MuGENT (Multiplex Genome Editing by Natural Transformation), which has demonstrated the simultaneous uptake and incorporation of multiple fragments in a single round of transformation (Figure 1.1) [32].

Genetic manipulation of *V. natriegens* has provided many strains with novel properties. Some of these strains offer more stable or productive platforms for protein expression. For instance, engineering of increased plasmid-borne gene expression and improved plasmid DNA integrity have been demonstrated [6]. The potential for

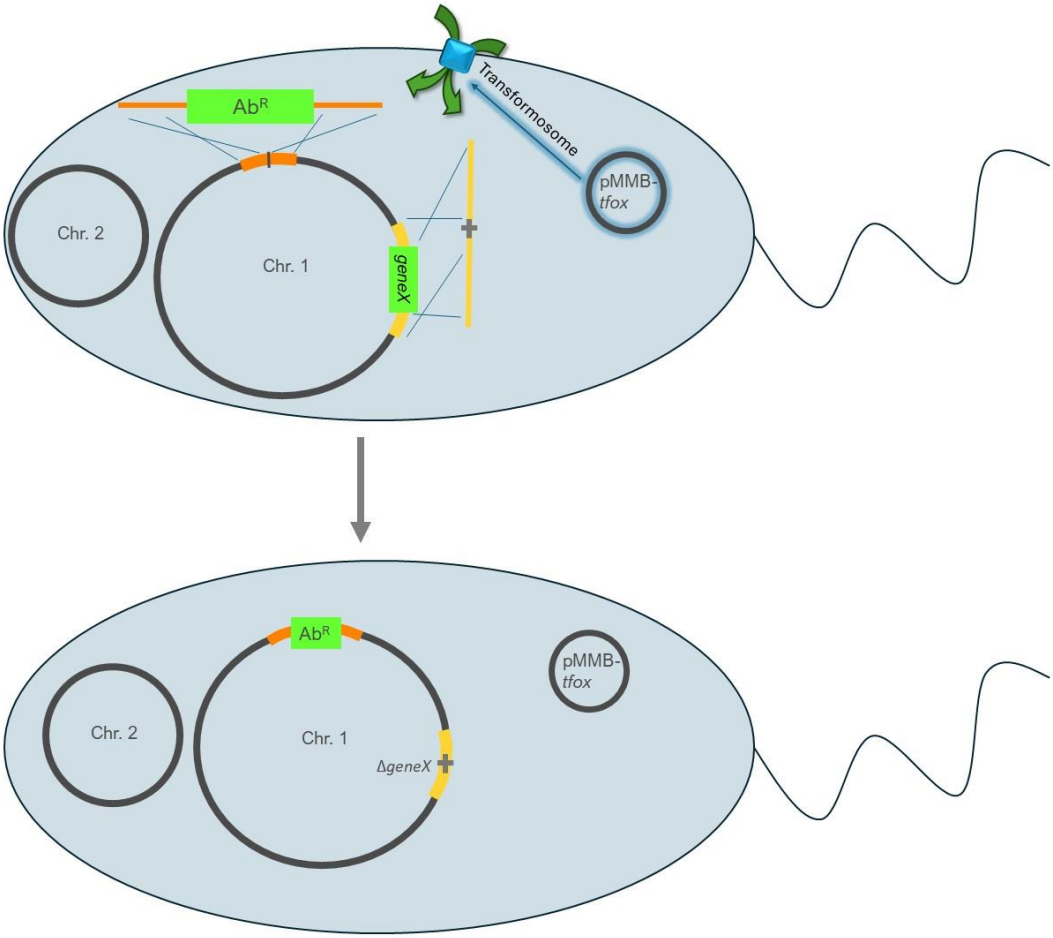

Figure 1.1 Schematic of Multiplex Genome Editing by Natural Transformation (MuGENT) in *Vibrio natriegens*. The diagram illustrates a simple example of MuGENT with just two pieces of DNA, one fragment creates a gene insertion event (Ab^R = antibiotic resistance gene), and the other fragment creates a gene deletion event (*gene X*). Open reading frames are represented by green rectangles. Expression of the *tfoX* gene from the plasmid, pMMB-*tfox*, signals formation of the transformosome. Linear DNA is brought into the cell and recombines with chromosomal DNA via homologous recombination. Homologous DNA segments are shown in orange and yellow.

genome minimization has also been explored where ~ 194 kb was iteratively deleted from one strain of *V. natriegens* to make it more similar to the type-strain ATCC 14048. This demonstrated the ability to remove loci including mobile elements, restriction-modification systems, and prophage genes [6]. Similarly, removal of prophage regions in ATCC 14048 has been explored and demonstrated higher growth rate, biomass yield, and pyruvate production under low salt conditions [24]. This is particularly considerable for industrial applications where high-salt culturing conditions may present a corrosivity problem. Likewise, removal of prophage regions abolished spontaneous induction and could provide a more stable platform for further engineering applications [24].

Lastly, other efforts have focused on heterologous protein expression from *V. natriegens* for industrially relevant purposes. For example, this has achieved production of industrially relevant compounds such as 1,3-propanediol, violacein, beta-carotene, and the bioplastic precursor poly-b-hydroxybutryate (PHB), [14, 32, 34]. Additionally, *V. natriegens* has been engineered to produce enzymes which break down a plastic derivative, polyester terephthalate (PET), as well as to utilize a desirable CO_2-derived feedstock, formic acid [12, 15]. Importantly, *V. natriegens* has shown great potential for genetic modification and as a platform for bioproduction. With the rapidly expanding wealth of literature on *V. natriegens,* it represents a highly attractive system for continued development.

Conclusions

Vibrio natriegens holds several innate properties that have the potential to transform molecular and synthetic biology research. Often promoted for its fast growth, *V. natriegens* has been acclaimed as a "powerhouse," and, "emergent synthetic biology chassis." Metabolic analyses and the development of efficient genetic tools have revolutionized utilization of this organism. Notably, engineering of *V. natriegens* has proven useful for industrial applications. However, a recent review highlights some aspects that require closer attention for scaling-up [29]. For instance, regarding *V. natriegens* physiology, understanding of metabolism and regulation currently relies on information from other related species. Recent transcriptome, proteome, and metabolome

analyses are beginning to address these gaps in knowledge [23, 31, 35, 36]. These types of studies will be essential to inform future biological analyses.

V. natriegens potential as a host for biotechnology is undisputed. Additionally, it represents a genetically tractable marine heterotroph and non-pathogenic member of the *Vibrio* genus. While many studies have characterized physical and genomic features under optimal conditions, a comprehensive understanding of *V. natriegens* physiology under ecologically relevant conditions and in combination with stressors is lacking. Such endeavors would provide insight to how *V. natriegens* responds to diverse conditions that could be critical for the expansion of laboratory and synthetic biology research applications.

Additionally, the ecological distribution, diversity, and evolutionary history of *V. natriegens* are relatively unknown. While *V. natriegens* has the potential to reveal the molecular underpinnings of fast growth, the evolutionary steps that led to this rare trait are intriguing. Similarly, one could speculate about its metabolic flexibility and high substrate uptake rates. Reflecting on this, while gene dispensability and genome minimization have been considered in the context of a more efficient synthetic chassis [6, 11, 24], *V. natriegens* also presents an interesting subject to investigate the molecular underpinnings of adaptive evolution.

In conclusion, *V. natriegens* has rapidly become a compelling host for diverse molecular and synthetic biology applications. It also holds potential as a representative marine heterotroph and member of the *Vibrio* genus. Finally, the relative ease of culturing and genetic manipulation provides accessibility to broad skill and resource levels. These characteristics push *V. natriegens* towards the epithet of model organism but, continued organismal comprehension is essential for this designation and will provide insight for future studies and applications.

Chapter summaries

The work presented in this dissertation expands the genetic toolkit of *V. natriegens*, investigates a physiologically important stress response to enhance

organismal understanding, and utilizes *V. natriegens* as a novel host to explore the adaptive evolutionary theory of genome streamlining.

First, genetic developments are described in Chapter 2. I show that an intergenic region can be used for selectable marker insertion to avoid the traditional disruption of coding genes for marker placement. I develop an effective plasmid curing protocol which is desirable for many downstream applications following genetic manipulation. I also describe protocols for rapid mutant screening, chromosomal gene complementation, and large genetic modification. These techniques are applied in Chapters 3 and 4.

In Chapter 3, a gene knockout approach is used to investigate the function and regulation of three catalase genes in *V. natriegens*. A significant role for peroxide degradation is found for each catalase gene during stationary phase. I also show involvement of regulatory genes, *oxyR* and *rpoS*. I finally analyze the phylogeny of catalase genes across *Vibrio* species and offer discussion of evolutionary and ecological implications for this work.

Lastly, adaptive evolution of genome streamlining is investigated by generating mutants with artificially streamlined genomes and carrying out a competitive evolution experiment. In Chapter 4, genome reduced mutants are constructed and competed against the parental strain under prolonged ammonium limitation. I report a stable coexistence is established between the parent and mutant pool.

To conclude, significant findings are reviewed in Chapter 5. Follow up experiments are suggested for the work presented in the research chapters. Finally, additional knowledge gaps and potential future directions are discussed.

CHAPTER TWO

Expanding the capabilities of Multiplex Genome Editing by Natural Transformation (MUGENT) for large-scale genetic engineering of the fastest-replicating species, *Vibrio natriegens*

Disclosure statement

A version of this chapter was published by Liz Glasgo, Katie Lukasiak, and Erik Zinser. Liz Glasgo carried out all experiments. Katie Lukasiak generated the deletion mutant. Liz Glasgo and Erik Zinser wrote the document.

Glasgo, L. D., Lukasiak, K. L., & Zinser, E. R. (2024). Expanding the capabilities of MuGENT for large-scale genetic engineering of the fastest-replicating species, *Vibrio natriegens*. *Microbiology spectrum*, e0396423. Advance online publication. https://doi.org/10.1128/spectrum.03964-23

Abstract

The fastest replicating bacterium *Vibrio natriegens* is a rising workhorse for molecular and biotechnological research with established tools for efficient genetic manipulation. Here we expand on the capabilities of multiplex genome editing by natural transformation (MuGENT) by identifying a neutral insertion site and show how two selectable markers can be swapped at this site for sequential rounds of natural transformation. Second, we demonstrated that MuGENT can be used for complementation by gene insertion at an ectopic chromosomal locus. Additionally, we developed a robust method to cure the competence plasmid required to induce natural transformation. Finally, we demonstrated the ability of MuGENT to create massive deletions; the 280 kb deletion created in this study is one of the largest artificial deletions constructed in a single round of targeted mutagenesis of a bacterium. These methods each advance the genetic potential of *V. natriegens* and collectively expand upon its utility as an emerging model organism for synthetic biology.

Importance

Vibrio natriegens is an emerging model organism for molecular and biotechnological applications. Its fast growth, metabolic versatility, and ease of genetic manipulation provide an ideal platform for synthetic biology. Here, we develop and apply novel methods that expand the genetic capabilities of the *V. natriegens* model system. Prior studies developed a method to manipulate multiple regions of the chromosome in a

single step. Here we provide new resources that diversify the utility of this method. We also provide a technique to remove the required genetic tools from the cell once the manipulation is performed, thus establishing "clean" derivative cells. Finally, we show the full extent of this technique's capability by generating one the largest chromosomal deletions reported in the literature. Collectively, these new tools will be beneficial broadly to the *Vibrio* community and specifically to the advancement of *V. natriegens* as a model system.

Introduction

Vibrio natriegens was first isolated and described in the late 1950's and early 1960's when it was found to have an astonishing doubling time of <10 minutes [1, 2, 5]. *V. natriegens* is Gram-negative, halophilic, non-pathogenic, and offers a broad range of metabolic capabilities [6, 9]. However, it was not until roughly the past decade that it gained attention as a promising model organism for industrial applications such as heterologous protein synthesis and small molecule production [17, 32, 34, 37]. Traditional genetic methods for *V. natriegens*, though labor intensive [6, 9, 11, 17], have been utilized in initial efforts to create strains of *V. natriegens* with more efficient substrate production and higher biomass yield by eliminating non-essential, potentially destabilizing, and/or resource costly regions of the genome [6, 24].

The development of multiplex genome editing by natural transformation (MuGENT) offers an advancement in these applications as a fast and efficient technique for genetic manipulation [32]. Briefly, MuGENT exploits natural transformation of linear PCR products into *V. natriegens* to make genome edits at multiple loci in a single round of transformation. Development and optimization of MuGENT in other *Vibrio* species, *V. cholerae* and *V. parahaemolyticus*, has included the ability to cure the inducer plasmid [32, 38-40], an important step currently lacking in *V. natriegens*. With the development of MuGENT, the potential to rapidly reduce the genome of *V.natriegens* in search of creating a more efficient chassis for heterologous expression is more feasible than ever, and importantly with the availability of comparative genomics data [11], identification of potentially dispensable genes is also easily achievable.

MuGENT requires the inclusion of a selectable marker to identify successful transformants. Traditionally during MuGENT, non-selectable products, that are designed to make the desired genome edit(s), are cotransformed with a selectable product that replaces the endonuclease gene, *dns*, with an antibiotic resistance marker [32]. This mutation did not impact growth in rich media, however, mutations that eliminate functional genes may not be neutral in all environments. Another approach is to directly replace a gene of interest with the selectable marker itself, rather than cotransforming two separate products. While this may work if only a single deletion is needed, it limits the user's ability to create multiple genome edits. Therefore, we sought to identify an alternative fitness neutral insertion site in *V. natriegens'* genome that avoids replacing a coding sequence to preserve cells as close to wildtype as possible.

Induction of natural transformation in *Vibrio natriegens* is achieved by ectopic expression of the competence regulator gene, *tfoX,* cloned on the plasmid pMMB*tfoX* [32]. Plasmid curing after genome editing is important for subsequent physiological studies of the transformants but has proven challenging for this system. One efficient way to cure cells is to counterselect against a plasmid-encoding gene, such as *sacB* from *Bacillus subtilis*. *sacB* encodes levansucrase and when expressed in Gram-negative bacteria causes lethality in the presence of sucrose [38]. Strains cured of the plasmid are enriched amongst the colonies growing on sucrose plates and can subsequently be verified by PCR screening for the plasmid. Notably, *sacB* has been shown to function in *V. natriegens* as a counter-selection marker for allelic exchange on the *V. natriegens* chromosome [17]. Here, we demonstrate that a *sacB*-containing derivative of pMMB*tfoX* (pMMB*sacBtfoX*) developed for *V. parahaemolyticus* [38] can also be used for plasmid curing in *V. natriegens*.

Complementation is the gold standard method to confirm a mutation is responsible for a specific phenotype. While plasmid-based complementation is commonplace in genetic studies we wanted to test the ability to complement directly on the chromosome. Phenotypic rescue from a single copy located elsewhere on the chromosome may be preferrable to rescue from copies on a multicopy plasmid if gene dosage is an important consideration. Complementation from the chromosome offers the

additional advantage of a stably integrated gene that does not require selective pressure for maintenance of the carrier plasmid (e.g., antibiotic resistance). We show that deletion of *oxyR*, a regulator of antioxidant genes [41], creates sensitivity to hydrogen peroxide. We complement this phenotype by inserting *oxyR* at a distant location on the chromosome.

Prior use of MuGENT has targeted the creation of only small deletions, 50-500 bp [32, 40], and the possibility of creating large, multi-gene deletions was unexplored. Therefore, we wanted to apply MuGENT to test the capability of generating large-scale genome deletions. As a proof of concept for the methods we developed, we generated a 280 kb deletion of Chromosome 2, the largest known deletion created using MuGENT and one of the largest created for any bacterium. Subsequently, sucrose counterselection allowed us to cure the deletion mutant of the pMMB*sacBtfoX* plasmid required for transformation. Importantly, and in distinction from *V. parahaemolyticus*, we find that curing of pMMB*sacBtfoX* was dependent on drastic reduction but not elimination of salt in the sucrose selection medium. We show that despite the removal of 239 genes, the Δ280 kb strain is viable in complex medium and suffers only a small growth rate defect compared to WT growth. The methods reported here provide valuable genetic tools for *V. natriegens* and demonstrate the potential for quick and efficient engineering of *V. natriegens* genome.

Materials and methods

Bacterial strains and culturing conditions

Vibrio natriegens ATCC 14048 and *Vibrio natriegens* ATCC 14048 harboring competence plasmid pMMB*tfox*, generously provided by Dr. Ankur Dalia, were used as the parent strains in this study. All strains and plasmids used in this study are listed in Table A2.1. *V. natriegens* was routinely grown in LB3 (LB with 3% w/v NaCl), and antibiotics were added at 100 μg/mL erythromycin (erm), 250 μg/mL spectinomycin (spec), 250 μg/mL kanamycin (kan), and 150 μg/mL ampicillin (amp) when appropriate, unless otherwise stated. All reagents were purchased from Thermo Fisher unless otherwise indicated. As an extension of the initial development of the MuGENT system

in *V. natriegens* all cultures in this study were likewise grown at 30 °C [32]. All liquid cultures were grown in an orbital shaker unless otherwise noted.

Generation of selectable markers and mutant construction

Selectable markers and deletion mutant constructs were created with three-piece or two-piece SOE (splicing-by-overlap extension) PCR essentially as previously described [32, 42]. For selectable markers and *oxyR* complementation, 3 kb upstream and 3 kb downstream regions flanking the location of insertion were amplified by F1/R1 and F2/R2 primers, respectively (Table A2.2), and *oxyR* or antibiotic resistance markers (erm^R or $spec^R$) were amplified from genomic or plasmid sources, respectively (Table A2.2). R1 and F2 primers have 20-23 bp nucleotide sequences added to the 5' ends that are homologous to sequences added to the primers used to amplify the desired insert. This allows the sequences to be 'stitched' together in SOE PCR. For three-piece SOE PCR, purified PCR products were added in a 50ng:50ng:50ng ratio as the template DNA. PCR was run for 10-15 cycles without primers and then the F1/R2 primers were added and PCR was run for an additional 25-30 cycles. Thermocycler conditions were as follows, 1) 98 °C – 30 seconds, 2) 98 °C – 10 seconds, 3) 60 °C – 10 seconds, 4) 72 °C – 30 seconds/kb, 5) repeat steps 2-4 10-30x, 6) 72 °C – 5 minutes, 7) 4 °C – hold. SOE PCR products were gel purified with QIAquick Gel Extraction Kit (Qiagen) and used in transformations. The *ΔoxyR* and Δ280 kb constructs were generated in a similar manner, amplifying the 3kb- upstream and downstream regions flanking the site of deletion. These two pieces were purified using the QIAquick PCR Purification Kit (Qiagen) and added together in a 50ng:50ng ratio as the template DNA for SOE PCR and run as described above. After purification, this product was used in transformation. All primers are listed in Table A2.2. All PCRs were performed using Phusion Plus Polymerase (Thermo Scientific) according to manufacturer's protocols. Products were visualized on 1.5% agarose gels using Midori Green (Bulldog Bio).

***pMMBsacBtfoX* conjugation**

To incorporate the pMMB*sacBtfoX* plasmid into our WT strain of *V. natriegens*, the plasmid was first introduced into a diaminopimelic acid (DAP) auxotroph strain of *E.coli* WM3064 (Table A2.1) [43] via heat shock transformation. Overnight *E.coli*

WM3064 cells were diluted 1:1000 and grown for 3 hrs at 37 °C to mid-log. Cells were pelleted and resuspended in 100 μL of 0.1 M $CaCl_2$. 3 μL of plasmid were added to the cells and the mixture was placed on ice for 5 minutes. Then, the mixture was heat shocked at 42 °C for 1 minute. Cells were placed back on ice while 0.4 mL of LB were added, then the cells were grown out for 30 minutes at 37 °C in a roller drum. Cells were plated onto LB + 50 μg/mL kanamycin + 500μM DAP. To conjugate the plasmid into *V. natriegens*, overnights of each strain were grown, *E.coli* WM3064-pMMB*sacBtfoX* was grown in LB supplemented with kanamycin and DAP at 37 °C and *V. natriegens* was grown in LB3 at 30 °C. Cells were pelleted and resuspended three times in fresh LB. Cells were mixed together in various ratios of donor to recipient 1:9, 9:1, 1:4, 4:1, 1:1, 0:1, 1:0 in total volumes of 100 μL. The mixtures were spotted onto LB plates and incubated for 3-5 hours at 30 °C. The cells were then resuspended from the plates with 1mL of LB and plated onto LB3+kanamycin plates lacking DAP (to eliminate the *E.coli* donor strain) and incubated at 30°C overnight. Colonies formed on plates for the 1:9, 9:1, and 1:1 dilutions, but not for the 1:4, 4:1, or the donor alone or recipient alone controls (1:0; 0:1).

Natural transformation/MuGENT

Natural transformation was performed as previously described [32]. Briefly, cells containing the competence plasmid pMMB*tfox* or pMMB*sacBtfoX* were grown overnight at 30 °C, shaking (250 rpm) in LB3 supplemented with 100 μM IPTG and appropriate antibiotic. Cells were then diluted 1:1000 into 350 μL of Instant Ocean (28 g/L; Spectrum Brands) with 100 μM IPTG. For natural transformation of selectable markers 50 ng of PCR construct was added. For MuGENT, 50 ng of selectable marker and 250 ng of the non-selectable PCR construct were added. Cells were incubated statically with the transforming DNA (tDNA) for 5 hrs at 30 °C then grown out in 1mL LB3 for 2hrs, serially diluted, and plated onto antibiotic plates. Transformations were additionally plated onto non-selective medium when calculating transformation efficiency.

To verify transformation products were incorporated into the genome, DNA was extracted from transformants and additional rounds of PCR were performed. For selectable markers, PCR primers matching the homologous sequences facilitating SOE

PCR were used to confirm insertion of the antibiotic gene (Table A2.2). For the *oxyR* and 280 kb deletions, a process similar to MASC (multiplex allele-specific colony) PCR was performed, previously described [32]. "Scar" primers were designed to amplify a ~600 bp or ~2 kb product if a deletion was successful and a ~1.6 kb or ~282 kb region if not, respectively. For *oxyR* complementation, primers amplified a ~1.8 kb product if insertion was successful and a ~1.5 kb product if insertion was unsuccessful (Table A2.2). Transformants were cryopreserved in a 96-well microtiter plate at -80 °C in LB+10% glycerol and thawed for subsequent screening. To rapidly screen isolates for incorporation of tDNA, PCR was first performed on pools of nine colonies. Colonies were added to 100 μL of sterile water and incubated at 90 °C for 10 minutes. Cell debris was pelleted by centrifugation and the supernatant was used as the DNA template in PCR. Individual colony PCR was performed subsequently to identify specific isolates that incorporated the tDNA. Colony PCR reactions were performed using Gotaq polymerase (Promega) according to manufacturer's protocols using thermocycler conditions as follows, 1) 95°C – 2 minutes, 2) 95 °C – 1 minute, 3) 55 °C – 1 minute, 4) 72 °C – 1 minute/kb, repeat steps 2-4 25-30x, 72 °C – 10 minutes, 4 °C – hold. Products were visualized by Midori Green (Bulldog Bio) stain after gel electrophoresis (1.5% agarose). To confirm the deletion *via* Sanger sequencing, DNA was extracted using the DNeasy Blood and Tissue Kit (Qiagen) according to manufacturer's protocol for Gram negative bacteria. PCR of the deletion scar was performed using Phusion Plus Polymerase according to manufacturer's protocol. Thermocycler conditions were as follows, 1) 98 °C – 30 seconds, 2) 98 °C – 10 seconds, 3) 60 °C – 10 seconds, 4) 72 °C – 30 seconds/kb, repeat steps 2-4 25-30x, 72 °C – 5 minutes, 4 °C – hold. The PCR reaction was purified with QIAquick PCR Purification Kit (Qiagen) and Sanger sequencing was performed by the UT Genomics Core or Eurofins Genomics.

***pMMBsacBtfoX* plasmid curing**

To cure *V. natriegens* Δ280 (EZ284) of pMMB*sacBtfoX* cells were grown overnight in LB3, serially diluted and plated onto LB0.1 (LB with 0.1% NaCl) supplemented with 15% sucrose. Plates were incubated at 30 °C. Single colonies from sucrose-containing plates were transferred with sterile toothpicks to non-selective plates

and kanamycin plates to confirm loss of the plasmid *via* kanamycin sensitivity. Colonies that were both able to grow on sucrose and sensitive to kanamycin were considered putatively cured of the plasmid. PCR targeting the plasmid origin of replication was subsequently performed to confirm loss of the entire plasmid rather than just loss of the *sacB* and kan^R genes. DNA was extracted using the DNeasy Blood and Tissue Kit (Qiagen) following instructions for Gram negative bacteria, and PCR was performed using Phusion Plus Polymerase according to manufacturer's protocols, using primers internal to the plasmid origin (Table A2.2). Thermocycler conditions were as follows, 1) 98 °C – 30 seconds, 2) 98 °C – 10 seconds, 3) 60 °C – 10 seconds, 4) 72 °C – 30 seconds/kb, repeat steps 2-4 25-30x, 72 °C – 5 minutes, 4 °C – hold. The same process was used to create a plasmid cured strain of *Vibrio natriegens* ATCC 14048 harboring the $spec^R$ marker (EZ278).

Fitness assays

Vibrio natriegens ATCC 14048 pMMB*tfoX* was used as the WT strain in fitness assays compared to strains marked with erm^R (EZ262) or $spec^R$ (EZ263). Strains were grown overnight in 3 mL of LB3 at 30 °C, shaking (250 rpm). Overnight cultures were diluted 1:1000 into 3 mL of fresh LB3 medium. Growth curves of monocultures were obtained by viable count assay on non-selective LB3 medium. Cocultures of WT and antibiotic resistant (Ab^R) strains were established by inoculating 3 µL of each overnight culture together into 3 mL LB3, and were titered onto both non-selective and antibiotic selection plates. CFU/mL of Ab^R cells was calculated from growth on relevant antibiotic plates. CFU/mL of WT cells was calculated by subtracting the CFU/mL of Ab^R cells from the total CFU/mL calculated on non-selective plates.

Complementation of *ΔoxyR* was assessed by comparing the survival of WT (EZ262), *ΔoxyR* (EZ274), and the *ΔoxyR* complement strain (EZ292) after exposure to 1.5 µM hydrogen peroxide in marine heterotroph minimal media (MHM; AMP-A with 10x trace metals [44-46]). Strains were grown overnight in MHM + 1 % acetate at 30 °C, shaking (250 rpm), diluted 1:1000, and grown overnight again. Cells were pelleted and washed three times in MHM and diluted 1:1000 into 5 mL of fresh MHM. Cultures were

incubated at 30 °C, shaking (250 rpm) for 24 hours, then exposed to 1.5 mM hydrogen peroxide. Cell abundances were measured by viable count assay.

Plasmid cured strains of WT *Vibrio natriegens* ATCC 14048 marked with $spec^R$ (EZ278) and the Δ280 kb mutant marked with erm^R (EZ289) were assayed for relative growth. Overnight cultures were diluted 1:1000 in 10 mL LB3 and grown to an optical density (OD_{600}) of ~0.2. Each culture was then diluted back to an OD_{600} of 0.1 and inoculated 1:100 in triplicate into test tubes with 3ml LB3. Cultures were titered onto LB3 plates to calculate CFU/mL. Growth rates were calculated as the growth constant from the regression of cell number over time of four consecutive time points during exponential growth.

Results

A prophage region can serve as a neutral site for antibiotic resistance gene insertion

In the study that adapted MuGENT from *V. cholerae* to *V. natriegens*, the *dns* locus was chosen as the site for insertion of the kanamycin- or spectinomycin-resistance marker because loss of *dns* did not impact growth or viability in rich medium[32]. Notably, loss of *dns,* which encodes an extracellular/periplasmic endonuclease, did not affect MuGENT transformation efficiency in *V. cholerae* [40, 47]. While the Δ*dns*::kan^R and Δ*dns*::$spec^R$ mutations showed no obvious fitness defect in rich medium in the *V. natriegens* study, we sought to identify a new location for selectable marker insertion with minimal impact on gene expression and physiology, and may prove selectively neutral under most or all experimental conditions. Iterative mutagenesis with MuGENT requires two different drug resistance markers (see below), which would normally be satisfied with the kan^R and $spec^R$ markers used previously. However, because the *sacB* curable derivative of the transformation plasmid (see below) confers kanamycin resistance, we substituted this marker with a new one for MuGENT: erythromycin resistance (erm^R).

Two genomic locations on Chromosome 1 were tested as potential targets. Neutrality was defined as the absence of growth defects of the Ab^R marked strains compared to WT. The first insertion site was an intergenic region between two genes

(HD-GYP domain-containing protein CDS; locus tag PN96_RS00670, and methyl-accepting chemotaxis protein CDS; locus tag PN96_RS00745), transcribed in opposing directions (Figure A2.1A), reasoning that insertion into this location would avoid disruption of any intergenic gene regulation elements. However, unexpectedly, insertion of an erm^R gene into this site resulted in a growth defect (Figure A2.1B). This result highlights the unknown aspects of *V. natriegens* genome and gene regulation. The second insertion site was located within a prophage region between two genes (tyrosine-type recombinase/integrase CDS; locus tag PN96_RS07070, and hypothetical protein CDS; locus tag PN96_RS07075), (Figure 2.1), reasoning that this location would not disrupt fitness impacting processes of the cell. Insertion into the prophage region yielded no fitness defects from erm^R or $spec^R$ gene insertions when the strains were grown in monoculture or cocultured with wild type cells in rich medium (Figures 2.2A and 2.2B, respectively).

Iterative MuGENT mutagenesis via marker swapping

Multiple rounds of engineering via MuGENT are possible so long as each selection event utilizes a different resistance marker than that of the prior selection. One means to facilitate endless iterations of MuGENT transformation is to simply alternate back and forth between two marker genes that replace each other via homologous recombination of flanking DNA at the same neutral site. To test this approach at the neutral site described above, transformation efficiencies were first calculated when either erm^R or $spec^R$ markers were introduced into WT. Subsequently, transformation efficiencies were determined for replacing one marker for the other.

Rates of marker replacement were sufficiently high suggesting this approach can facilitate multiple rounds of mutation via MuGENT (Figure 2.3). Notably, however, the transformation efficiency of insertion of the erm^R marker into WT was significantly higher than all others. Interestingly, the first round of transformation with either selectable marker required extended incubation, 24-36 hours, to form full sized colonies. Whereas, subsequent swapping of the markers required ≤16-18 hours for colonies to fully form. All strains grew normally after initial isolation (Figure 2.2A and 2.2B).

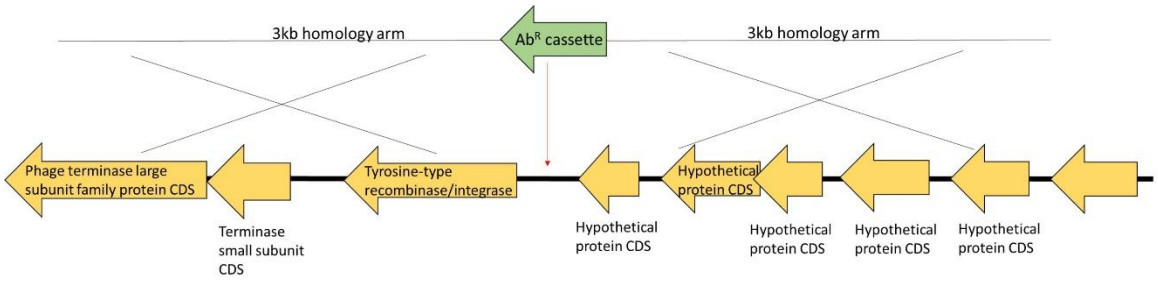

Figure 2.1 Location of a neutral site within a prophage region for antibiotic resistance marker insertion.

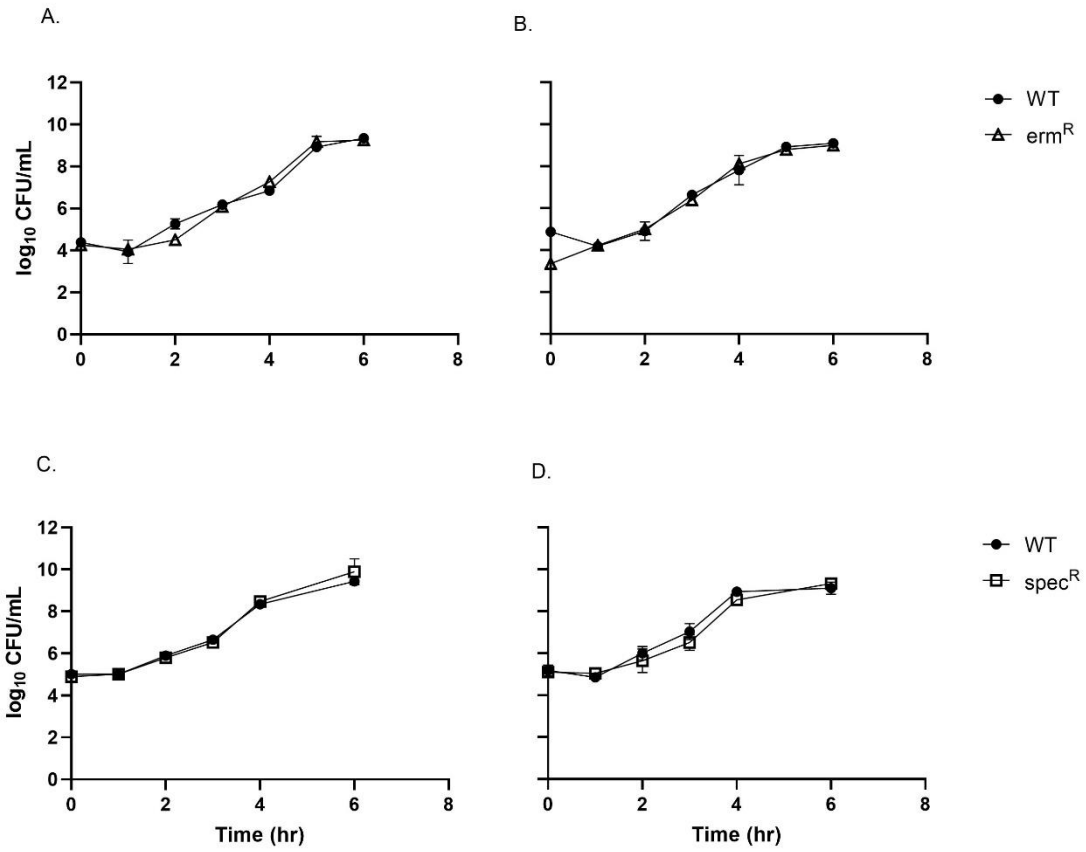

Figure 2.2 Antibiotic resistance gene insertion into a prophage region results in no growth defects. Growth of WT and antibiotic resistant marked strains of *Vibrio natriegens* in monocultures (A and C) and cocultures (B and D) in LB3 at 30 °C (n=3; ± SD of the geometric mean).

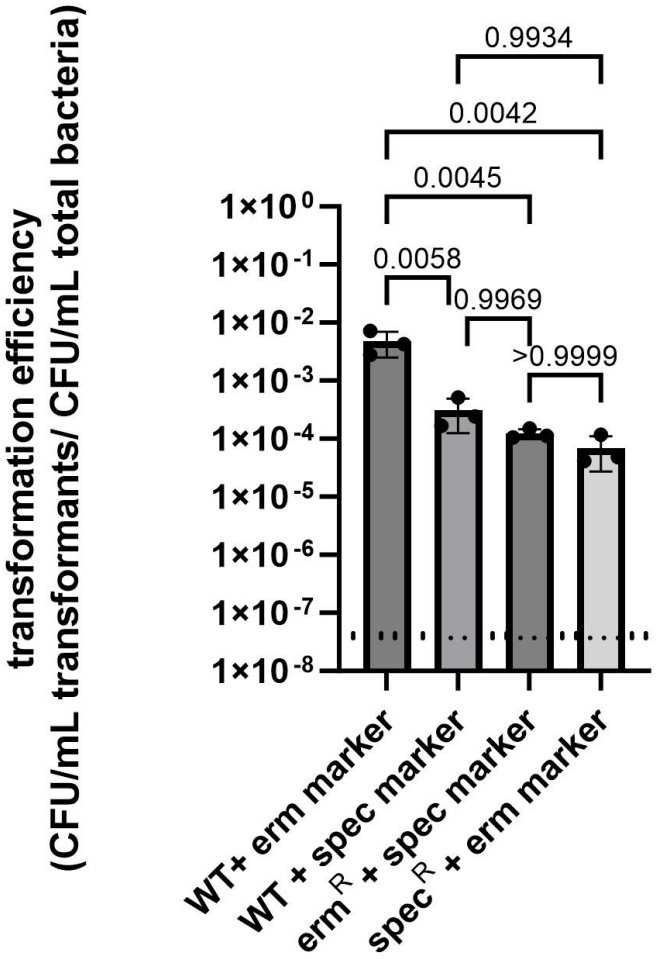

Figure 2.3 Antibiotic marker swapping efficiency. Efficiencies were calculated as CFU/mL on antibiotic-containing plates/ CFU/mL on non-selective plates. P-values were calculated from three biological replicates using a One-way ANOVA multiple comparisons test with Tukey's correction. The dashed line indicates the limit of detection calculated as the ratio of CFU/mL of negative control transformations (no tDNA added) on antibiotic-containing plates versus negative control transformations on non-selective plates. There were no colonies obtained from negative control transformations plated on 100 μg/mL erythromycin plates, however it was found that there is a low rate (4.5-9.7 $x10^{-8}$) of spontaneous spectinomycin resistance that arises when the negative control mock transformations are plated on media containing 250 μg/mL spectinomycin.

Chromosomal complementation of *oxyR*

Complementation of deletion mutations in *V. natriegens* has been achieved by plasmid-based expression systems and reversion mutations [23, 40, 48]. However, to our knowledge complementation of a deleted gene by insertion of that gene at an ectopic chromosomal locus has not yet been developed. To assess this, we created a knockout mutant of *oxyR*, Δ*oxyR* (EZ274), which resulted in cells with an increased sensitivity to hydrogen peroxide compared to WT (EZ262) (Figure 2.4B)**,** consistent with studies in other bacteria [49-51]. We then complemented Δ*oxyR* by replacing the *dns* open reading frame and promoter region (-138 to -1 bp) with those of *oxyR* (promoter region = -124 to -1 bp), creating Δ*oxyR* Δ*dns::oxyR* (EZ292). This construct includes 50 bp of the 3' UTR of *oxyR* placed upstream of the 3' UTR of *dns*. We reasoned that this site has previously been used for selectable marker insertion (see above) and could be used to validate the concept of chromosomal complementation. In the absence of hydrogen peroxide cell viability of Δ*oxyR* and Δ*oxyR* Δdns::*oxyR* did not differ from WT (Figure 2.4A). Whereas, Δ*oxyR* abundance declined rapidly and fell below the limit of detection (100 cells/mL) within 72 hours of hydrogen peroxide exposure, while Δ*oxyR* Δ*dns*::*oxyR* retained cell counts similar to WT (Figure 2.4B). Notably, a small but not statistically significant decrease in Δ*oxyR* Δ*dns*::*oxyR* counts relative to WT was observed by 72 hours after hydrogen peroxide exposure.

Natural transformation can be used to create deletions up to 280 kb in the genome of *Vibrio natriegens* in a single round of mutagenesis

MuGENT has been shown to be an incredibly efficient method for creating markerless point mutations, small indels and single gene deletions [32, 38, 40, 52], but the maximum size of deletions has not been constrained. Chromosome 2 contains only 6 genes essential for growth in rich medium and they are separated by large regions of non-essential genes [11], making the chromosome an ideal target for deletion analysis. For the initial attempt we targeted a 280,441 bp region lacking essential genes (Figure 2.5A). Natural transformation was used to co-transform the erm^R marker and Δ280-creating construct into *V. natriegens* pMMB*sacBtfoX*. Colonies were isolated on erythromycin

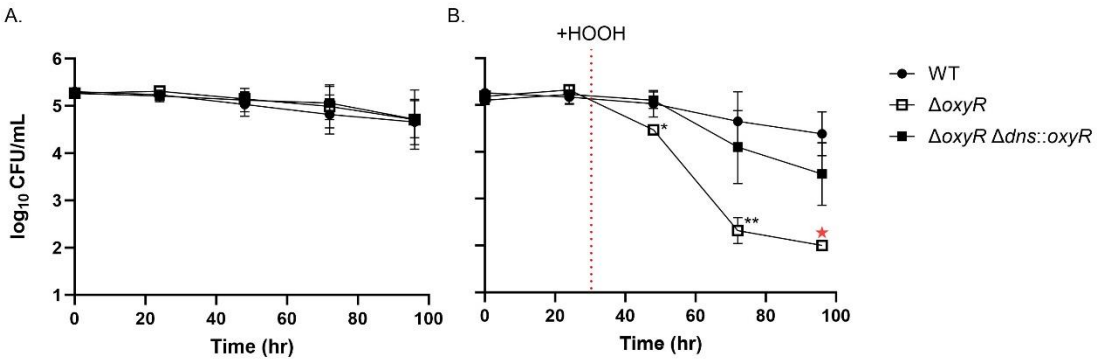

Figure 2.4 Chromosomal complementation of Δ*oxyR* rescues cells exposed to hydrogen peroxide. Cell viability of WT, Δ*oxyR*, and Δ*oxyR* Δ*dns*::*oxyR* in MHM without hydrogen peroxide (HOOH) (A), and with exposure to HOOH (B). Red dashed line indicates addition of 1.5 μM HOOH. Red star indicates cell densities below the limit of detection (<100 CFU/mL). P-values were calculated from three biological replicates using a One-Way ANOVA multiple comparisons test with Dunnett's correction, * $P \leq 0.05$, ** $P \leq 0.01$.

Figure 2.5 Homologous recombination achieves deletions up to 280 kb. A) Schematic depicts the location at which a 280,441 bp deletion was created. Orange circles represent the 3 kb amplicons that were adjoined through PCR to create the construct used in natural transformation. The blue dashed line represents the removal of the segment of DNA between the two deletion endpoints. In the resulting deletion strain the two- 3 kb amplicons, are linked together by a 20-23 bp scar. B) Grouped colony PCR identifies subsets of colonies containing the deletion. Number ranges indicate the isolate #'s groups together in the PCR. C) Individual colony PCR confirms individual colonies containing the deletion. Numbers indicate the isolate # ran in each column. The Thermofisher™ Gene Ruler Express Ladder is used in all gels pictured. D) Sanger sequencing of PCR product aligned to *V.natriegens* genome. Red boxes highlight the sequence is mapped to the endpoints, indicating the two distal segments are now connected and everything in between has been deleted. The zoomed in image shows the presence of the 23 bp scar sequence (red box). Green arrows represent open reading frames (ORFs), right- and left-pointing arrows are encoded on top and bottom stand, respectively.

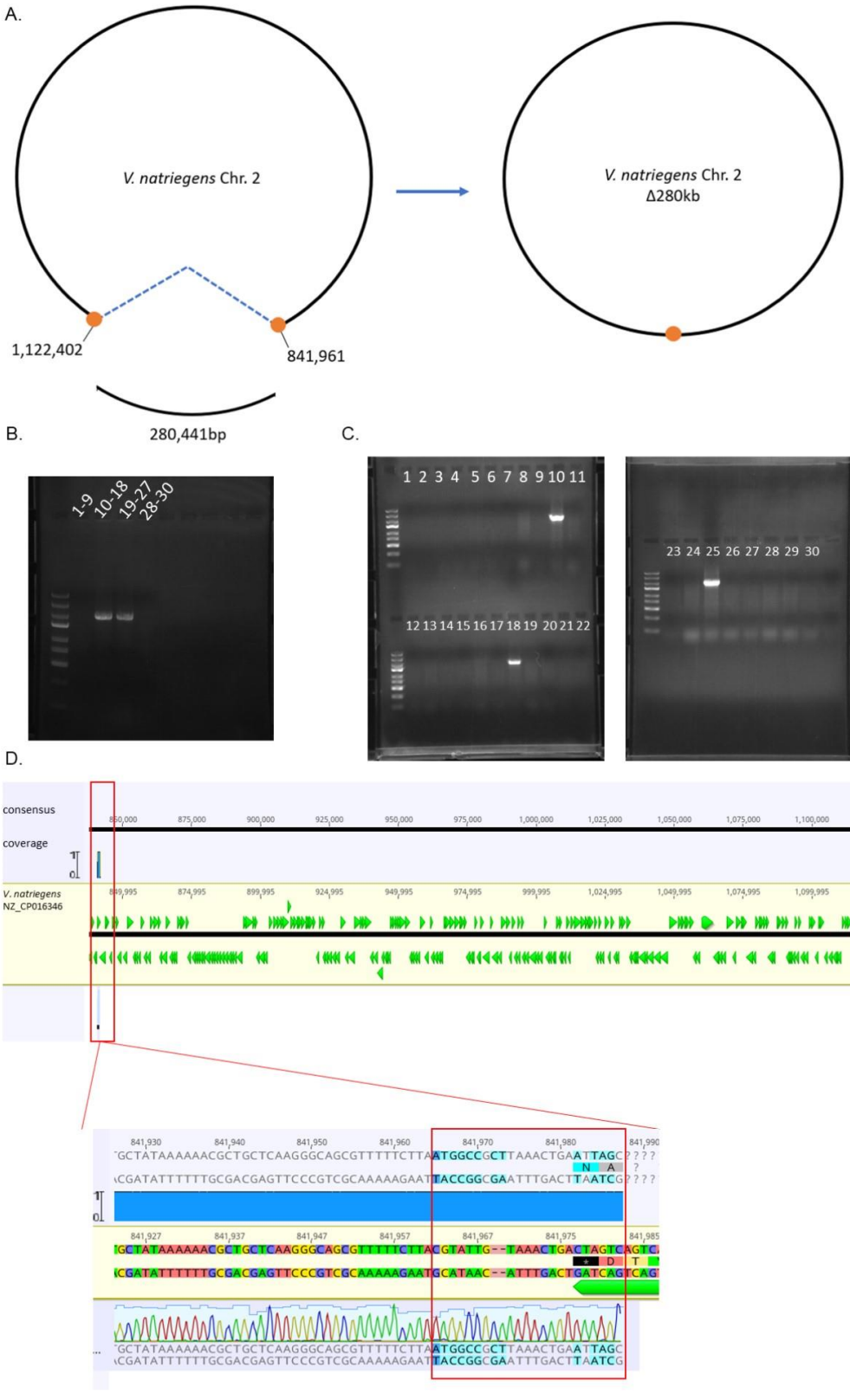
A.
V. natriegens Chr. 2
1,122,402
841,961
280,441bp
V. natriegens Chr. 2
Δ280kb
B.
1-9
10-18
19-27
28-30
C.
1 2 3 4 5 6 7 8 9 10 11
12 13 14 15 16 17 18 19 20 21 22
23 24 25 26 27 28 29 30
D.
consensus
coverage
V. natriegens
NZ_CP016346

containing medium following transformation and cryopreserved in a 96-well plate. To rapidly screen colonies for the deletion, PCR was first performed on pools of nine colonies using the deletion scar primers, 840291F and 1122735R (Table A2.2). This screen indicated two pools contained putative deletions of 280 kb (Figure 2.5B). Colony PCR was performed for every isolate to verify the pooled colony result and to identify those individual isolates with the deletion (Figure 2.5C). Individual screening results were consistent with the pooled screening result and identified that 3/30 of the colonies screened obtained the 280 kb deletion. Sanger Sequencing confirmed loss of the 280 kb and presence of the scar (Figure 2.5D). The deletion of 280 kb removed 239 genes including ones involved in transcriptional regulation, catabolism, iron transport, chemotaxis, oxidative stress, and osmotic stress (Attachment 2.1.xlsx).

To determine whether the size of the targeted deletion impacts mutation efficiency, we compared deletion rates for the 280 kb region (~10%, Figure 2.5C) versus a single gene (2172 bp) that constituted one end of the 280 kb deletion region. The gene target was one of three copies of *katG* (locus tag BA890_RS19750). Natural transformation was performed exactly the same as with the 280 kb deletion, and 30 colonies (transformants that acquired at minimum the antibiotic resistance gene) were screened for *katG* deletion using flanking primers (Table A2.2). Of the 30 colonies screened, 9 showed the deletion (Figure A2.2). Therefore, co-transformation to create a 280 kb deletion was roughly 3 times less efficient than a 2 kb deletion sharing one deletion end, though the lower rate was still well within the scope of feasibility by the MuGENT technique.

sacB **counter-selection permits curing of competence plasmid pMMB*sacBtfoX* from *V. natriegens***

Natural transformation in *V. natriegens* is dependent on plasmid-borne expression of a competence regulator gene, *tfoX*. Being able to cure the plasmid is beneficial for downstream analysis when it is no longer needed and maintaining a multi-copy plasmid may lower fitness. However, *V. natriegens* is quite recalcitrant to losing the plasmid and a robust curing technique has not yet been developed for this organism. One report indicated successful curing by strongly inducing *tfox* expression to increase metabolic

burden and promote plasmid loss; however, screening efficiency for this method was not reported [53]. It has recently been shown that addition of a *sacB* gene onto pMMB*tfox* could be used to cure the plasmid from *V. parahaemolyticus via* sucrose counterselection [38]. We tested whether this *sacB* harboring plasmid, pMMB*sacBtfoX*, can also be lost from *V. natriegens* by sucrose counterselection.

After the pMMB*sacBtfoX* plasmid was used to create the Δ280 kb mutant we implemented counter-selection on sucrose for plasmid curing. Successful curing was achieved by plating on medium containing 15 % sucrose and low salt, 0.1 % NaCl (LB0.1 + 15% sucrose). The addition of 0.1% NaCl, while low, was found to be necessary for growth of *V. natriegens* on these plates. Plating cultures on LB0.1 + 15 % sucrose resulted in a 1000-fold reduction in the number of colonies compared to growth on non-selective medium (Figure 2.6A). Single colonies on LB0.1 + 15 % sucrose were transferred to LB3 (no sucrose) plates containing kanamycin to confirm loss of the kan^R-conferring plasmid. Some colonies showed the desired kan^S phenotype; however, some colonies retained kanamycin resistance (Figure 2.6B). This indicated that the sucrose selection allows for some false positives to arise. For the putative cured $sucrose^R$-$kanamycin^s$ colonies, DNA extraction and PCR amplification of the plasmid *ori* further confirmed loss of the plasmid (Figure 2.6C). It should be emphasized that the reduced salt content of the medium was essential for sucrose counterselection: in full strength (3%) salt media no reduction in colony formation was seen, even in the presence of 15 % sucrose, and no $kanamycin^s$ colonies were

Deletion of 280 kb impacts cell growth in rich media

To assess possible growth defects of the Δ280 kb deletion we compared monoculture growth curves for plasmid cured strains of Δ280 kb (EZ289) marked with erm^R and WT *V. natriegens* marked with $spec^R$ (EZ278). In LB3 medium, Δ280 (EZ289) achieved a lower maximum growth rate than WT but both strains reached similar final abundances (Figures 2.7B and 2.7A, respectively). Thus, despite the removal of 239 genes, the deletion mutant remained viable and had the same growth yield as WT with only a small defect in growth rate.

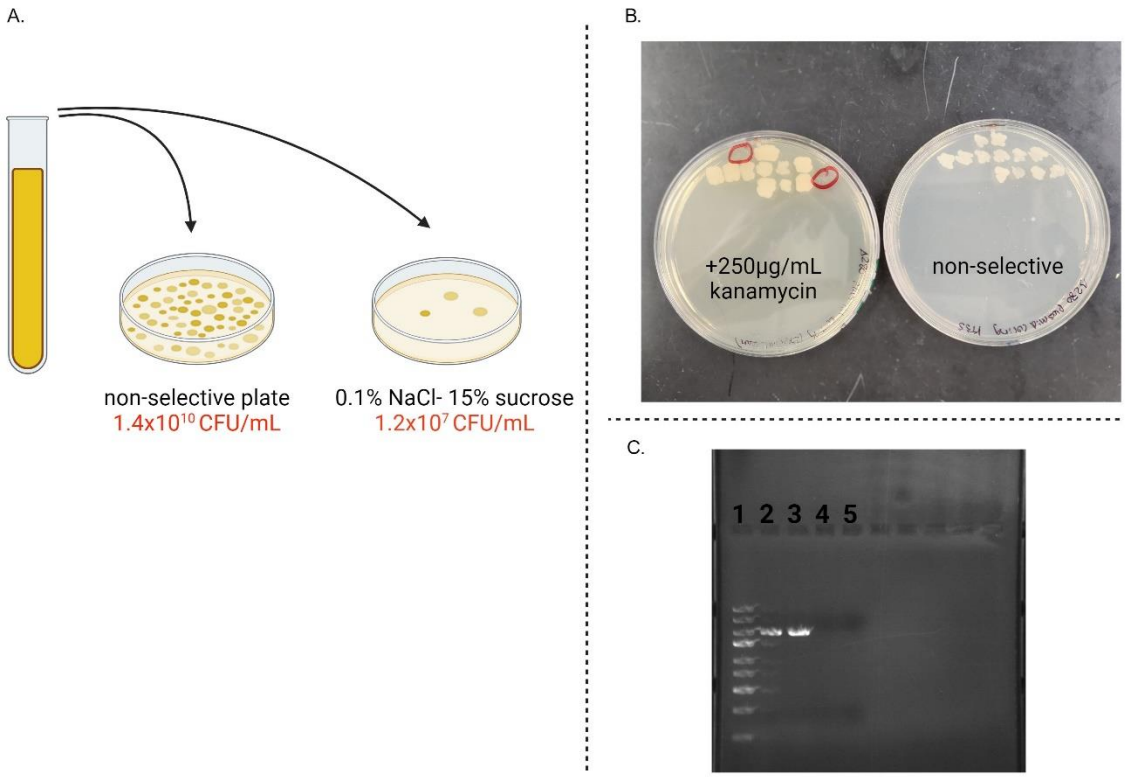

Figure 2.6 Plasmid curing accomplished with *sacB*-mediated selection. A) CFU/mL calculation of Δ280-pMMB*sacBtfox* bacterial culture plated on non-selective and sucrose-containing media. B) Growth of individual colonies from sucrose-containing plate on non-selective and kanamycin-containing plates. Red circles highlight the colonies that were kanamycin sensitive. C) DNA was extracted from both sucrose^{R}-kanamycin^{s} strains. Thermofisher™ GeneRuler Express Ladder (column 1), PCR amplification of the Δ280 scar (columns 2 and 3) and the plasmid *ori* (columns 4 and 5) were performed to confirm loss of the plasmid. Created with Biorender.com

A.

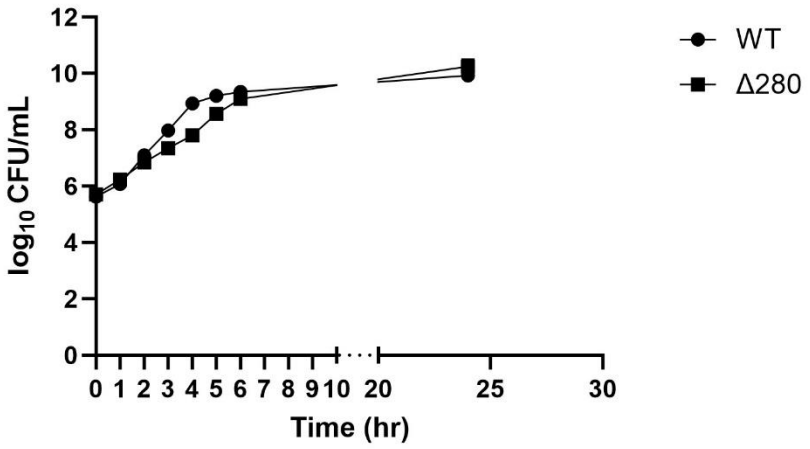

B.

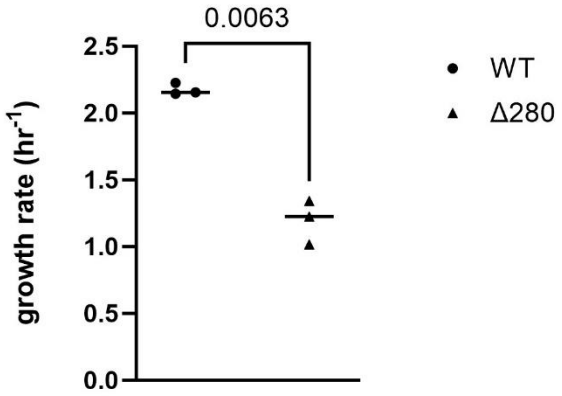

Figure 2.7 Fitness of Δ280 kb strain. A) Monoculture growth curves and B) growth rates (hr^{-1}) of WT and Δ280 kb strains of *V. natriegens* in LB3 medium at 30°C (n=3; ±SD of the geometric mean). P-value was calculated using a two-tailed, unpaired t-test with Welch's correction.

Discussion

This work expands the genetic toolset for *V. natriegens* and advances the genomic engineering capabilities of this emerging model organism. We identified a neutral site for selectable marker insertion within a prophage region of Chromosome 1, providing an alternative target that does not require disruption of the *dns* gene. Additionally, we demonstrated the ability to select for transformants in iterative rounds of MuGENT with high efficiency *via* marker swapping at each round. Here we implemented selectable markers establishing erythromycin or spectinomycin resistance, but a number of antibiotics have been used for the selection of *V. natriegens* after transformation [28], and should be feasible to use. We further applied this to create a knockout mutant of *oxyR*, and subsequent insertion of *oxyR* at a different locus, and showed chromosomal complementation permits phenotypic rescue of *oxyR* mutants. To demonstrate the ability of MuGENT to make massive edits to the genomic chassis in single transformations, we created a 280 kb markerless deletion, removing 239 genes from the genome with some loss of maximum growth rate but no apparent decrease in cell yield. Finally, as a useful cleanup step after mutagenesis, we established a protocol of curing the transformants of the plasmid necessary for MuGENT using the *sacB* counterselection method.

The new marker insertion site is found within a prophage region on Chromosome 1. It should be noted that a previous study has characterized this prophage region, finding that excision can be induced by DNA damaging agent, mitomycin C, and it can undergo spontaneous induction, but at a low rate of <1 % in exponentially growing cells and 0.001 % in stationary phase cells [24]. Prophage induction could theoretically lead to marker loss from the chromosome, but induction should culminate in cell lysis and mortality, and in either case loss of drug resistance can be screened readily.

Notably, our transformation efficiencies were 2-3 fold lower than previously reported [32] and initial insertion of either marker at the prophage locus resulted in a longer incubation time (24-36 hours) for colonies to fully form. The cause of this delay is unknown, but perhaps the insertion of the selectable marker triggers an elevated rate of spontaneous induction that slows colony enlargement through the release and lytic infection by the phage within the growing population. Alternatively, there could be a lag

in expression of the selectable marker, which would result in some initial cell death and thus slower colony formation. However, and importantly, subsequent culturing of the strains harboring selectable markers showed no difference in fitness compared to wildtype cells and in iterative rounds of transformation that replace one marker with another, colonies form normally (16-18 hours). Finally, initial insertion of the erythromycin marker into WT had a significantly higher transformation efficiency than all other marker insertions. It is notable that the erythromycin marker used here has also been described as a superior marker for use in *V. fischeri* because it resulted in higher recovery of transconjugants and lower rates of spontaneous resistance [54]. While several antibiotics have been shown to work as selective markers in *V. natriegens,* future studies could benefit from a comprehensive understanding of marker efficiencies to optimize mutagenesis protocols in *V. natriegens* and other *Vibrio* species.

Deletion of *oxyR* resulted in hypersensitivity to hydrogen peroxide, indicating a likely familiar role in activation of antioxidant genes during oxidative stress [55]. It should be noted that this phenotype was observed after 24-hour acclimation in minimal medium and exposure to 1.5 mM hydrogen peroxide. These conditions were chosen to more closely mimic environmental conditions than rich medium typically used for laboratory culturing, and proved useful for exhibiting a detectable phenotype.

Chromosomal complementation of *ΔoxyR* was successful in rescuing the deletion phenotype, demonstrating the feasibility of single-copy, chromosomal complementation. We used the *dns* gene as the location for this ectopic expression, providing the native promoter region of *oxyR* and leaving the 3' UTR of *dns* intact. This method provides an alternative to plasmid-based complementation and can be useful when plasmid maintenance and/or expression of genes on multicopy plasmids are undesired.

Higher growth rate [56], cell density [56, 57], recombinant protein production [56-59] , improved genetic stability [56, 60], and greater DNA uptake efficiency [60] have all been observed in deletion constructs of bacteria with bioproduction potential (see also reviews [61, 62]). As such, much effort has been given to investigating effects of genome reduction, the minimal set of genes required for life, and to creating a reduced chassis desirable for bioproduction applications, as recently reviewed [63, 64]. One major

challenge in these areas is the labor-intensive process to create deletions. Our work illustrates the ease of using *V. natriegens* and provides a framework to apply *V. natriegens* in the aforementioned areas of research. Here we have demonstrated the ability to delete 280 kb of DNA in a single round of targeted mutagenesis. To our knowledge this is the largest deletion made by MuGENT and one of the largest deletions made in a single round of mutagenesis of a bacterial chromosome [65]. The upper bound of possible deletion size using this methodology is unknown but presumably set by the maximum distance between essential genes. Chromosome 2 of *V. natriegens* contains regions >500 kb lacking any predicted essential genes and so future studies may successfully generate deletions larger than 280 kb. However, challenges facing the creation of larger deletions using this method may include the physical distance between recombination sites and the DNA topology of the chromosome that the tDNA must interact with for recombination to occur. Additionally, the definition of "essentiality" should be considered. Caution should be taken as there are additional "growth supporting" genes (required for rapid growth in rich medium) throughout the chromosome [11]. The deletion of growth supporting genes in our 280 kb deletion (e.g. *pyrC*, a DEAD/DEAH box helicase, a hypothetical protein, an Sco family protein, and an iron chelate uptake ABC transporter family permease subunit) likely contributed to the growth defect we observed. Consideration should be given to growth conditions which may impact gene essentiality, and to the possibility of conditionally lethal genes, which may impede multi-gene deletions [66]. Furthermore, it has been shown that deletions of 'dispensable' genomic loci sometimes result in unexpected negative effects [59, 67, 68].

Our pooled colony screening technique proved useful to rapidly screen multiple transformation isolates simultaneously, with 100% accuracy of identifying pools that contained isolates with our targeted deletions. We also found that deletion of 280 kb occurred in 10% of colonies screened, while deletion of a single gene (2 kb) occurred in 30% of colonies screened. Both the size of PCR constructs to create these deletions and transformation protocols used were performed the same for both deletion lengths. One simple interpretation of this difference is that the proximities of the two deletion ends are different for the two construct sizes due to chromosomal packaging, and this proximity

contributes to overall recombination efficiency. Another, non-mutually exclusive explanation is that the gene function(s) lost in the large deletion contribute in some way to (initial) colony formation, though subsequent rounds of growth show no loss in plating efficiency for the deletion mutant.

Finally, we report successful implementation of *sacB*-mediated plasmid curing in *V. natriegens*. This cleanup step removes the plasmid from the host genome, decreasing metabolic burden on the host and removing the necessity of maintaining the culture under antibiotic selection to ensure genetic homogeneity between treatment groups in downstream analysis of the mutants (i.e., all groups should have the plasmid, or not have the plasmid, to prevent ambiguity that can occur if spontaneous curing happens in absence of selection). Plasmid curing was only achievable when we reduced salt from the selection media. We hypothesize the reduction in salt concentration improved *sacB*-mediated cell death by enriching the osmolyte pool with sucrose: addition by subtraction. Similarly, reducing or removing salt entirely from the media has been shown to increase sucrose sensitivity in *sacB*-harboring cells of *Escherichia coli* K12 and *Burkholderia pseudomallei* [69, 70], but to our knowledge the mechanisms behind this have not been experimentally determined. In *Bacillus subtilis,* it has also been shown that NaCl influences expression of *sacB,* however, it was found that higher NaCl concentrations induced higher expression of *sacB* [71], suggesting a different mechanism may be responsible for the improved counter-selection phenotype seen here. Importantly, this method worked only when salt was reduced but not eliminated. Elimination of salt prevented growth of *V. natriegens* in our media, which is consistent with prior reports that substrate uptake and cell proliferation by this organism is dependent on the availability of salt ions [1, 3, 72].

Acknowledgements

We thank Ankur Dalia and Kim Orth for strains and valuable advice.

Funding

This work was supported by a Student/Faculty Research Award from the University of Tennessee, Knoxville to L.D. Glasgo and E.R.Z and NSF OCE-2023680 to E.R.Z.

Appendix

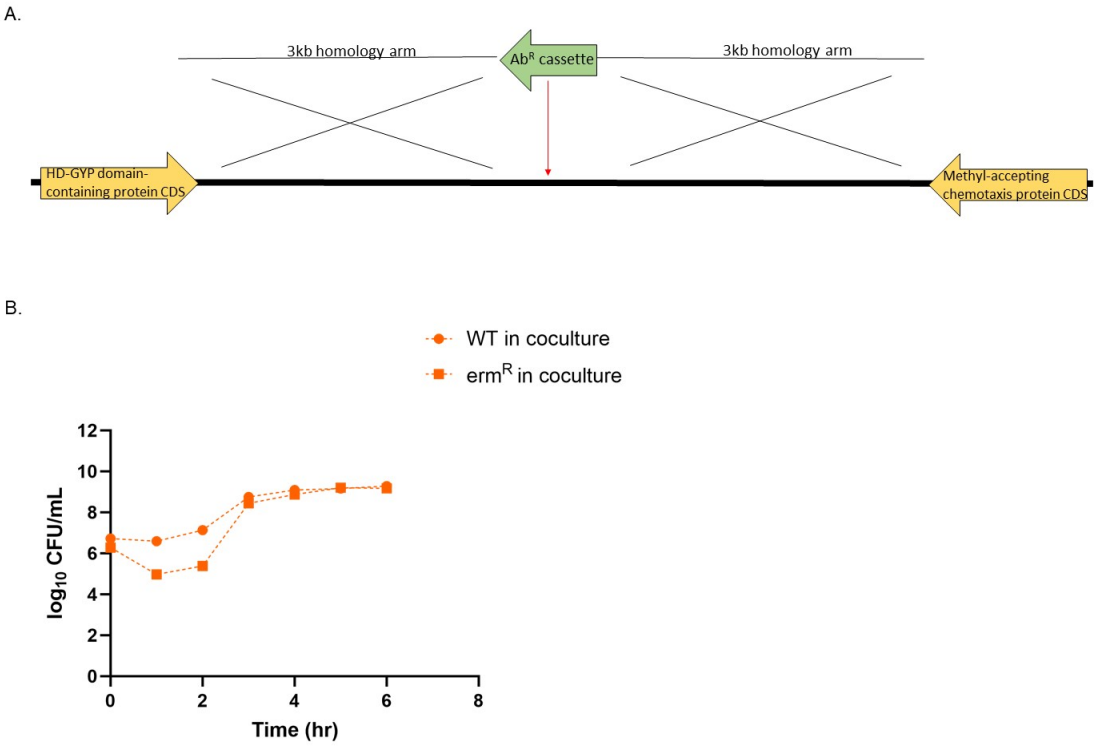

Figure A2.1 Antibiotic resistance gene insertion into an intergenic region results in growth defect. A) Intergenic location for antibiotic resistance gene insertion. B) Growth curves of WT and erm^R resistant marked strains of *Vibrio natriegens* grown together in coculture. Performed in duplicate biological replicates, in LB3 media at 37°C.

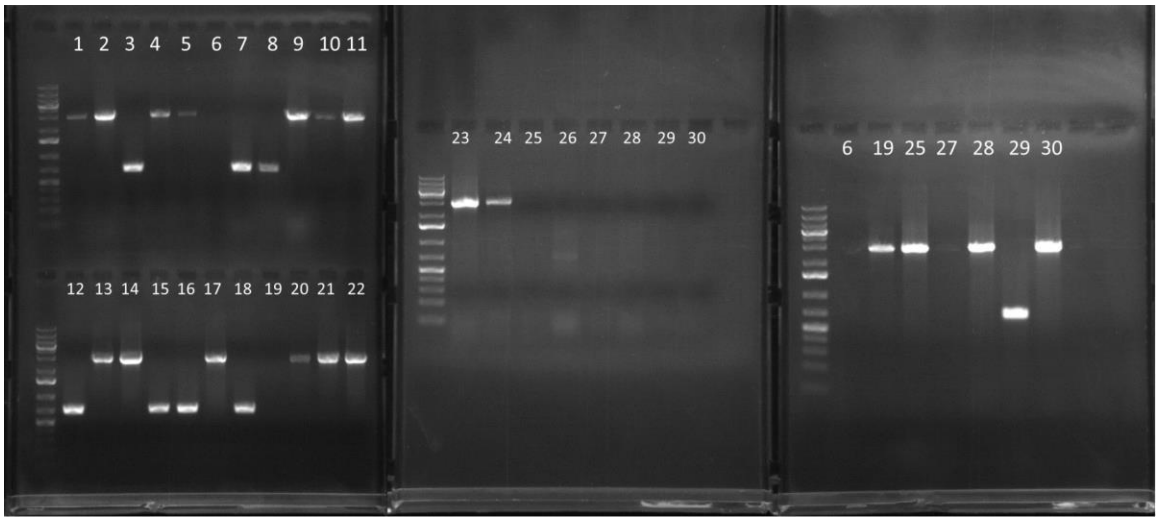

Figure A2.2 Colony PCR for single gene deletion efficiency analysis. Colony PCR was performed on individual colonies obtained from transformation with a construct targeting deletion of a single gene, *katG*, ~2kb in size. A band of ~3kb indicates no deletion occurred, while a band of ~800kb indicates that the deletion did occur. Numbers represent the colony isolate # ran in each column. The far right gel shows re-runs of failed reactions from the first two gels. The Thermofisher™ GeneRuler 1kb Plus Ladder was used in all gels.

Table A2.1 Strains and plasmids used in this study.

Name	**Description**	**Source**
Vibrio natriegens ATCC 14048 SAD1302	WT	Ankur Dalia
Vibrio natriegens ATCC 14048 pMMB*tfox* TND1964	Amp^R	Ankur Dalia
E.coli WM3064	*thrB1004 pro thi rpsL hsdS lacZDM15 RP4-1360 D(araBAD)567 DdapA1341::[erm pir],* pir^+	[43]
pMMB*sacBtfoX*	Carries kan^R, $sucrose^s$	Kim Orth [38]
Vibrio natriegens ATCC 14048 pMMB*tfox* erm^R (EZ262)	Chr.1 Δ1,520,008-1520031::erm^R, Amp^R	This study
Vibrio natriegens ATCC 14048 pMMB*tfox* $spec^R$ (EZ263)	Chr.1 Δ1,520,008-1520031::$spec^R$, Amp^R	This study
Vibrio natriegens ATCC 14048 pMMB*sacBtfoX* (EZ276)	Kan^R,	This study
Vibrio natriegens ATCC 14048 (EZ278)	Chr.1 Δ1,520,008-1520031::$spec^R$	This study
Vibrio natriegens ATCC 14048 pMMB*tfox* Δ*oxyR* (EZ274)	Chr.1 Δ1,520,008-1520031::erm^R, Amp^R, ΔPN96_RS15030 [chr.1 Δ3,218,138 – 3,219,076]	This study
Vibrio natriegens ATCC 14048 pMMB*tfox* Δ*oxyR* Δ*dns*::*oxyR* (EZ292)	Chr.1 Δ1,520,008-1520031::$spec^R$, Amp^R, ΔPN96_RS15030 [chr.1 Δ3,218,138 – 3,219,076], ΔPN96_RS00885 [chr.1 171,347-172,168] :: ΔPN96_RS15030 [chr.1 3,218,016 – 3,219,099]	This study
Vibrio natriegens ATCC 14048 pMMB*sacBtfoX* Δ280kb (EZ284)	Δ BA890_RS18565 – BA890_RS19750 [chr.2 Δ841,961 – 1,122,402], Chr.1 Δ1,520,008-1520031::erm^R, Kan^R	This study

Table A2.1 continued

Name	**Description**	**Source**
Vibrio natriegens ATCC 14048 Δ280kb (EZ289)	Δ BA890_RS18565 – BA890_RS19750 [chr.2 Δ841,961 – 1,122,402], Chr.1 Δ1,520,008-1520031::erm^{R}	This study

Table A2.2 List of primers used in this study. Underlined nucleotides specify homologous regions added for SOE PCR.

Primer name	**Primer sequence 5'->3'**	**Description**	**Template DNA**
IGRF1	TCGTGAGGAAG GTAGTGTGT	Upstream arm of intergenic site, forward primer	*V. natriegens* ATCC14048, NZ_CP009977
IGRR1	ACACAATCGCT CAAGACGTGCG CCTTAGGGGTC GACTTAC	Upstream arm of intergenic site, reverse primer	*V. natriegens* ATCC14048, NZ_CP009977
IGRF2	CTAATTCCCATG TCAGCCGTCCG AAAGGCGTAGT CGATGG	Downstream arm of intergenic site, forward primer	*V. natriegens* ATCC14048, NZ_CP009977
IGRR2	CGCCCAACACA CACCACATA	Downstream arm of intergenic site, reverse primer	*V. natriegens* ATCC14048, NZ_CP009977
PF1	CACAGTGAGGA CAGATTAAACG A	Upstream arm of phage region, forward primer	*V. natriegens* ATCC14048, NZ_CP009977
PR1	ACACAATCGCT CAAGACGTGAC GATTACGTATCT CTGATGCGA	Upstream arm of phage region, reverse primer	*V. natriegens* ATCC14048, NZ_CP009977
PF2	CTAATTCCCATG TCAGCCGTCCA AAGGGTCACCA CCGTAA	Downstream arm of phage region, forward primer	*V. natriegens* ATCC14048, NZ_CP009977
PR2	GTGACAGAGAC GCAGGACTC	Downstream arm of phage region, reverse primer	*V. natriegens* ATCC14048, NZ_CP009977
ErmFwd	CACGTCTTGAG CGATTGTGTAA CTGAGGATCCG GTGATTG	Erm^R gene forward primer	pEVS170
ErmRev	ACGGCTGACAT GGGAATTAGGA AGCAAACTTAA GAGTGTGTTGA	Erm^R gene reverse primer	pEVS170

Table A2.2 continued

Primer name	**Primer sequence 5'->3'**	**Description**	**Template DNA**
SmRFwd2	CACGTCTTGAG CGATTGTGTATG ACCCTGCTGATT GGTTC	$Spec^R$ gene forward primer	pAM5057
SmRRev2	ACGGCTGACAT GGGAATTAGGA TGTTATGGAGC AGCAACG	$Spec^R$ gene reverse primer	pAM5057
pKD4KanF	CACGTCTTGAG CGATTGTGT	Ab^R scar forward primer	
pKD4KanR	ACGGCTGACAT GGGAATTAG	Ab^R scar reverse primer	
OxyRF1	GCCGTAACGTT GGCCTATAA	Upstream arm of Δ*oxyR*, forward primer	*V. natriegens* ATCC14048, NZ_CP009977
OxyRR1	GCTAATTCAGTT TAAGCGGCCAT CACACGATTCG CTTCTATTTAGT G	Upstream arm of Δ*oxyR*, reverse primer	*V. natriegens* ATCC14048, NZ_CP009977
OxyRF2	ATGGCCGCTTA AACTGAATTAG CAGCTATTGGCT CCCCTTGTT	Downstream arm of Δ*oxyR*, forward primer	*V. natriegens* ATCC14048, NZ_CP009977
OxyRR2	CACGACCGCGA ACTCTATTT	Downstream arm of Δ*oxyR*, reverse primer	*V. natriegens* ATCC14048, NZ_CP009977
3217813F	GAGGCAAATGG CTTGAAGAA	Δ*oxyR* scar, forward primer	*V. natriegens* ATCC14048, NZ_CP009977
3219406R	CCTTGGTCAAG GCCAAGTAT	Δ*oxyR* scar, reverse primer	*V. natriegens* ATCC14048, NZ_CP009977
endAF1	CTAACATGGCT AAGCACCTG	Upstream arm of Δ*dns*, forward primer	*V. natriegens* ATCC14048, NZ_CP016345
endAR1	ACACAATCGCT CAAGACGTGAC TGAGGATTAGG AAAGCTGGA	Upstream arm of Δ*dns*, reverse primer	*V. natriegens* ATCC14048, NZ_CP016345

Table A2.2 continued

Primer name	**Primer sequence 5'->3'**	**Description**	**Template DNA**
endAF2	ATGGCCGCTTAAACTGAATTAGCCCTCACCAATCGCGACAATC	Downstream arm of Δ*dns*, forward primer	*V. natriegens* ATCC14048, NZ_CP016345
endAR2	TAAGGTGTCTCAAATCTCAATCTAGG	Downstream arm of Δ*dns*, reverse primer	*V. natriegens* ATCC14048, NZ_CP016345
oxyRcompF1	CACGTCTTGAGCGATTGTGTTCGGCTCGTGTCTGTTCTG	*oxyR* complement, forward primer	*V. natriegens* ATCC14048, NZ_CP009977
oxyRcompF2	GCTAATTCAGTTTAAGCGGCCATAACAACAAGGGGAGCCAATAG	*oxyR* complement, reverse primer	*V. natriegens* ATCC14048, NZ_CP009977
2728836F	TTCCCTATTCCCAGCCTGAC	Δ*dns*::*oxyR* scar, forward primer	*V. natriegens* ATCC14048, NZ_CP016345
2730429R	CTACGCGCTCAGAGATGTCT	Δ*dns*::*oxyR* scar, reverse primer	*V. natriegens* ATCC14048, NZ_CP016345
838941F	GCTGGCACATTTTACGCATAG	Upstream arm of Δ280, forward primer	*V. natriegens* ATCC14048, NZ_CP016346
841961R	GCTAATTCAGTTTAAGCGGCCATTAAGAAAAACGCTGCCCTTG	Upstream arm of Δ280, reverse primer	*V. natriegens* ATCC14048, NZ_CP016346
KatG3F2	ATGGCCGCTTAAACTGAATTAGCTCGCTAAGCTAGCATAAGCTCT	Downstream arm of Δ280, forward primer	*V. natriegens* ATCC14048, NZ_CP016346
KatG3R2	GGATTCTGACTGGAGCAAGC	Downstream arm of Δ280, reverse primer	*V. natriegens* ATCC14048, NZ_CP016346
840291F	CGGCTAATCTGACCATGAAC	Δ280 scar, forward primer	*V. natriegens* ATCC14048, NZ_CP016346

Table A2.2 continued

Primer name	**Primer sequence 5'->3'**	**Description**	**Template DNA**
1122735R	GTTCCGGAGAT ATCGGACAA	Δ280 scar, reverse primer	*V. natriegens* ATCC14048, NZ_CP016346
KatG3F1	ATAGCCACCAT CGGTTGAGA	Upstream arm of Δ*katG*, forward primer	*V. natriegens* ATCC14048, NZ_CP016346
KatG3R1	GCTAATTCAGTT TAAGCGGCCAT CTGGCTTTTTGC GTATCCAT	Upstream arm of Δ*katG*, reverse primer	*V. natriegens* ATCC14048, NZ_CP016346
KatG3F2	ATGGCCGCTTA AACTGAATTAG CTCGCTAAGCT AGCATAAGCTC T	Downstream arm of Δ*katG*, forward primer	*V. natriegens* ATCC14048, NZ_CP016346
KatG3R2	GGATTCTGACT GGAGCAAGC	Downstream arm of Δ*katG*, reverse primer	*V. natriegens* ATCC14048, NZ_CP016346
1119752F	GCCAGACATCC TAATGCCTTT	Δ*katG* scar, forward primer	*V. natriegens* ATCC14048, NZ_CP016346
1122735R	GTTCCGGAGAT ATCGGACAA	Δ*katG* scar, reverse primer	*V. natriegens* ATCC14048, NZ_CP016346
pMMBOriVF	AACCTGCAAAC CCAGCAG	pMMB*sacBtfoX* origin forward primer	pMMB*sacBtfoX*
pMMBOriVR	CCGCTAAAGCG GCTAAAAG	pMMB*sacBtfoX* origin reverse primer	pMMB*sacBtfoX*

CHAPTER THREE

Structure and function of three catalase-peroxidases in *Vibrio natriegens*

Disclosure statement

A version of this chapter has been submitted for publication in the Journal of Bacteriology. Liz Glasgo planned, executed, and supervised the work presented in this chapter. Spiridon Papoulis gathered sequence data used for abundance and diversity analysis. Emily Chase generated phylogenetic trees and provided expertise on tree presentation and interpretation. Kennedi Hambrick generated the *oxyR* mutants. Luke Qualey carried out the peroxide tolerance experiments with the parental strain and the ampicillin peroxide degradation assay. Liz Glasgo and Erik Zinser wrote the manuscript. Spiridon, Emily, Kennedi, Luke, and Steven Wilhelm helped edit.

Abstract

Vibrio natriegens is an emerging model organism in laboratory and biotechnology research that is known for its fast growth rate and diverse metabolic capabilities. However, little is known about its response to oxidative stress. Reactive oxygen species (ROS) are ubiquitous stressors for most aerobic life and without mitigation can lead to cellular damage and sometimes death. *V. natriegens* are unusual amongst the *Vibrio* genus and Proteobacterial phylum in having three copies of *katG* encoding the bifunctional ROS defense enzyme catalase-peroxidase, with two of them arising recently via duplication and divergence. Analysis of single, double, and triple Δ*katG* constructs confirmed a role of each *katG* gene product during exposure to hydrogen peroxide (HOOH) under stationary phase conditions but found the genes were dispensable for HOOH resistance during exponential growth. We also demonstrated the involvement of the OxyR and RpoS regulons in *V. natriegens* oxidative stress response in stationary phase and found evidence that two of the *katG* genes are under RpoS control. As an outcome of this investigation, we identified and repaired several spontaneous loss-of-function mutations of *rpoS* in laboratory cultures of the *V. natriegens* type strain ATCC 14048. Together, these results provide physiological and evolutionary insights into *V. natriegens* ROS response.

Importance

The importance of oxidative stress is evident in a diversity of research areas, such as bacterial ecology, host-microbe interactions, and tolerance to antimicrobials. The use of *V. natriegens* as a model organism to study oxidative stress offers the advantages of an easily tractable system that can be used as a model organism in marine ecology research and as a non-pathogenic representative of the *Vibrio* genus. To our knowledge this is the first case study into the multiplicity of *katG* genes and oxidative stress response of *V. natriegens*. This work advances our understanding of *V. natriegens* as a rising model organism and contributes to the broader fields of bacterial oxidative stress response and marine ecology.

Introduction

Following the Great Oxygenation Event 2.4 billion years ago, cellular life became threatened by harmful reactive oxygen species (ROS). ROS molecules [*e.g.* superoxide (O_2^-), hydrogen peroxide (HOOH), and hydroxyl radicals (OH•)], induce damage through oxidization and destabilization of cellular components including DNA, proteins, and lipids [73, 74]. In aerobic environments, production of ROS occurs ubiquitously through biotic and abiotic processes [75]. Consequently, adaptations to combat oxidative stress are diverse and widespread.

Bacteria often encode multiple antioxidant genes with specialized function and regulation [76]. Small molecules, metals, and pigments are thought to be early evolutionary oxidant defenses [73, 77-79], while stronger defenses arose that directly degrade ROS. Superoxide dismutase (SOD) converts O_2^- into O_2 and HOOH, and catalases and peroxidases neutralize HOOH [76, 80, 81]. Catalases have been further grouped into two main families: HPII (*e.g.,* KatE) – monofunctional catalase enzymes, and HPI (*e.g.,* KatG) – bifunctional catalase-peroxidase enzymes. A well-developed functional and regulatory understanding of these systems has been established for model organisms [82-84]. For instance, in *Escherichia coli*, *katG* expression is induced by transcriptional regulator and HOOH sensing molecule, OxyR [85], while *katE* is not.

However, both genes are under control of RpoS and increase in expression during stationary phase [86, 87].

The ability of *Vibrio* species to tolerate oxidative stress has been implicated as an important mechanism for survival of pathogenic species such as *V. cholerae, V. parahaemolyticus, V. vulnificus,* and *V. harveyi* [51, 88-90]. More recently, studies of *V. parahaemolyticus* identified the presence of two *katE* and two *katG* genes [91, 92]. All four are regulated by OxyR, but *katE*1 and *katE*2 were reported to respond to extrinsic HOOH during exponential and early stationary phase [91-93], while *katG*1 and *katG*2 were additionally found to be regulated by RpoS, and expressed during stationary phase [91, 92, 94]. Additionally, the expression of each set of duplicate enzymes was found to differ. Notably, this regulation differs from that in *E. coli* and demonstrates non-redundant function of each enzyme.

Vibrio natriegens is a close relative of *V. parahaemolyticus*, yet few studies have reported on its response to oxidative stress [6, 95]. Here, we report *V. natriegens* harbors three copies of the bifunctional catalase-peroxidase encoding gene, *katG,* we designate *katG1, katG2,* and *katG3*. We investigated the HOOH degradation activity, regulation, and phylogenetic relationship of each gene product. Importantly, we report that commonly used type strains of *V. natriegens* contain one of several mutations in *rpoS,* encoding the stationary phase sigma factor s^s (RpoS). We constructed a "wild type" *rpoS* allele that maximizes oxidative stress response and show that *katG1* and *katG2* are regulated by *rpoS,* while *katG3* is not. We find that *katG* multiplicity is conditionally important for cells lacking a functional *rpoS,* the multiplicity of *katG* genes being critical during prolonged stationary phase conditions. We demonstrate the involvement of the transcription factor, OxyR, in *V. natriegens* oxidative stress response and show probable governing of a larger regulon. We also provide phylogenetic analysis suggesting an early ancestor possessed two copies of *katG* but a more recent duplication event led to the occurrence of three *katG* copies in *Vibrio natriegens,* a rare feature within the *Vibrio* genus. This work provides novel insights into the function and evolution of *katG* genes in *V. natriegens* and importantly, uncovers physiologically important characteristics of this emerging model system.

Materials and methods

Bacterial strains and culturing conditions

Vibrio natriegens ATCC 14048 carrying plasmid pMMB*tfox* (EZ260) was used as the parent strain in this study to generate the strains listed in Table A3.1. All strains were frozen in LB+10% glycerol and stored at -80° C. Cultures were routinely grown in Minimal Marine Heterotroph Medium (MHM) [96] with carbon sources (acetate or glucose) as indicated. Experiments were performed in acid-washed glassware unless otherwise stated. Glassware was soaked in 1 N HCL for at least 24 hours, then rinsed 6 times with MilliQ water before being filled with MilliQ and autoclaved. All cultures were incubated at 30° C in an orbital shaker (200-250 rpm) in the dark. Media was supplemented with 150 μg/mL ampicillin (amp), 100 μg/mL erythromycin (erm), and 250 μg/mL spectinomycin (spec), as needed.

Statistical analysis

One-way ANOVAs with multiple comparisons tests and Dunnett's corrections were performed when comparing greater than two populations at once. Single deletion mutants were compared to the parental strain and double deletion mutants were compared to the triple deletion strain, unless otherwise stated.

Mutant design and Multiplex Genome Editing by Natural Transformation (MuGENT)

Mutant constructs were created with splicing by overlap (SOE) PCR as previously described [32]. Deletion constructs were generated with two-piece SOE and selectable markers and complementation constructs were generated with three-piece SOE. Briefly, 3 kb upstream and 3 kb downstream regions flanking the gene of interest or site of insertion were amplified. For two-piece SOE, primers added 20-23 bp homologous nucleotide sequences to the 3' end of the upstream region and 5' end of the downstream region. Three-piece SOE was performed similarly but included amplification of the desired insert (middle piece) with primers that added homologous nucleotide sequences to each of its ends. Point mutations in *rpoS* were targeted with three-piece SOE with slight modification. Primers did not contain an additional 20-23 bp homologous nucleotide sequence. The desired point mutations were embedded into middle piece primer

sequences. The upstream reverse primer and downstream forward primer were completely homologous to the middle piece primers. The resulting nucleotide sequence was confirmed by Sanger sequencing. Complementation constructs were also constructed with three-piece SOE and replaced the *dns* 5' UTR and open reading frame with that of the gene of interest, as previously described [96]. All primers are listed in Table A3.2 and all PCRs were run with Phusion Plus Polymerase (Thermo Scientific) according to manufacturer's protocols. Products were visualized on 1.5 % agarose gels using Midori Green (Bulldog Bio). Amplicons were purified with QIAquick PCR purification Kit (Qiagen) and added together in and equal concentration, 50 ng each, as the template DNA for SOE PCR. SOE PCR was run as described [96]. SOE products were gel purified with QIAquick Gel Extraction Kit (Qiagen) and used in transformations.

Vibrio natriegens pMMB*tfox* was used as the parent strain for Multiplex Genome Editing by Natural Transformation (MuGENT) and transformations were performed as previously described [32]. The selectable markers conferred erm^R or $spec^R$ and inserted into a prophage region on Chromosome1 [96]. Strains containing multiple edits were constructed through iterative rounds of MuGENT that exchanged the antibiotic markers to maintain selection of transformants. Δ*katG* and Δ*oxyR* mutants were selected on plates containing appropriate antibiotic and 1 mM sodium pyruvate (Sigma Aldrich) to scavenge any hydrogen peroxide in the agar [97-99] that may hinder growth of the mutants. Colonies isolated from natural transformation were stored at –80° C in 96-well microtiter plates [96]. Incorporation of the non-selective tDNA (transforming DNA) was verified by additional PCRs targeting amplification of the mutation site. Notably, incorporation of the *rpoS* SOE construct generates single nucleotide changes that would not be detectable by PCR amplicon size. Instead transformants were screened by bubbling assay (see below) and/or Sanger sequencing. Sanger sequencing was performed by the UT Genomics Core or Eurofins Genomics.

Cell viability and hydrogen peroxide (HOOH) assays

Parental and mutant strains of *V. natriegens* were assayed for cell viability and ability to degrade hydrogen peroxide (HOOH). Strains were inoculated from frozen stocks and incubated overnight in MHM with 1 % carbon (acetate or glucose, as

indicated). Cultures were diluted 1:100 and grown again for 20-22 hours. 2 mL of overnight cells were pelleted and resuspended three times in fresh medium matching experimental conditions before being inoculated into 5 mL cultures. Importantly, ampicillin was not added to HOOH degradation assays as it has been found to quench chemiluminescent signal [100], which was corroborated here as seen in Figure A3.10. HOOH measurements were performed on the Orion-L Luminometer with an acridinium ester chemiluminescent method [101]. Cell abundances were monitored by viable count assay on YTSS plates (per L: 5 g tryptone, 2.5 g yeast extract, 15 g Sigma Aldrich sea salts, 12 g agar), supplemented with 1 mM sodium pyruvate.

To screen for catalase activity *via* bubbling (O_2 production), frozen stocks were streaked onto YTSS agar plates and incubated at 30° C overnight. Single colonies were picked with sterile toothpicks are transferred to a new YTSS agar plate. Plates were incubated for 48 hours at 30° C, then 30 % HOOH (Fisher Scientific) was spotted onto the bacterial colonies. Notably, the incubation time of 48 hours was critical to observe bubbling.

Biofilm assays

Overnight cultures were grown as indicated above. Biofilm assays were setup as previously described [102]. Briefly, overnight cultures were diluted 1:100 directly into microtiter plate wells containing 99 μL of medium. Strains assayed for their ability to form biofilms in the presence of HOOH were supplemented with ~ 1500 nM HOOH at the start of the experiment. Plates were incubated statically for 24 hours at 30° C. Biofilm disruption by HOOH was assayed by allowing microtiter plates to incubate statically at 30° C for 24 hours prior to the addition of ~ 1500 nM HOOH. Plates were incubated an additional 24 hours after HOOH addition. After incubation liquid medium and planktonic cells were removed from wells by inverting plates onto paper towels and briskly tapping. 125 μL of 0.1 % crystal violet was added to wells and allowed to incubate for 10-15 minutes at room temperature. Crystal violet was gently rinsed from wells by four successive rinses in larger beakers of water, gently shaking water out of wells between each rinse. After the final rinse and shake step, plates were briskly tapped on paper towels to remove as much remaining water from the wells as possible. Plates were

allowed to air-dry for at least 24 hours. To resuspend crystal violet, 200 μL of 95 % ethanol was added to wells and incubated at room temperature for 10-15 minutes. OD600 was measured with a Bio Tek Cytation 5 Cell Imaging Multimode Reader (Agilent, Santa Clara, CA.) Clara, CA.)

Enumeration of *katG* and *katE* homologs

RefSeq proteomes were downloaded (Attachment 3.1 csv; remote_assemblies.csv) and hmmsearch, version 3.3.2, was used to search all proteomes for catalase (PFAM ID: PF00199.22) and peroxidases (PF00141.26) with gathering cutoffs. Data was filtered by phylum or genus to pull out Proteobacteria, *Vibrio spp.* and *Aliivibrio spp.* hits. The number of uniquely identified targets of KatE (PF00199.22) and KatG (PF00141.26) per organism accession were quantified. Values for bubble plots were generated by determining the ratio of KatE and KatG hits per organism and summing the number of organisms that fell into each numerical combination.

Percent identity matrix

To compare the KatG sequences of *V. natriegens* ATCC 14048 a percent identity matrix of KatG1 (WP_020334780.1), KatG2 (WP_020335989.1), and KatG3 (WP_020333524.1) amino acid sequences was generated using Clustal Omega v2.1.

Taxonomic relationships with genus *Vibrio* using *16S rRNA*

To elucidate taxonomic relationships within the genus *Vibrio* a *16S* phylogeny was produced using 16S sequences curated by Refseq [103]. Sequences were downloaded, collapsed at 100% using CD-HIT v. 4.8.1 [104], and all partial 16S sequences or sequences including unresolved nucleotides (*i.e.*, "N") were removed giving a total of 177 sequences. Sequences were aligned in MAFFT v7.310 [105] with default parameters and 500 iterations. Alignment trimming was conducted using trimAl v1.4.rev15 with these gappyout algorithm [106], producing an alignment of 1430 bp. IQ-TREE v2.2.2.3 was used to produce a tree (1000 bootstrap replicates) using the built in model test selection [107]. Based on BIC (Bayesian Information Criterion), a time dependent model with invariable sites and a gamma distribution with 4 discrete categories (*i.e.*, TIM3e+I+G4) was chosen. The resulting tree was based on an alignment

of 1110 constant sites, 277 parsimoniously informative sites, and 93 singleton sites. The tree was visualized using iTol online tool with modifications [108].

KatG based phylogeny tree

Refseq proteomes under the taxonomic ID 662 (Attachment 3.2.csv; remote_assemblies_TAXID662.csv) were downloaded and KatG sequences were identified as described above. Sequences were manually curated to remove partial sequences (number of sequences = 2189). Alignment and tree production was conducted in the same way as described above (*16S rRNA* gene tree), producing a protein alignment of 841 positions, with 177 constant sites, 576 parsimoniously informative sites, and 88 singleton sites. A JTT+I+G4 phylogenetic model was chosen (*i.e.,* protein time dependent model), and the resulting tree was again visualized using iTol with modifications [108].

Results

***V. natriegens* tolerance to hydrogen peroxide**

Total coastal abundances of *Vibrio spp.* have been reported as $10^2 – 10^5$ cells/mL [109], and measurements of HOOH in coastal and brackish waters range from 0.1 nM – 4.5 μM [110]. We therefore investigated responses of *V. natriegens* to HOOH amendments with inocula and HOOH concentrations within these ranges. In Minimal Marine Heterotroph Medium (MHM) + 1 % glucose, exposures up to 800 nM HOOH caused no change in growth rate or yield for the *V. natriegens* type strain ATCC 14048 (Figure 3.1A). However, cultures exposed to 10 μM and 200 μM experienced an initial lag or decrease in cell abundance, respectively, though they eventually recovered, and final cell abundances for all HOOH treatments matched the unamended control at ~5 x 10^8 CFU/mL (Figure 3.1A). Growth of the cultures was concurrent with degradation of HOOH over time (Figure 3.1B). Notably, growth on 1 % glucose resulted in a decrease in pH (5-5.5) but did not contribute to cell mortality over the course of the 13 hour assay (Figure 3.1A). This pH drop likely occurred from fermentation of the glucose, yielding organic acids (sometimes referred to as overflow metabolism [22, 29]) that overwhelmed the medium buffer (1mM TAPS, kept low to prevent interference with our HOOH detection method).

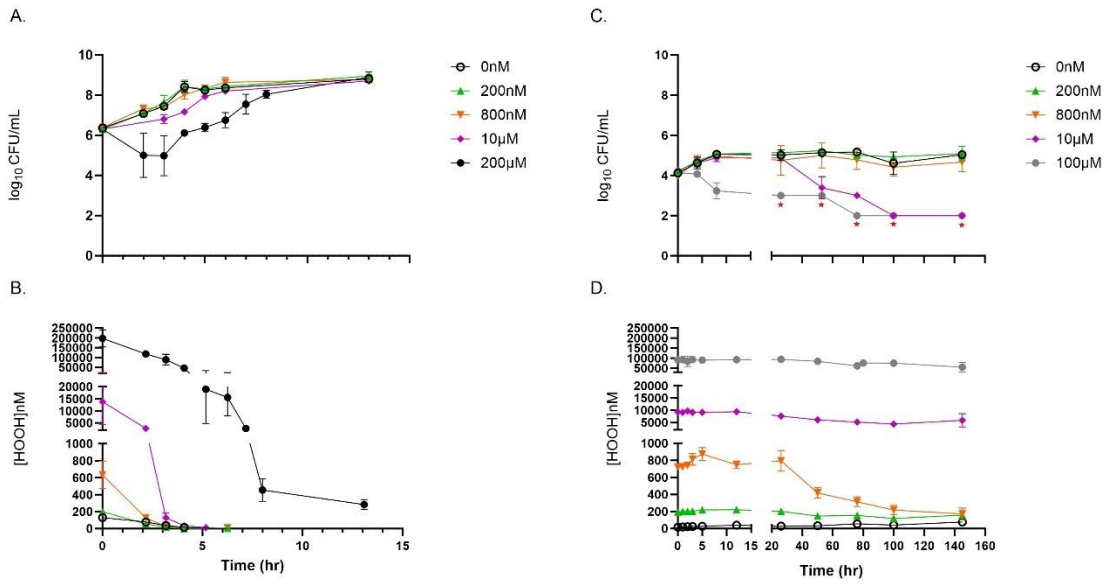

Figure 3.1 *Vibrio natriegens* tolerance to hydrogen peroxide. (A) Cell viability and (B) HOOH degradation of *Vibrio natriegens* ATCC 14048 in MHM + 1 % glucose (1 mM TAPS). (C) Cell viability and (D) HOOH degradation of *Vibrio natriegens* ATCC 14048 in MHM + no carbon (n=3; ± SD of the geometric mean). Red stars indicate measurements fell below the limit of detection.

The above experiments characterized the response of V. natriegens with replete organic carbon. To simulate resource-limited conditions that V. natriegens may experience in coastal and brackish waters, we repeated the HOOH exposures in MHM medium lacking additional carbon input and thus restricting growth to the trace organic contaminants of the artificial medium [44]. When exposed to 0, 200, or 800 nM HOOH, final cell densities reached ~10^5 CFU/mL (Figure 3.1C). Notably, degradation of 800 nM HOOH began after ~24 hours and continued until ~145 hours (Figure 3.1D). Exposure to 10 or 100 μM HOOH resulted in a loss of cell abundance below the limit of detection (<100 cells/mL) (Figure 3.1C). This corresponded with little to no measurable degradation of HOOH (Figure 3.1D). Importantly, limiting carbon availability achieved conditions where *V. natriegens* cells were resistant to ecologically relevant levels of HOOH (0 – 800 nM) but became sensitive at relatively high concentrations (10 – 100 μM). These results suggest growth substrate and/or cellular abundance influence the response of *V. natriegens* to HOOH and help to constrain conditions which detect a sensitivity to HOOH.Richness of oxidative stress response enzymes in *V. natriegens*

Richness of oxidative stress response enzymes in *V. natriegens*

The robust response of *V. natriegens* to hydrogen peroxide prompted us to explore the genetic underpinnings of its oxidative stress response, beginning with catalase. Diversity and richness of oxidative stress response enzymes can vary widely across bacterial phyla [80, 111]. Strikingly, three copies of *katG* are annotated on Chromosome 2 of *V. natriegens* ATCC 14048. Studies of other *Vibrio spp.* have similarly found two copies of *katG* or *katE* [92, 94]**,** but to our knowledge this is the first report of a *Vibrio spp.* with over two copies of *katG.* To determine how widespread or unique this characteristic is, we quantified the number of KatG (PF00141.26) and KatE (PF00199.22) homologs in Proteobacterial species and within *Vibrio* and *Allivibrio* species using available RefSeq proteomic sequence data.

Analysis of Proteobacterial species revealed a wide distribution in the number of KatE and KatG homologs per proteome, reaching up to nine KatE copies and five KatG copies in a single species (Figure A3.1). However, most organisms contained only 1 – 2

copies of each enzyme. A notable trend was the decline in copy number of KatE or KatG when the copy number of the other enzyme (KatE or KatG) increased. For example, KatG copies rarely exceeded three, when the number of KatE homologs were greater than or equal to two, and KatE copies rarely exceeded two, when the number of KatG homologs were greater than or equal to three (Figure A3.1). *Vibrio* and *Allivibrio* species data shared this trend on a smaller scale. The number of KatE and KatG homologs per proteome ranged between 1 – 3, with most species containing a single copy of one or both enzymes (Figure 3.2). *V. natriegens* has three copies of KatG and zero copies of KatE. Only one other species fell into this category which was identified as *Vibrio nitrifigilis*.

Diversity of Genus *Vibrio* KatG protein sequences

We named the three *katG* genes of *V. natriegens "katG1", "katG2",* and *"katG3"* based on their relative positions from the origin on reference genome (NCBI Refseq accession NZ_CP016346: locus tags BA890_RS15465, BA890_RS16825, and BA890_RS19750, respectively). We next performed sequence and phylogenetic analyses to gain insight into the molecular diversity of *V. natriegens'* KatG enzymes. First, protein sequence alignments of KatG1 (WP_020334780.1), KatG2 (WP_020335989.1), and KatG3 (WP_020333524.1) revealed that KatG2 and KatG3 share the highest amino acid percent identity at 88.93%, while KatG1 shares 80.36% and 78.67% amino acid identity with KatG2 and KatG3, respectively (Table 3.1). These results indicate a particularly high divergence of KatG1 with KatG2 and KatG3.

Next, to gain insight into the evolution of KatG proteins among *Vibrio spp*. a phylogenetic tree was constructed based on a manually curated set of KatG protein sequences (Figure 3.3). Sequences were collapsed at 100% and each branch represents a unique KatG sequence. Twelve species were identified with greater than one phylogenetically distinct KatG sequence. The divergence of KatG sequences within a single species can be observed by the distance between individual or clusters of KatG sequences from the same species, denoted by color strips (Figure 3.3). As a general trend, KatG sequences from different species are more closely related than KatG's within the same species or even closely related species (the latter indicated by comparison to the

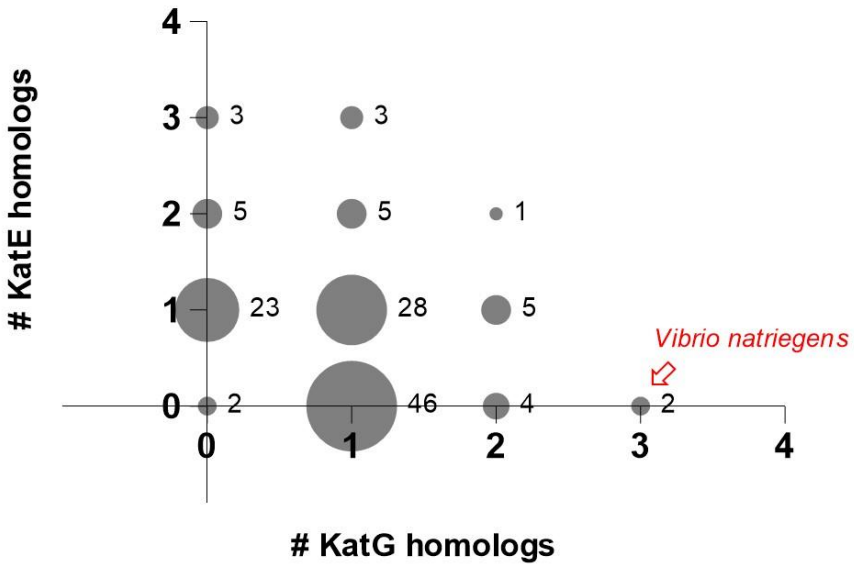

Figure 3.2 Enumeration of KatE (PF00199.22) and KatG (PF00141.26) within *Vibrio spp.* and *Aliivibrio spp.* proteomes (Refseq proteomes accessed February 2022).

Table 3.1 Clustal Omega alignment percent identity matrix of *Vibrio natriegens* ATCC 14048 KatG amino acid sequences. KatG1 = WP_020334780.1, KatG2 = WP_020335989.1, KatG3 = WP_020333524.1.

	KatG1	**KatG2**	**KatG3**
KatG1	100	80.36	78.67
KatG2	80.36	100	88.93
KatG3	78.67	88.93	100

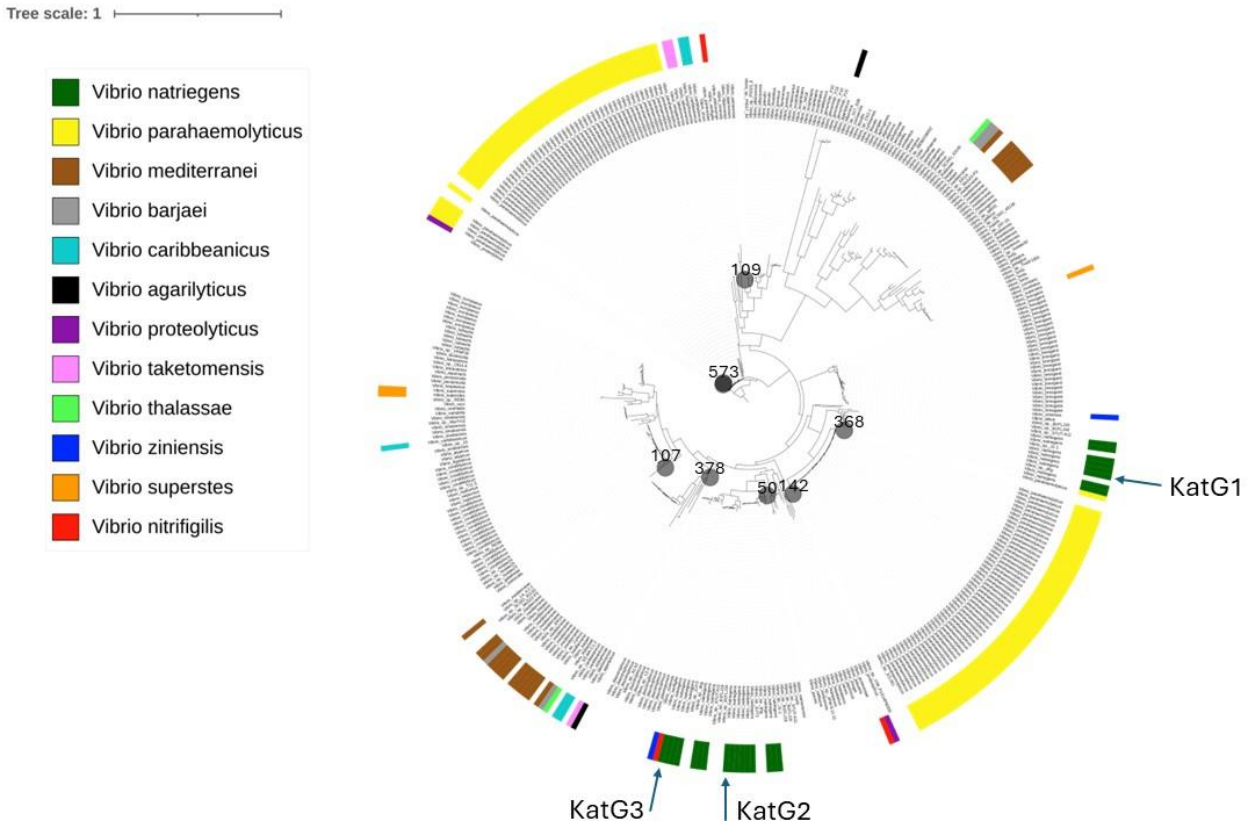

Figure 3.3 *Vibrio spp.* KatG based phylogeny. Species containing greater than one KatG (PF00141.26) copies are indicated by color strips. *V. natriegens* ATCC 14048 KatG proteins indicated by blue arrows (KatG1 = WP_020334780.1, KatG2 = WP_020335989.1, KatG3 = WP_020333524.1.). Collapsed branches are represented by grey circles.

16S rRNA gene tree (Figure A3.2). However, the sequence similarity and close phylogenetic distance between KatG2 and KatG3 in *V. natriegens* suggests recent duplication and divergence events was responsible for the establishment of the three KatG copies in this species (Figure 3.3). The unusual array of catalase-peroxidases within *V. natriegens* prompted a genetic analysis of their functions and regulation.

Impact of growth phase on Δ*katG* mutant responses to HOOH

Single, double, and triple Δ*katG* mutants were constructed to assess the role of each *katG* gene product under different nutrient conditions and exposures to HOOH. Importantly, mutant strains did not exhibit defects in growth rate or yield in the absence of HOOH (Figure A3.3).

The protective role of each *katG* gene of *V. natriegens* was assessed during lag, exponential growth, and early stationary phase in MHM + 24 μM acetate medium. This medium enabled growth via aerobic respiration to final yield of ~10^6 cells/mL. Parental and Δ*katG* strains were first grown for 24 hours in MHM + 1 % acetate, then washed and inoculated at ~10^3 cells/mL in MHM + 24 μM acetate with or without HOOH amendment. Mutants lacking one, two, or three *katG* genes exhibited no defects in growth or HOOH degradation during lag and exponential growth phase when exposed to 1400 nM HOOH (Figure A3.4). Notably, for all strains significant HOOH degradation did not occur within the first nine hours of growth but degradation was complete by 30 hours, after significant population growth and entry into stationary phase occurred.

To investigate the HOOH dynamics in stationary phase specifically, cultures were inoculated in MHM + 24 μM acetate as before, but not exposed to 1400 nM until 24 hours post inoculation. All genotypes experienced an order of magnitude drop in viable counts during the first 24 hours of stationary phase, even the parental strain without the HOOH amendment (Figure 3.4A and 3.4C). After this initial decline, viable counts stabilized for the parental strain and all *katG* mutants including the triple deletion, showing no clear protective effect for any of the *katG* copies.

However, significant differences were observed in HOOH degradation rates for some mutants during this stationary phase period (Figure 3.4B and 3.4D). The Δ*katG2*

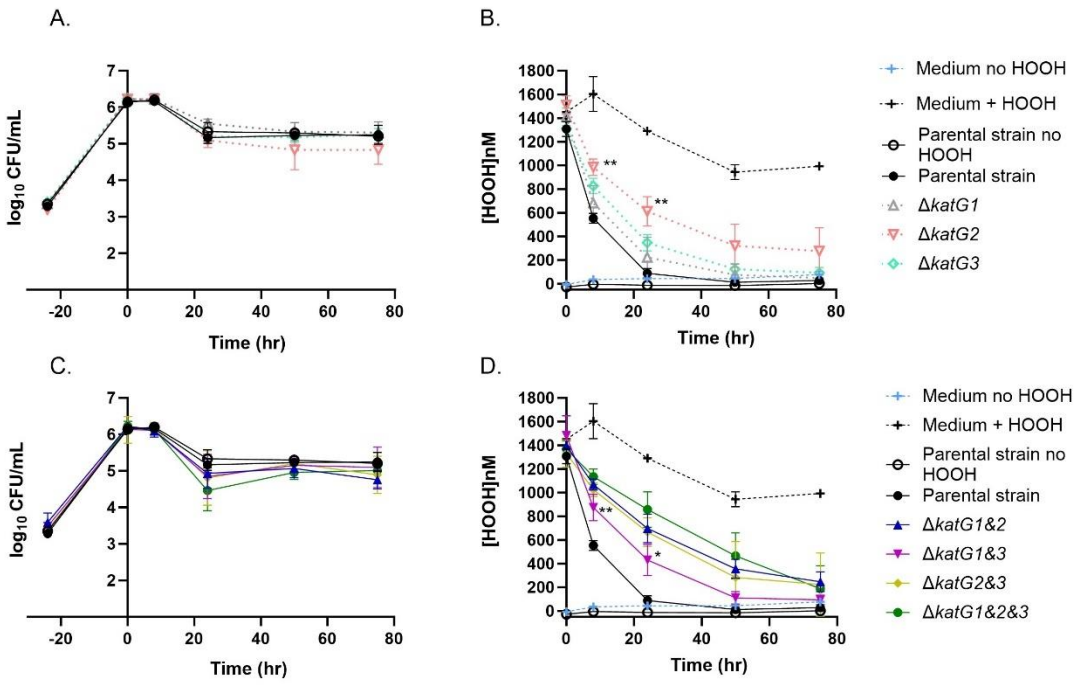

Figure 3.4 (A and C) Cell viability and (B and D) HOOH degradation by *V. natriegens* parental and mutant strains in MHM + 24 μM acetate, (n=3; ± SD of the geometric mean). HOOH exposure at time 0, cells in stationary phase. P-values were calculated using One-way ANOVA multiple comparisons with Dunnet's correction, * $P \leq 0.05$, *** $P \leq 0.001$: (B) Single *katG* deletions compared to parent strain, (D) double deletions compared to triple *katG* deletion.

strain (EZ265) had significantly decreased ability to degrade HOOH at early time points (Figure 3.4B). While not significant, this trend continued through later time points and Δ*katG2* cultures ended with higher HOOH concentrations. Likewise, differences between the parental and Δ*katG1* (EZ264) or Δ*katG3* (EZ266) strains were non-significant, however, early time points trend with higher HOOH concentrations.

To assess the contribution of each individual *katG* gene to HOOH degradation, *katG* double knockouts were compared to the triple mutant lacking all *katG* copies. As for the single knockouts above, there was a trend with all *katG* double knockouts, where HOOH degradation was higher due to the presence of a *katG* gene. However, only Δ*katG1&3* (EZ268) differed significantly from Δ*katG1&2&3* (EZ270), and only at early time points (Figure 3.4D). This indicates that KatG2 significantly contributes to HOOH degradation under these conditions. Together, the results from all mutant genotypes suggest that all three KatG's and especially KatG2 are active and degrade HOOH during stationary phase. Notably, the triple mutant lacking all three KatG's maintained significant HOOH degradation activity, suggesting peroxidases are also functioning under these early stationary phase conditions.

Exposing *V. natriegens* to extended stationary phase revealed a greater dependency on the three catalase-peroxidases for survival. In this variation of the experiment, cells from the stationary phase cultures grown in MHM + 1% acetate were inoculated into MHM without a carbon source and incubated 24 hours prior to the 1400 nM HOOH addition. Similar to early stationary phase, the parental strain was completely resistant to the HOOH exposure in extended stationary phase conditions (Figure 3.5A), but in distinction did not completely remove HOOH from the medium and left ~400 nM behind (Figure 3.5B). In contrast to the phenotype in early stationary phase exposure (Figure 3.4D), the triple *katG* mutant exhibited no ability to remove HOOH during extended stationary phase, suggesting that the catalase-peroxidases were the only enzymes that could scavenge exogenous HOOH during prolonged starvation (Figure 3.5D).

During extended stationary phase conditions two of the *katG* genes were functional and contributed to survival of HOOH exposure. Cells lacking *katG2* (*katG1+*

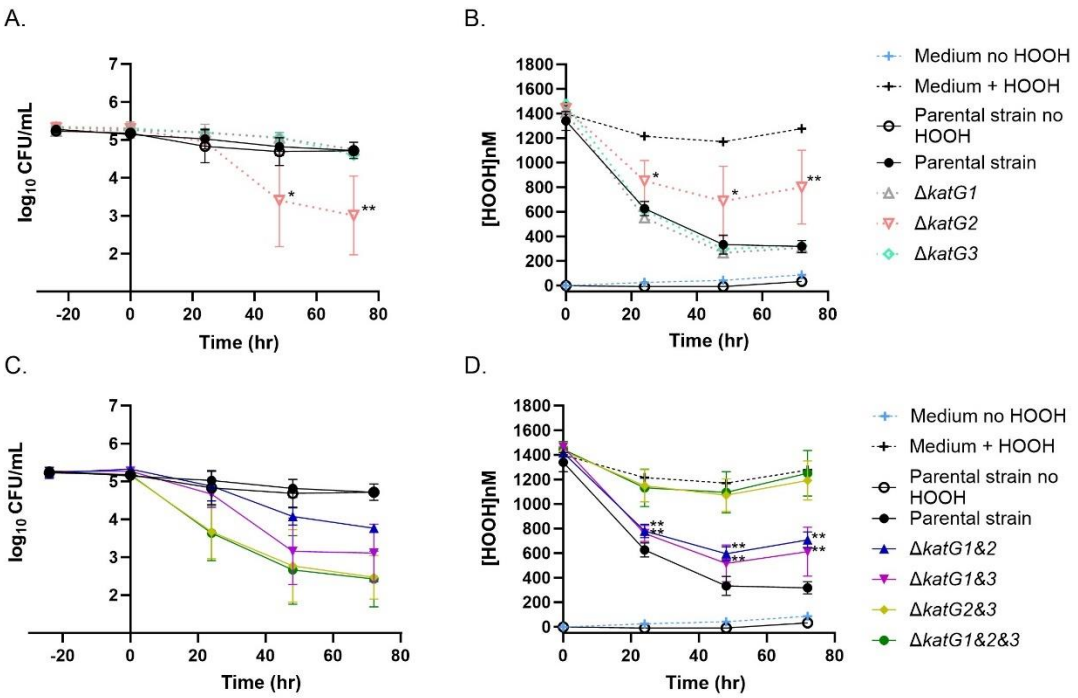

Figure 3.5 (A and C) Cell viability and (B and D) HOOH degradation by *V. natriegens* parental and mutant strains in MHM + no carbon, (n=3; ± SD of the geometric mean). HOOH exposure at time 0, after 24 hours of starvation. P-values were calculated using a One-way ANOVA multiple comparisons with Dunnet's correction, * $P \leq 0.05$, ** $P \leq 0.01$: (B) single *katG* deletions compared to parental strain, (D) double *katG* deletions compared to triple *katG* deletion.

and *katG3+*) exhibited slower HOOH decay and a decline in cell viability by 48 hours post exposure (Figure 3.5A and 3.5B). Cells lacking *katG1* and *katG2* (*katG3+*), and cells lacking *katG1* and *katG3* (*katG2+*) had lower HOOH decay and higher death compared to the parental strain, but significantly higher HOOH decay and less death than the triple mutant lacking all catalases. In contrast, cells lacking *katG2* and *katG3* (*katG1+*) were indistinguishable from the triple mutant, suggesting it is not contributing to HOOH removal and cell survival under these conditions (but see section on *rpoS*, below). However, comparison of Δ*katG3* (*katG1+* and *katG2+*) to Δ*katG1&3* (*katG2+*) suggests that the presence of *katG1* does improve cell viability and HOOH degradation when working in combination with *katG2*. Notably, these results demonstrate that during nutrient starvation any single *katG* gene is insufficient to maintain parental levels of cell viability or HOOH degradation.

Impact of HOOH on biofilm formation and disruption

V. natriegens readily forms biofilms in microtiter well assays (Figure A3.5), so the effects of HOOH and HOOH scavenging enzymes during and after biofilm formation was assessed. To assess if HOOH would disrupt biofilm formation, cells were inoculated into wells containing MHM + 24 μM acetate + 1500 nM HOOH and biofilms were stained with crystal violet after 24 hours of incubation. No significant difference was observed between the parental strain or Δ*katG1&2&3* with and without HOOH. However, there was a significant increase between the parental strain and Δ*katG1&2&3* both with HOOH (Figure A3.5A).

Following indication that early and prolonged stationary phase mutant cells were more sensitive to HOOH in liquid cultures, the ability of HOOH to disrupt established biofilms was examined. Cells were diluted into MHM + 24 μM acetate or MHM with no carbon source and incubated for 24 hours. HOOH was added, the plates were incubated an additional 24 hours before being stained. No significant differences were observed in crystal violet staining between parental and Δ*katG1&2&3* mutant (Figure A3.5B and A3.5C).

***Vibrio natriegens* oxidative stress response regulators OxyR and RpoS**

Due to the variation observed in HOOH degradation capabilities of *V. natriegens' katG* genes, we sought to investigate potential regulatory mechanisms. First, we examined mutants lacking OxyR, a transcription factor known to regulate oxidative stress response genes in other species [41, 55] including *katG* in *V. parahaemolyticus* [94]. Our prior work indicated *oxyR* mutants of *V. natriegens* are sensitive to HOOH [96], and we hypothesized some or all of this sensitivity could be due to dysregulation of the *katG* genes.

Here, *ΔoxyR* (EZ274) and Δ*oxyR&katG1&2&3* (EZ275) strains were exposed to HOOH during different growth phases and under extended stationary phase conditions as described above. Like *ΔkatG* strains, Δ*oxyR* mutants were not impacted during lag or exponential growth in MHM + 24 μM acetate + 1400 nM HOOH (Figure 3.6A and 3.6B). When HOOH was added in early stationary phase, mutants demonstrated reduced HOOH degradation compared to the parental strain (Figure 3.6C and 3.6D). Notably, HOOH degradation was slightly greater in Δ*oxyR* than Δ*oxyR&katG1&2&3* suggesting OxyR may regulate other HOOH degrading enzymes in addition to the catalase-peroxidases. HOOH addition during extended stationary phase conditions led to decreased cell viability below the limit of detection (Figure 3.6E), and little to no HOOH degradation by either mutant (Figure 3.6F). Notably, this was a more dramatic loss in cell viability compared to Δ*katG1&2&3* (*oxyR*+) (Figure 3.6E).

RpoS is a sigma factor and global regulator of stress response and stationary phase genes and it is known to regulate *katG* in other species [94, 112]. Considering the results above demonstrated that loss of *katG* genes in *V. natriegens* was most critical during early and prolonged stationary phase conditions, we next wanted to examine the role of *rpoS*. However, *Vibrio natriegens* ATCC 14048 (EZ260), from which all strains in this study were derived, was found to contain two single nucleotide polymorphisms in *rpoS* relative to published NCBI accessions (e.g. NZ_CP160345 and NZ_CP009977): a nonsense mutation relatively early in the open reading frame (E71→ *, GAA→TAA) and a missense mutation (N123 → I, AAC → ATC) (Raphael, Slimak and Slonczewski, pers. comm.). Based on the sequence provided on the ATCC website (sequenced August 27,

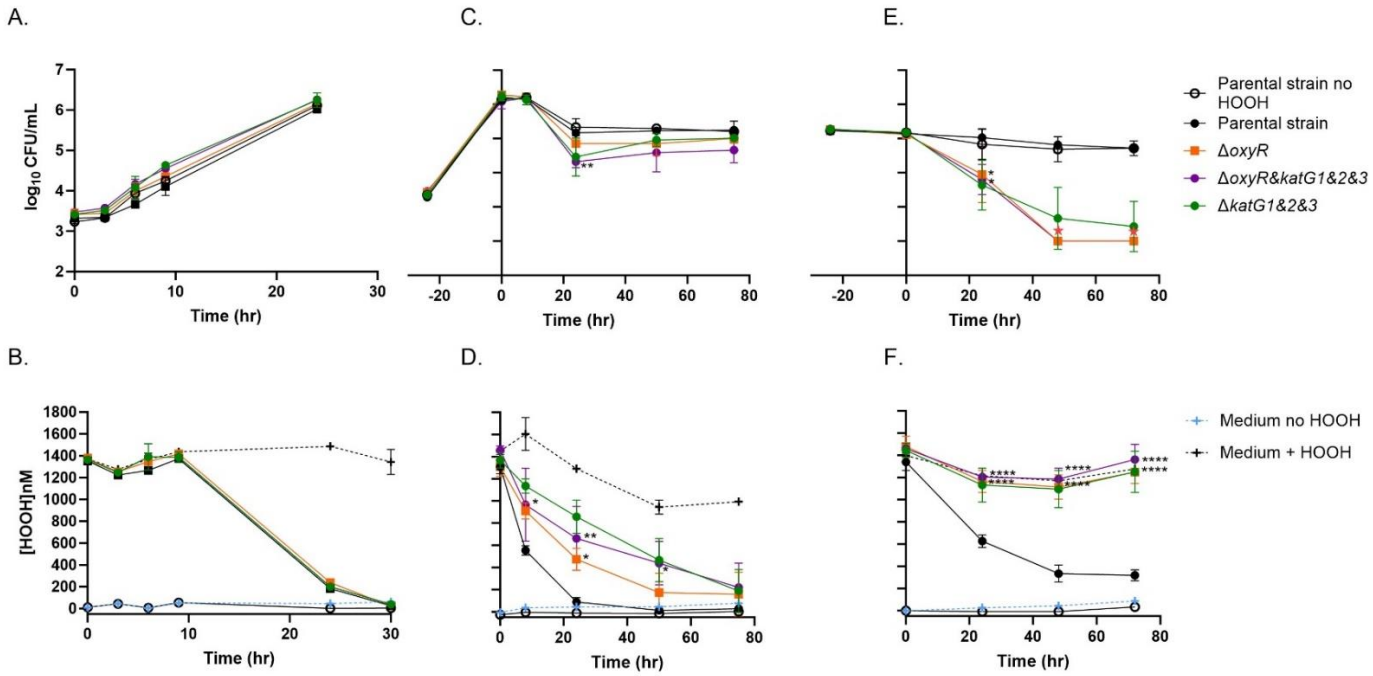

Figure 3.6 (A, C, and E) Cell viability and (B, D, and F) HOOH degradation of *V. natriegens* parental and Δ*oxyR* mutants, (n=3; ± SD of the geometric mean). HOOH exposure during (A and B) lag, (C and D) stationary, and (E and F) starvation. Red stars indicate viable count measurements fell below the limit of detection. P-values were calculated using a One-way ANOVA multiple comparisons test with Dunnett's correction, * $P \leq 0.05$, ** $P \leq 0.01$, **** $P \leq 0.0001$: *oxyR* deletions compared to parental.

2019), the polymorphisms in our parental strain were present when the strain was purchased. Hypothesizing that the nonsense mutation likely rendered RpoS null in our strains we constructed various combinations of the two polymorphisms. Our studies on HOOH decay, discussed below, indicate that the "true" wildtype *rpoS* allele – that maximizes HOOH decay – is neither the NCBI nor the ATCC allele, but rather a combination of E71 + I123 (Figure A3.6).

During strain construction we noted that only the combination of E71 + I123 provided maximal "bubbling" (*i.e.*, oxygen generation via catalase activity) when HOOH was pipetted onto colonies (Attachment 3.3.mp4, Figure A3.7, and see Materials and Methods). The NCBI allele E71 + N123 provided marginal bubbling and the ATCC allele of *71 + I123 provided almost no bubbling. These bubbling phenotypes correlate with the phenotypes in liquid culture (see below). Hence, we denote E71+I123 as WT *rpoS*.

Next, we repeated the HOOH exposure during extended stationary phase experiments with the E71+I123 (WT) allele and E71+N123 allele of *rpoS*. Parental with WT *rpoS* cultures fully degraded the HOOH and showed no loss in viable counts (Figure 3.7A and 3.7B), the former result an improvement compared to the nonsense *rpoS* mutant (Figure 3.5B). In the WT *rpoS* background, survival during HOOH exposure improved for the *katG* triple mutant but still showed significant loss in viable counts by the end of incubation (Figure 3.7A). Presence of any of the three *katG* genes significantly improved viability, indicating they all played a protective role in this condition (Figure 3.7A).

Importantly, *rpoS* allelic state had a significant impact on the activity of the KatG1 enzyme when working in solo. This is evident by the significant decay of HOOH in the restored wild type *rpoS* background (Figure 3.7B) compared to non-decay in the nonsense mutant background (Figure 3.5D) for the Δ*katG2&3* double mutant. Of note, Δ*katG2&3 rpoS*E71N123 demonstrated slower HOOH degradation than Δ*katG2&3 rpoS*E71I123 (WT), consistent with the bubbling assay.

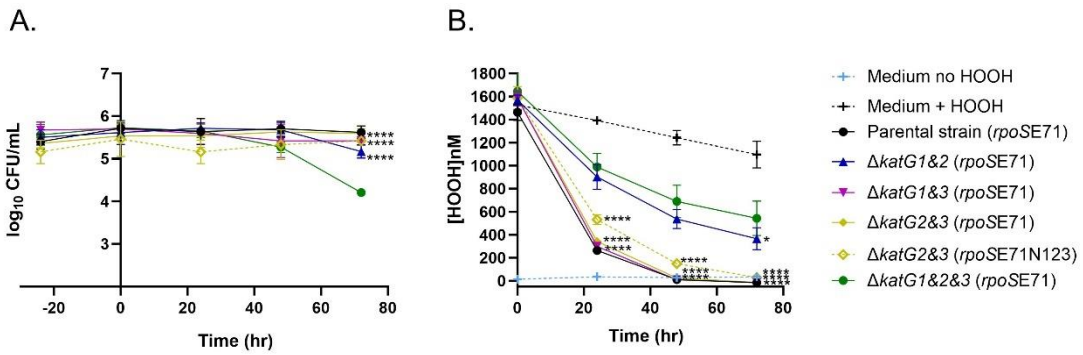

Figure 3.7 (A) Cell viability and (B) HOOH degradation by *V. natriegens* parental and mutant strains with indicated *rpoS* alleles (n=3; ± SD of the geometric mean). HOOH exposure at time 0, after 24 hours of starvation in MHM + no carbon. P-values were calculated using a One-way ANOVA multiple comparisons test with Dunnett's correction, * $P \leq 0.05$, ** $P \leq 0.01$, **** $P \leq 0.0001$: double *katG* deletions compared to triple *katG* deletion.

HOOH degradation by solo *katG2* (*i.e.*, Δ*katG1&3*) was improved in the *rpoS* WT background and was indistinguishable from the *rpoS* WT strain containing all three *katG* genes (Figure 3.7B). In the *rpoS* WT background, HOOH degradation by solo *katG3* (*i.e.*, Δ*katG1&2*) showed marginal improvement relative to the triple *katG* mutant that was less pronounced than in the *rpoS* nonsense mutant background (Figure 3.5D). Finally, we noted greater degradation of HOOH by Δ*katG1&2&3* in WT *rpoS* (Figure 3.7B) than in the nonsense *rpoS* background (Figure 3.5D), consistent with RpoS control of HOOH-degrading enzymes other than the three KatG's.

Phenotypic complementation of *katG1, katG2,* or *katG3* deletion was tested by placement of a WT gene copy with native promoter on the chromosome rather than on a multicopy plasmid; this was done to minimize artefactual elevated activity due to overexpression of any one of these single copies of *katG*. Copies were inserted ectopically into the *dns* locus of Δ*katG1&2&3 rpoS*E71I123 creating strains with single *katG* genes in one copy per chromosome; Δ*katG1&2&3 rpoS*E71I123 *Δdns:: katG1* (EZ310), Δ*katG1&2&3 rpoS*E71I123 *Δdns:: katG2* (EZ311), and Δ*katG1&2&3 rpoS*E71I123 *Δdns:: katG3* (EZ312). HOOH exposure during prolonged stationary phase was performed with the complement strains, each demonstrated successful restoration of HOOH degradation and complementation of the *katG* genes (Figure A3.8).

Discussion

This study examined the oxidative stress response of *V. natriegens* ATCC 14048 under ecologically relevant conditions. The presence of three catalase-peroxidase genes (*katG1,2,3*) is rare amongst *Vibrio* species and likely a consequence of two independent acquisition events followed by a duplication and divergence of one of the acquired copies. All three *katG* genes are conditionally required for full protection during early and prolonged stationary phase conditions but are dispensable during exponential growth or under biofilm conditions. Both OxyR and RpoS regulons are likewise involved in stationary phase HOOH survival but dispensable during growth in the presence of this ROS. This work also led to the identification of two different *rpoS* point mutations in frequently cited laboratory strains of ATCC 14048 *rpoS* and we show that both

negatively impact catalase activity. Notably, we infer that the true wildtype sequence of *rpoS* contains a glutamic acid (E) at position 71 and an isoleucine (I) at position 123.

The presence of multiple catalases per genome is common in Proteobacterial and *Vibrio* species (Figure 3.2 and Figure A3.1) but in most cases this involves a combination of *katG* (bifunctional catalase-peroxidase) and *katE* (monofunctional catalase) versions of the enzyme. Why *V. natriegens* took the rare evolutionary pathway of acquiring three copies of *katG* (and no *katE*'s) is a matter of speculation. However, if we assume selection rather than drift as the evolutionary driver, we suspect that the dual activity of the *katG*'s provide greater fitness to *V. natriegens* in its native environment. The peroxidase function of *katG* has a higher substrate affinity than catalase and can thus mitigate lower levels of peroxide stress where the catalase reaction can stall [81]. For *V. natriegens* which resides in coastal and estuarine environments where peroxide levels are often in the nanomolar range, this may provide an advantage. Finally, a scenario can be imagined that necessitates the acquisition of three *katG* genes. We demonstrate that with a nonsense *rpoS* mutation, any singular *katG* was not sufficient to protect cell viability. Additionally, single *katG* deletions demonstrated that *katG2* was especially critical to maintain cell viability. Therefore, if *V. natriegens* once possessed only *katG1* and *katG3*, a *rpoS* mutation could become detrimental to survival during oxidative stress. This would provide a need for a third *katG* gene (*i.e., katG2*).

We determined that the *katG* genes as well as the global regulators *oxyR* and *rpoS* are dispensable for HOOH resistance during exponential growth in liquid batch cultures and biofilm formation. Interestingly, planktonic cell cultures exposed to HOOH during lag phase demonstrated unaltered growth and complete HOOH degradation by 30 hours. Although cell growth appeared normal during the first nine hours after inoculation of batch cultures, there was a curious absence in HOOH degradation during this time. It is possible that actively growing and dividing cells of *V. natriegens* mitigate damage through other means such as DNA repair mechanisms and/or asymmetric division of damage to daughter cells [113, 114]. This would explain why growth was not impacted although HOOH was not being degraded.

We recently reported that a *V. natriegens* mutant lacking *oxyR* is sensitive to HOOH [96], consistent with its function in other species. This study extends that initial observation and shows that the OxyR regulon contributes to HOOH degradation during stationary phase (Figure 3.5). *In silico* analysis of the *oxyR* regulon using Virtual Footprint [115] and the *oxyR* (MX000154) matrix predicts *oxyR* binding sites upstream of promoters for several enzymes capable of degrading HOOH: glutathione peroxidase (locus tag BA890_RS21710; Chr. 2), AhpC and AhpF (locus tags BA890_RS19985 and BA890_RS19990; Chr.2), and importantly all three KatG's: *katG1* (-75 to -61), *katG2* (-164 to -150 and -269 to -255), and *katG3* (-258 to -272) (Figure A3.9). The existence of a greater *oxyR* regulon beyond the three catalases is supported by our finding during prolonged stationary phase that Δ*oxyR* had a greater sensitivity to HOOH than *oxyR*$^{+}$ Δ*katG1&2&3* (Figure 3.5E). Importantly, OxyR binding sites are not predicted for the Dyp-type peroxidase (locus tag BA890_RS10740; Chr.1), and thioredoxin-dependent thiol peroxidase (locus tag BA890_RS10800; Chr. 1). These putative OxyR-independent enzymes could account for the complete HOOH degradation by the Δ*oxyR&katG1&2&3* mutant (Figure 3.5B). A more extensive genome search for antioxidant genes and an in-depth study of the *oxyR* regulon is needed to confirm these predictions.

The analysis of the regulatory role of RpoS was complicated by the presence of a pre-existing null mutation within *rpoS* in our copy of the ATCC 14048 type strain. Reconstruction of the wild type *rpoS* allele – as assessed by HOOH degradation activity - indicated a clear role in HOOH defense and ultimately suggested *katG1* and *katG2* are under RpoS control. Survival in extended stationary phase in the presence of HOOH improved dramatically, even in mutants lacking all three catalase-peroxidases (Figure 3.6). This result suggests that, like OxyR, the RpoS regulon involves protection beyond the three catalase-peroxidases. The protective effect of *katG1* improved dramatically when *rpoS*+ was restored, and an *in silico* analysis predicts that RpoS may exert direct control of *katG1* and *katG2* expression through promoter binding. In *V. parahaemolyticus* a predicted *rpoS* binding site (CTGTTTT) was found upstream of *katG1* [92]. Alignment of the 5' UTRs of *V. parahaemolyticus' katG1* and *V. natriegens' katG1* found an extended overlapping sequence including this proposed binding motif:

GACTACGCTGTTTT (-89 to -76) and GACTACGCTGTTAT (-90 to -77), respectively. There was not a strong signal from the alignment of the 5' UTR of *V. natriegens' katG2* but sequence gazing similarly found "CTGTTTT" at -56 to -50 (Figure A3.9).

Notably, our results also demonstrated *katG2*- and *katG3*-mediated protection from HOOH in the *rpoS* nonsense mutation background (Figure 3.4) suggesting alternative transcriptional controls. Consistently, promoter analysis performed with BPROM (Bacterial PROMoter prediction program [116]) predicted σ^{70} binding sites in the 5' UTRs of *katG1, katG2,* and *katG3* (Figure A3.9). Predictions for *katG2* and *katG3* indicate long 5' UTR sequences (144 and 212 bp, respectively), consistent with predictions of a 206 – 237 bp 5' UTR for the *katG* in *V. cholerae* [117]. Hence, one or more of these *katG*'s may be regulated by the housekeeping sigma factor which could contribute to *rpoS*-independent *katG* expression.

Loss of function mutations in *rpoS* may occur frequently in laboratory cultures of *V. natriegens* and this may extend beyond strain ATCC 14048. A previous study reported that *V. natriegens* strain CCUG 16347 has low intrinsic catalase activity informed by the lack of bubbling when spotted with HOOH and a cold temperature sensitivity that could be rescued by plating cells with exogenous catalase [6]. An investigation of the published genome of that strain revealed that the *rpoS* gene contains a stop codon mutation at amino acid 59 due to an upstream frameshift mutation (FS S49/L50 (+C). Notably, this is a different nonsense mutation than found in ATCC 14048, but may likewise be responsible for the low catalase activity in the strain. Additionally, loss of function mutations in *rpoS* have been reported extensively for lab cultures of other species such as *E. coli*. Storage and transport conditions are credited for unintentional selection of *rpoS* mutants in *E. coli* collections and mutations in *rpoS* can provide a fitness advantage [118]. Notably, surveys of fresh environmental isolates indicate that *rpoS* mutations are rare in natural *E. coli* populations [119, 120]. In *V. natriegens* the diversity of *rpoS* alleles and frequency of mutations is unknown. Similar analyses of new isolates and laboratory collections could provide beneficial insight for the community.

As a final observation, the extent of extracellular HOOH degradation exhibited condition and genotype dependence. In the *rpoS* nonsense mutant background, complete

degradation occurred when cells were exposed during early stationary phase, whereas roughly 400 nM HOOH was left behind when exposed during extended stationary phase (Figure 3.4 and 3.5, respectively). A potential explanation for the incomplete HOOH degradation is that cells in extended stationary phase lack significant reductant to operate peroxidases and thus must rely exclusively on catalase activity, which has a low affinity for HOOH [121] [82]. We note however that restoration of the WT *rpoS* allele facilitated complete HOOH degradation, perhaps through regulation of antioxidant enzymes and/or metabolic changes that provide reductant for the peroxidases.

In conclusion, these findings contribute to a new understanding of the oxidative stress response of *V. natriegens.* Several pieces of information suggest a complex network of multiple regulatory elements and many genes beyond *katG.* This is applicable toward culturing and ecological understanding of *V. natriegens.* Importantly, we highlight mutations in *rpoS* among culture stocks of *V. natriegens*. This provides useful awareness for the field of *V. natriegens* research and can heed caution regarding organism characterization and phenotype interpretation as research moves forward.

Acknowledgements

This work was supported by a Student/Faculty Research Award from the University of Tennessee, Knoxville to L.D. Glasgo and E.R.Z and NSF OCE-2023680 to E.R.Z. A portion of the computation for this work was performed on the University of Tennessee Infrastructure for Scientific Applications and Advanced Computing (ISAAC) computational resources. The authors would like to thank the High Performance & Scientific Computing (HPSC) group (UTK) for their support. We'd also like to thank Mike Gilchrist and Liz Fozo for valuable discussions, and Slaybrina Raphael, Zachary Slimak and Joan Slonczewski for alerting us to the *rpoS* mutation of the ATCC strain.

Appendix

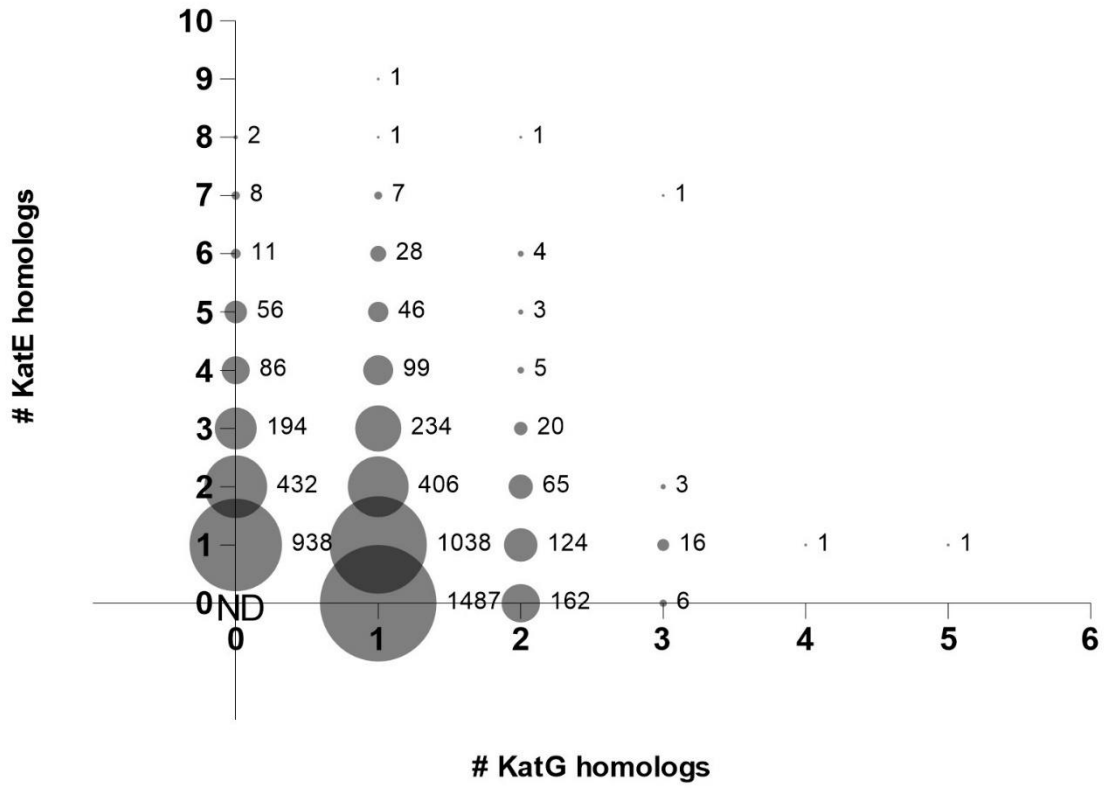

Figure A3.1 Enumeration of KatE (PF00199.22) and KatG (PF00141.26) within Proteobacteria proteomes. Refseq proteomes accessed February 2022), ND = no data.

Figure A3.2(A) Uncollapsed *Vibrio spp.* KatG based phylogeny tree. (B) *Vibrio spp. 16S rRNA* based phylogeny tree. Species containing greater than one KatG (PF00141.26) copies are indicated by color strips. Branches with bootstrap values between 80 (green) to 100 (blue) are indicated.

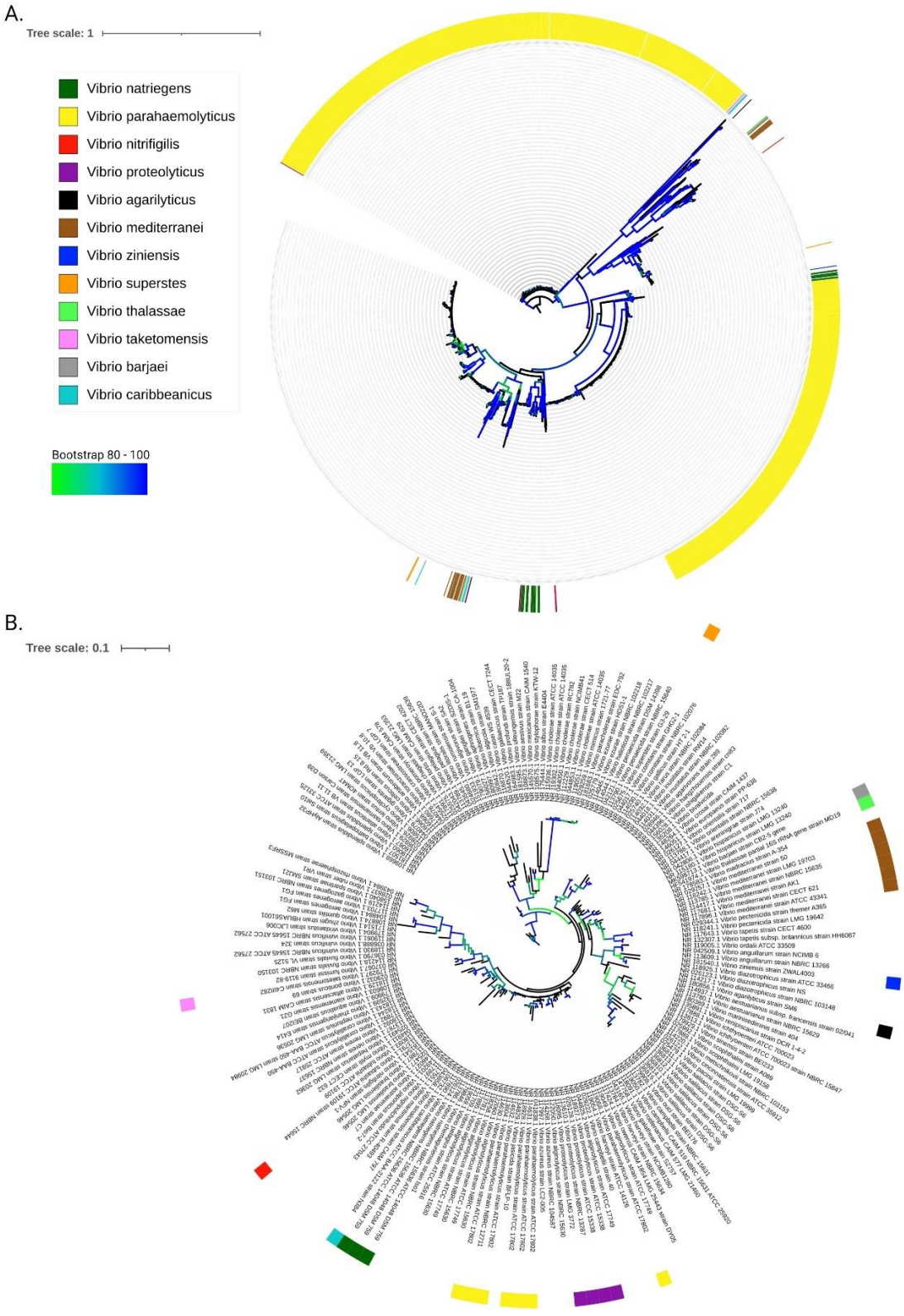
A.
Tree scale: 1
Vibrio natriegens
Vibrio parahaemolyticus
Vibrio nitrifigilis
Vibrio proteolyticus
Vibrio agarilyticus
Vibrio mediterranei
Vibrio ziniensis
Vibrio superstes
Vibrio thalassae
Vibrio taketomensis
Vibrio barjaei
Vibrio caribbeanicus
Bootstrap 80 - 100
B.
Tree scale: 0.1

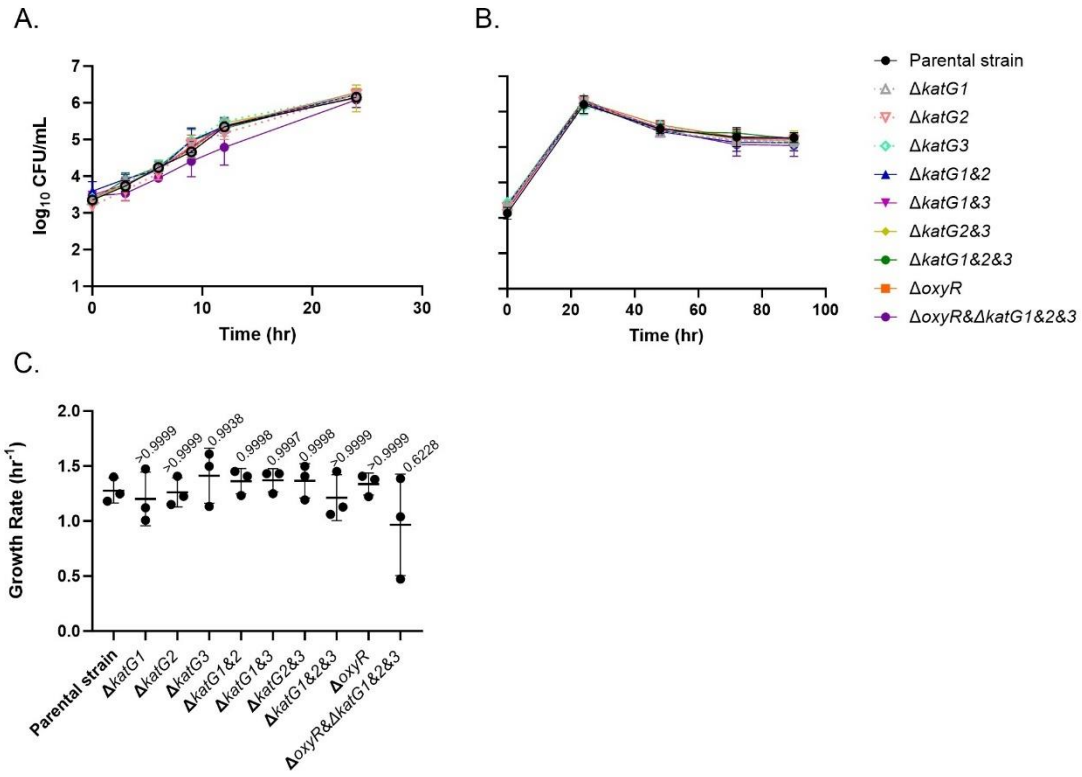

Figure A3.3 *V. natriegens* parental and mutant strains growth curves in MHM + 24 μM acetate. (A and B) viability counts, (C) growth rates (n=3; ± SD of the geometric mean). Growth rates were calculated from the regression of cell numbers over three consecutive time points during exponential growth. P-values were calculated using a One-Way ANOVA multiple comparisons test with Dunnett's correction.

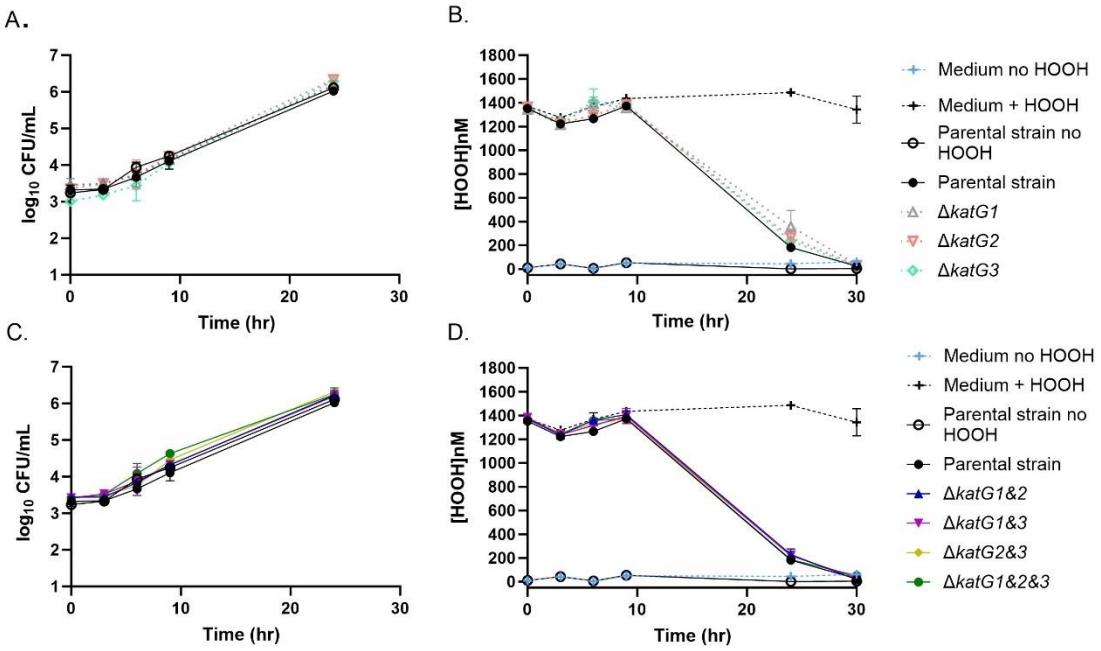

Figure A3.4(A and C) Cell viability and (B and D) HOOH degradation by *V. natriegens* parental and mutant strains in MHM + 24 μM acetate, (n=3; ± SD of the geometric mean). HOOH exposure at time 0.

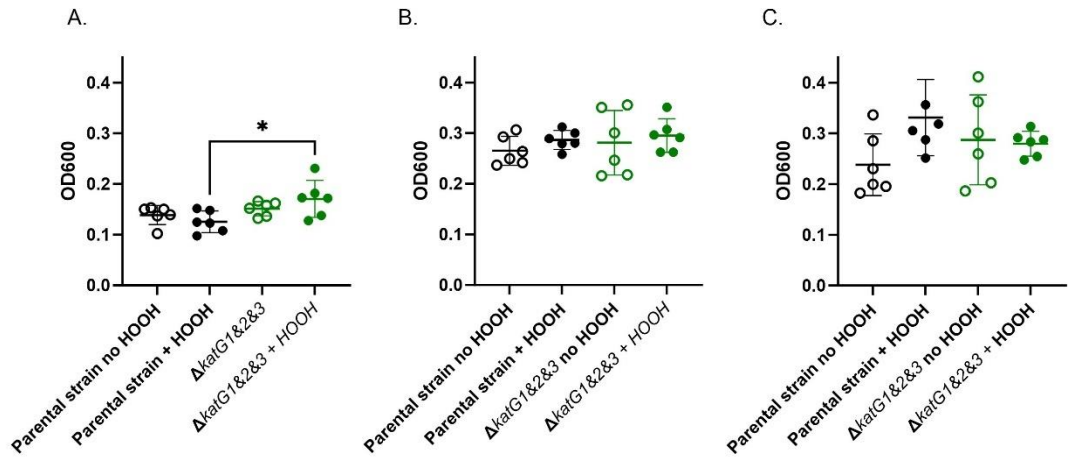

Figure A3.5 Crystal violet assays of *V. natriegens* parental and *ΔkatG1&2&3* strains. 1500nM HOOH added at (A) 0 hours or (B) 24 hours after incubation in MHM + 24 μM acetate, and (C) 24 hours in MHM + no carbon, (n=6; ± SD of the geometric mean). P-values were calculated using One-way ANOVA multiple comparisons with Tukey's correction, * $P \leq 0.05$.

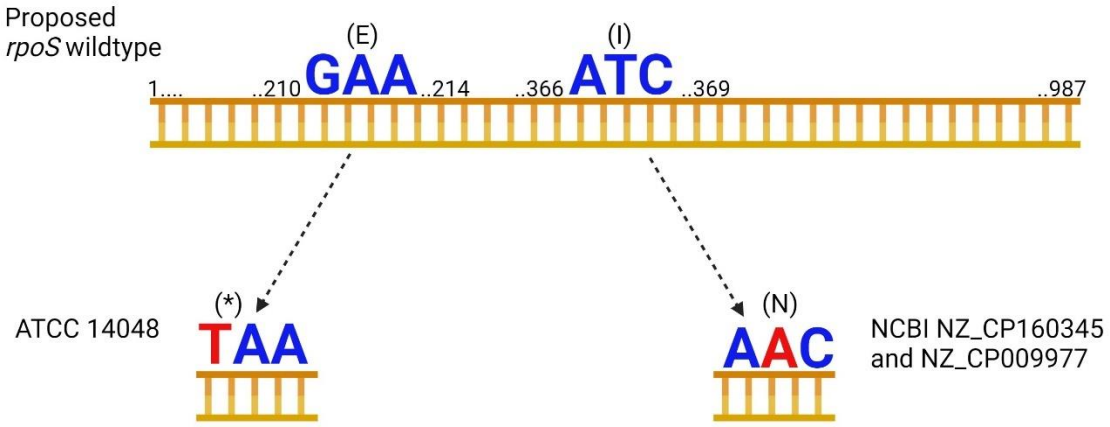

Figure A3.6 Illustration of *rpoS* genotypes. (Top) Proposed "wildtype" *rpoS* ORF with nucleotide numbers given in black text. Codons found to have sequence variants are enlarged with colored text. Letters in red indicate the nucleotides proposed as mutations. Symbols inside brackets indicate the encoded amino acid (E, I, and N) or stop codon (*). (Bottom) Codon variants found in the *rpoS* sequence of indicated strains. Created with BioRender.com.

Figure A3.7 Bubbling assay >5 minutes after HOOH exposure. Genotypes from left to right; *rpoS*$^{-}$: 1) parental 2) Δ*katG1&2* 3) Δ*katG1&3* 4) Δ*katG2&3*. *rpoS*$^{+}$: 1) parental *rpoS*E71 2) Δ*katG1&2 rpoS*E71 3) Δ*katG1&3 rpoS*E71 4) Δ*katG2&3 rpoS*E71 5)Δ*katG2&3 rpoS*E71N123.

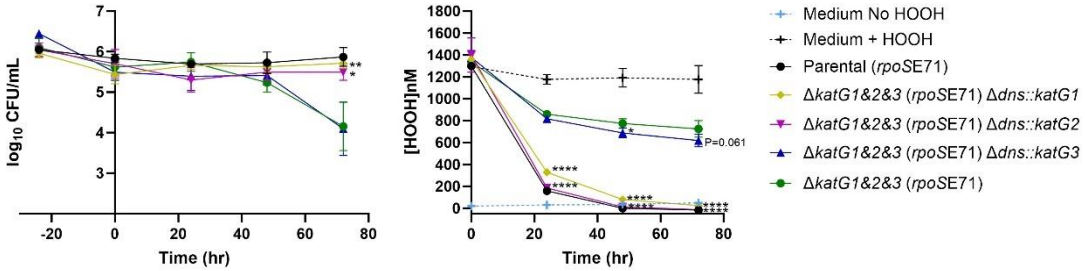

Figure A3.8 Complementation of *katG* genes. (A) Cell viability and (B) HOOH degradation, (n=3; ± SD of the geometric mean). All genotypes have the E71I123 *rpoS* allele abbreviated as *rpoS*E71. HOOH exposure at time 0, after 24 hours of starvation in MHM + no carbon. P-values were calculated using a One-way ANOVA multiple comparisons test with Dunnett's correction, * $P \leq 0.05$, **** $P \leq 0.0001$.

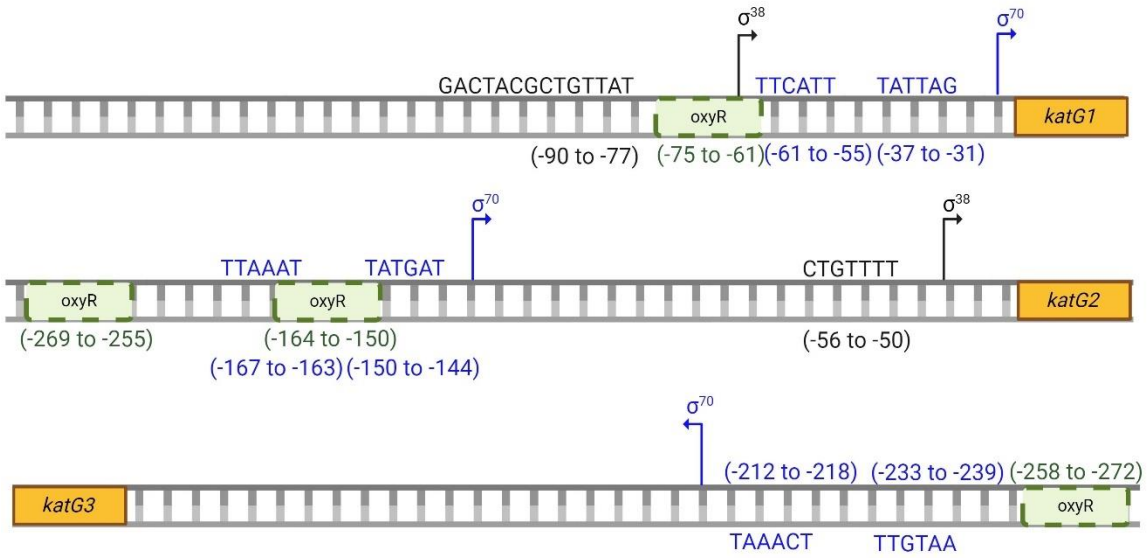

Figure A3.9 Schematic of sigma factor and OxyR binding sites for *katG1*, *katG2*, and *katG3* of *V. natriegens* ATCC 14048. Orange boxes indicate open reading frames. Blue text indicates predicted sigma 70 binding sites. Black text indicates predicted sigma 38 (RpoS) binding sites. Green boxes and text indicate OxyR, binding sites. Recognition sequences on the sense strain are located above the figure while recognition sequences on the antisense strain are located below the figure. Created with BioRender.com.

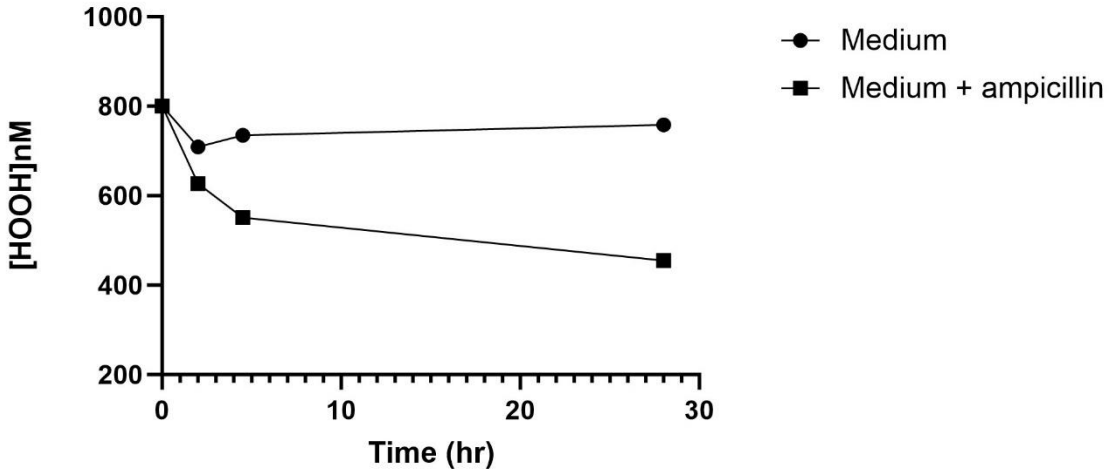

Figure A3.10 Ampicillin-dependent decrease in hydrogen peroxide detection. (n=3; ± SD of the geometric mean). Where not visible error bars are within the symbol.

Table A 3.1 Strains used in this study.

Strain Name	**Description**	**Source**
Vibrio natriegens ATCC 14048 pMMB*tfox* (EZ260)	Amp^R	[96]
EZ264	*ΔkatG1,* Chr.1 Δ1,520,008-1520031::erm^R, Amp^R	This study
EZ265	EZ260 *ΔkatG2,* Chr.1 Δ1,520,008-1520031::erm^R, Amp^R	This study
EZ266	*ΔkatG3,* Chr.1 Δ1,520,008-1520031::erm^R, Amp^R	This study
EZ267	*ΔkatG1, ΔkatG2,* Chr.1 Δ1,520,008-1520031::erm^R, Amp^R	This study
EZ268	*ΔkatG1, ΔkatG3,* Chr.1 Δ1,520,008-1520031::erm^R, Amp^R	This study
EZ269	*ΔkatG2, ΔkatG3,* Chr.1 Δ1,520,008-1520031::erm^R, Amp^R	This study
EZ270	*ΔkatG1, ΔkatG2, ΔkatG3,* Chr.1 Δ1,520,008-1520031::erm^R, Amp^R	This study
EZ274	*ΔoxyR,* Chr.1 Δ1,520,008-1520031::erm^R, Amp^R	This study
EZ275	*ΔkatG1, ΔkatG2, ΔkatG3, ΔoxyR ,* Chr.1 Δ1,520,008-1520031::erm^R, Amp^R	This study
EZ296	*rpos*E71, Chr.1 Δ1,520,008-1520031::erm^R, Amp^R	This study
EZ297	*ΔkatG1, ΔkatG2, rpoS*E71, Chr.1 Δ1,520,008-1520031::$spec^R$, Amp^R	This study
EZ298	*ΔkatG1, ΔkatG3, rpoS*E71, Chr.1 Δ1,520,008-1520031::$spec^R$, Amp^R	This study
EZ299	*ΔkatG2, ΔkatG3, rpoS*E71, Chr.1 Δ1,520,008-1520031::$spec^R$, Amp^R	This study

Table A3.1 continued

EZ300	*ΔkatG2, ΔkatG3*, *rpoS*E71N123 , Chr.1 Δ1,520,008-1520031::erm^R, Amp^R	This study
EZ308	*ΔkatG1, ΔkatG2, ΔkatG3,* *rpoS*E71, Chr.1 Δ1,520,008-1520031::spec^R, Amp^R	This study
EZ309	*ΔkatG1, ΔkatG2, ΔkatG3,* *rpoS*E71N123, Chr.1 Δ1,520,008-1520031::spec^R, Amp^R	This study
EZ310	*ΔkatG1, ΔkatG2, ΔkatG3,* *rpoS*E71, Chr.1 Δ1,520,008-1520031::erm^R, Amp^R Δ*dns*::*katG1*	This study
EZ311	*ΔkatG1, ΔkatG2, ΔkatG3,* *rpoS*E71, Chr.1 Δ1,520,008-1520031::erm^R, Amp^R Δ*dns*::*katG2*	This study
EZ312	*ΔkatG1, ΔkatG2, ΔkatG3,* *rpoS*E71, Chr.1 Δ1,520,008-1520031::erm^R, Amp^R Δ*dns*::*katG3*	This study

Table A3.2 Primer sequences used in this study. Underlined nucleotides indicate homologous regions added for SOE PCR.

Primer name	**5' -> 3' sequence**	**Description**
katG1F1	CCAATTGGTGGAGAGAGTGC	*ΔkatG1* Upstream forward primer
katG1R1	GCTAATTCAGTTTAAGCGGCCATCTCCTTTGTTAGGGGCACAG	*ΔkatG1* Upstream reverse primer
katG1F2	ATGGCCGCTTAAACTGAATTAGCCAAACGAGTTCTCTTAATTAACTGTC	*ΔkatG1* downstream forward primer
katG1R2	CTCGATGCAGGCGCTATT	*ΔkatG1* downstream reverse primer
133308F	TCTGTCGAGCTGATGCAAGT	*ΔkatG1* forward scar primer
136180R	AGAACCAATCATCGGGTTTG	*ΔkatG1* reverse scar primer
katG2F1	AGCTTCATCTTTTGCCATGC	*ΔkatG2* Upstream forward primer
katG2R1	GCTAATTCAGTTTAAGCGGCCATGCTGTTGTTCATAGGGTGTCC	*ΔkatG2* Upstream reverse primer
katG2F2	ATGGCCGCTTAAACTGAATTAGCGAAATGCACTTTGGTGCGTA	*ΔkatG2* downstream forward primer
katG2R2	CGCAGGACAACTGGAAAATA	*ΔkatG2* downstream reverse primer
447588F	GCACACGTTATCACCTCTCCT	*ΔkatG2* forward scar primer
450432R	AAAGAGAGCGCTGACCTGAG	*ΔkatG2* reverse scar primer
katG3F1	ATAGCCACCATCGGTTGAGA	*ΔkatG3* Upstream forward primer
katG3R1	GCTAATTCAGTTTAAGCGGCCATCTGGCTTTTTGCGTATCCAT	*ΔkatG3* Upstream reverse primer
katG3F2	ATGGCCGCTTAAACTGAATTAGCTCGCTAAGCTAGCATAAGCTCT	*ΔkatG3* downstream forward primer
katG3R2	GGATTCTGACTGGAGCAAGC	*ΔkatG3* downstream reverse primer

Table A3.2 continued

1119752F	GCCAGACATCCTAATGCCTTT	*ΔkatG3* forward scar primer
1122735R	GTTCCGGAGATATCGGACAA	*ΔkatG3* reverse scar primer
endAF1	CTAACATGGCTAAGCACCTG	*Δdns* upstream forward primer
endAR1	ACACAATCGCTCAAGACGTGACTGAGGATTAGGAAAGCTGGA	*Δdns* upstream reverse primer
endAF2	ATGGCCGCTTAAACTGAATTAGCCCTCACCAATCGCGACAATC	*Δdns* downstream forward primer
endAR2	TAAGGTGTCTCAAATCTCAATCTAGG	*Δdns* downstream reverse primer
KatG1compF	CACGTCTTGAGCGATTGTGTAAATCATCAGCAATCTGGTGT	*katG1* complement forward primer
KatG1compR	GCTAATTCAGTTTAAGCGGCCATGAGTCCGCCTGAATTTATCG	*katG1* complement reverse primer
KatG2compFH1	CACGTCTTGAGCGATTGTGTCCCGAGCTCCAACAATAGAT	*katG2* complement forward primer
KatG2compRH3	GCTAATTCAGTTTAAGCGGCCATGAGTCCGCCTGAATTTATCG	*katG2* complement reverse primer
KatG3compFH1	CACGTCTTGAGCGATTGTGAATGTCTGGCATGGATACGC	*katG3* complement forward primer
KatG3compRH3	GCTAATTCAGTTTAAGCGGCCATGCCCATCTTCCTATTGATTCTG	*katG3* complement reverse primer
2728836F	TTCCCTATTCCCAGCCTGAC	*Δdns::katG s*car forward primer
2730429R	CTACGCGCTCAGAGATGTCT	*Δdns::katG s*car reverse primer
rpoSF1	TCGTTTCTGCGCGTTTAGAG	*rpoS* upstream forward primer
rpoSE71R1	AAGCACTTCTTCTTCAGCAGT	*rpoS* upstream reverse primer
rpoSE71F2	ACTGCTGAAGAAGAAGTGCTT	*rpoS* middle piece forward primer

Table A3.2 continued

rpoSN123R2	TCTCAACTGCACGGTTCAAG	*rpoS* middle piece reverse primer
rpoSN123F3	CTTGAACCGTGCAGTTGAGA	*rpoS* downstream forward primer
rpoSR3	TTCACGTATCCTAAGCCGCT	*rpoS downstream* reverse primer
RpoSF	TGTCATGTCTTGCTAACTCGC	*rpoS* ORF forward primer
RpoSR	TTGGATACCCTGCTTAAAACGC	*rpoS* ORF reverse primer

CHAPTER FOUR

Apparent coexistence of parental *Vibrio natriegens* and genome reduced mutants under continuous ammonium limitation

Disclosure statement

The work in this chapter was carried out by Liz Glasgo. The document was written by Liz and edited by Erik Zinser.

Abstract

The genome streamlining theory suggests that selection favors smaller genomes during prolonged nutrient limited growth. In this study we created large-scale deletions to artificially reduce the genome of *V. natriegens* ATCC 14048. New and previously generated mutants comprised a small library of five genome-reduced strains possessing deletions between ~ 50 – 280 kb. We show that genome-reduced mutants exhibit robust growth in rich medium despite losses of 30 – 239 genes. We assessed fitness in terms of nutrient competition by coculturing all five mutant strains and wildtype *V. natriegens* simultaneously under continuous ammonium limitation. Population abundances tracked over ~ 400 generations show a coexistence between WT and the mutant pool, demonstrating resiliency in strains with sudden absences of up to several hundred genes. This study is the first of its kind to use *V. natriegens* to empirically evaluate the genome streamlining hypothesis.

Introduction

Bacterial genome sizes vary over two orders of magnitude and are in constant flux due to DNA acquisition through horizontal gene transfer and DNA loss through mutation and deletion [122]. Understanding the evolutionary forces acting on genome size and the impact that genome size has on cellular traits has guided research questions for decades. One particular interest is the subject of genome size reduction.

In endosymbiotic and free-living bacteria, DNA loss often occurs through mutation and erosion events, though how selection is acting on these populations differs [123, 124]. DNA loss in bacterial endosymbionts is facilitated by the *lack* of selection to maintain functions that overlap with the host [125]. In combination with population bottlenecks, decreased horizontal gene transfer, and small effective population sizes, these lifestyle characteristics increase fixation of deleterious mutations that are followed

by removal through deletion [126]. In contrast, genome reduction in free-living bacteria is thought to be facilitated by the *presence* of selection. Some of the smallest free-living bacteria belong to the heterotrophic SAR11 clade and the photosynthetic, cyanobacterial Genus *Prochlorococcus* [127, 128]. Both have large effective population sizes considered to be subject to natural selection. However, the mechanisms of DNA loss are less well understood. One contributing factor is thought to be the outsourcing of functions to the community, permitting gene loss, known as the Black Queen Hypothesis [129]. A selective advantage for gene loss in these species is proposed by the genome streamlining theory. The genome streamlining theory suggests that genome minimization can confer a reproductive advantage that outweighs the advantages of maintaining a large genetic repertoire. This is a scenario most likely to occur under stable, nutrient scarce conditions and high competition. For SAR11 and *Prochlorococcus* species which reside in oligotrophic surface waters, it is suggested that genome streamlining reduces elemental costs (*e.g.* nitrogen and/or phosphorus) of reproduction and increases resource utilization efficiency [130, 131].

The concept of improved cellular efficiency from DNA loss has become an attractive idea in synthetic biology. From a biotechnological perspective, industrially relevant species carry superfluous functions made negligible by the relatively narrow range of intended culturing conditions compared to the variation of a natural environment. Accordingly, removal of DNA has been carried out in aim of creating more efficient bacterial chassis. Artificial minimization by removal of phage genes, mobile genetic elements, genes of unknown function, and non-essential genes has been extensively studied in *Escherichia coli,* [132-134] but a number of other model systems have also been tried (*e.g. Bacillus subtilis* [59], *Pseudomonas putida* [56], and *Streptomyces avermitilis* [135]). While successes have been marked by increased biomass, growth rate, genetic stability, and homologous protein expression, impaired characteristics (growth, metabolic versatility and balance, and osmotic regulation), or lack of improvements have demonstrated the limitations of synthetic genome reduction [60, 67, 136-139].

Though inspired by the natural evolutionary process, few studies of simulated genome reduction have measured fitness using conditions outlined by the genome streamlining theory: nutrient limitation and stability. System stability is a challenge in traditional batch cultivation techniques where nutrients are drawn down over time and semi-continuous techniques where culture transfers lead to bottle necks and cyclic feast-and-famine regimes. Chemostat culturing addresses these issues through steady replenishment of growth medium [140]. The central premise of the chemostat is that a steady state can be achieved through the constant addition of fresh medium and simultaneous removal of culture. In steady state, population growth will be equal to the inflow of fresh medium, known as the dilution rate of the culture. In principle, medium providing everything in excess except a single resource will enable long-term selection for cell growth under steady, resource-limited conditions.

In this study, *Vibrio natriegens* was chosen as the host for artificial genome reduction. *V. natriegens* is a marine heterotroph, naturally found in coastal and estuary environments [2]. It is also a generalist and copiotroph owing to its large genetic repertoire encoded on two chromosomes totaling 5.2 Mbp [3, 8, 10]. Efficient tools for genetic manipulation have enabled genome reduction in *V. natriegens* including the recently reported deletion of 280 kb in a single round of mutagenesis facilitated by Multiplex Genome Editing by Natural Transformation (MuGENT) [6, 24, 96]. These attributes prompted the use of *V. natriegens* for simulated genome streamlining.

Here we utilized genome-reduced strains of *V. natriegens* possessing deletions of ~ 50 – 280 kb to explore the theory of genome streamlining. We tested the hypothesis that genome reduction will lead to a competitive fitness advantage under constant ammonium limitation. The data presented here shows a co-existence of the reduced mutants and non-reduced parental strain when cocultured over 400 generations in an ammonium-limited chemostat. While this result does not demonstrate a competitive fitness advantage due to genome reduction it highlights the underlying complexity of natural genome evolution and provides useful mutant characterization and experimental insights for future studies.

Materials and methods

Bacterial strains and culturing conditions

Vibrio natriegens ATCC 14048 harboring plasmid pMMB*sacBtfoX* (EZ276) was used to create all genotypes listed in Table A4.2. In this study, cells were cultivated in LB3 (LB + 3 % NaCl) or Minimal Marine Heterotroph Media (MHM) with 1 % acetate, as indicated [96]. For chemostat culturing, a variation, MHM-C, was developed here which contains 0.02% tryptone, 20 mM TAPS buffer, and 40 mM ammonium sulfate, ($1/10^{th}$ the MHM concentration). For growth assays, overnight cultures were started from frozen glycerol stocks and grown overnight 20-22 hours, then diluted 1:1000 into fresh medium and grown overnight again. Cultures were grown at 30 °C in an orbital shaker (250 rpm) and experiments were performed in acid-washed glassware unless otherwise noted. Media was supplemented with 250 μg/mL kanamycin (kan), 100 μg/mL erythromycin (erm), and 250 μg/mL spectinomycin (spec), as needed.

Generation of deletion and selectable marker PCR constructs

Transforming DNA (tDNA) fragments to be used in Multiplex Genome Editing by Natural Transformation (MuGENT) were created with splicing-by-overlap (SOE) PCR [32]. Deletion-creating constructs were generated with two-piece SOE, while selectable markers were generated with three-piece SOE [96]. Four deletion constructs were designed here, targeting deletion sizes of ~ 50 kb, 100 kb, 183 kb, 201 kb, located on Chromosome 2 (NZ_CP016346) (Figure 4.1). Notably, this exact methodology was used to create a 280 kb deletion, reported previously [96]. Briefly, two 3 kb fragments flanking the desired region of deletion were amplified with PCR primers that added 20-23 bp homologous sites to the 3´ end of the upstream fragment and the 5´ end of the downstream fragment. Each PCR product was purified and added in equal concentration (50 ng : 50 ng) for SOE PCR, to “stich” the pieces together. Similarly, for selectable marker construction, three-piece SOE PCR was performed by amplifying a 3 kb upstream fragment, a 3 kb downstream fragment, and additionally, an antibiotic resistance marker ($erythromycin^R$), as a middle fragment. The middle fragment contains 20 – 23 bp homologous sites on both ends that match the upstream and downstream fragments. Selectable marker upstream and downstream fragments share homology to a region

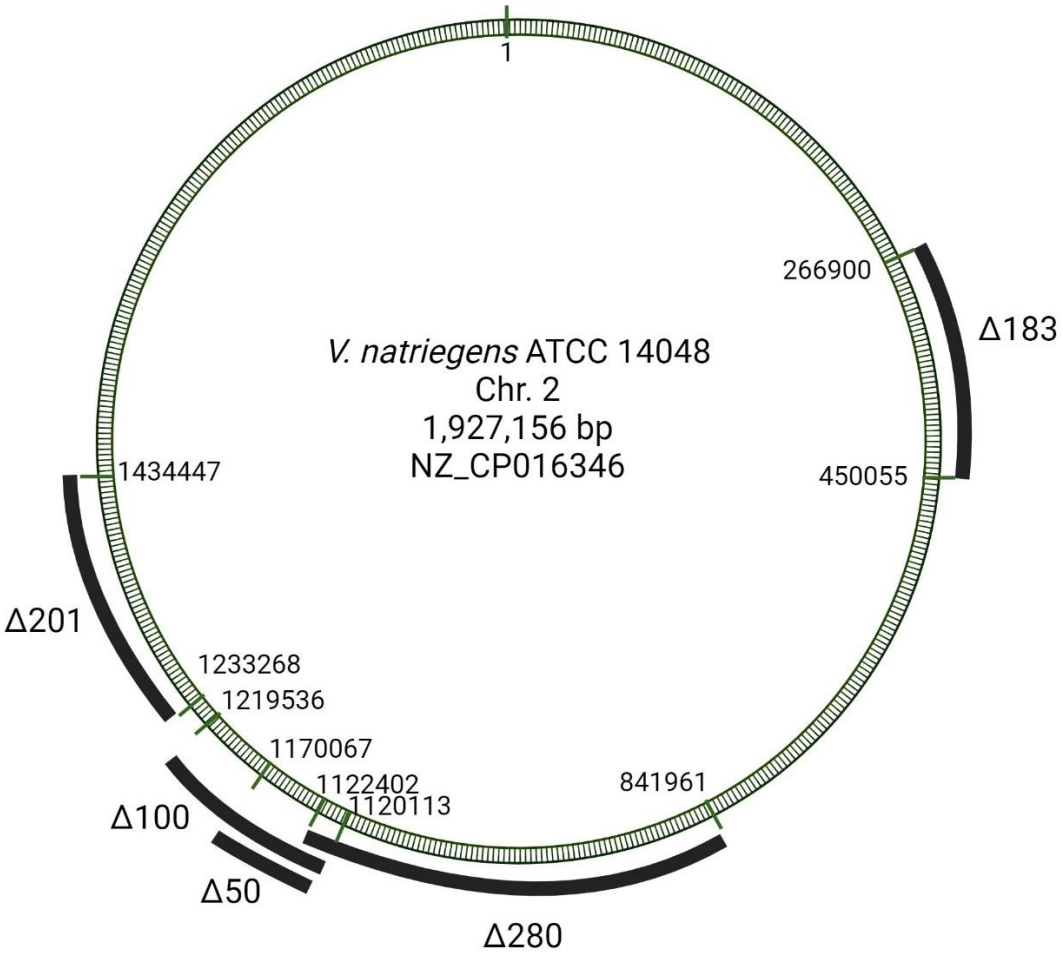

Figure 4.1 Map of deletions created on *V. natriegens* Chromosome 2. Reference genome NZ_CP016346. Numbers indicate deletion endpoints (in bp).

located on Chromosome 1, targeting insertion of the antibiotic marker into an intergenic location within a prophage region as described previously [96]. Each purified piece was added in equal concentration (50 ng : 50 ng: 50 ng) to perform SOE PCR. All primers are listed in Table A4.3.

All PCRs were performed with Phusion Plus Polymerase (Fisher Scientific) using manufacturers protocols, thermocycler conditions were as follows: 1) 98 °C – 30 seconds, 2) 98 °C – 10 seconds, 3) 60 °C – 10 seconds, 4) 72 °C – 30 seconds/kb, repeat steps 2-4 25-30x, 72 °C – 5 minutes, 4 °C – hold. PCR reactions were purified with QIAquick PCR Purification Kit (Qiagen). SOE PCR was performed exactly as previously described [96]. Briefly, PCR with Phusion Plus Polymerase is performed as above except the reaction is set up without primers and run for 10-15 cycles. Then, the reaction is stopped, the upstream forward primer and downstream reverse primer are added, and thermocycler conditions are resumed for an additional 25 – 30 cycles. All PCR products were visualized on 1.5 % agarose gels with Midori Green stain (Bulldog Bio). Upstream, downstream, and middle fragments were purified with the QIAquick PCR Purification Kit (Qiagen). SOE PCR products were gel purified with QIAquick Gel Extraction Kit (Qiagen) and used in transformations.

Multiplex Genome Editing by Natural Transformation (MuGENT)

Multiplex Genome Editing by Natural Transformation (MuGENT) was performed as previously described [32]. *Vibrio natriegens* ATCC 14048 cells harboring plasmid pMMB*sacBtfoX* (EZ276) were grown overnight in LB3 supplemented with 100 μM IPTG and 250 μg/mL kanamycin at 30 °C in an orbital shaker (250 rpm). Cells were diluted 1:1000 into 350 μL Instant Ocean (28 g/L) supplemented with 100 μM IPTG. 50 ng of selectable marker (erm^R) SOE construct and 250 ng of deletion-creating SOE construct were added to the cells. The mixture was incubated statically for 5 hours at 30 °C. The transformation reaction was then transferred to a glass culture tube containing 1 mL LB3 and grown out at 30 °C, shaking for 2 hours. Cells were serially diluted and plated onto agar plates containing 100 μg/mL erythromycin and incubated at 30 °C overnight. Individual colonies were picked with sterile toothpicks, grown in sterile 96-

well microtiter plates, shaking at 30 °C, then cryopreserved in 10 % glycerol (final v/v) at -80 °C.

To screen for incorporation of the non-selectable tDNA into the genome, PCR primers were designed that would generate a ~1500 – 3300 bp amplicon if the deletion was successful, designated as "scar" primers (Table A4.3**)**. No amplicon was expected if incorporation of the non-selectable product was unsuccessful because products would be 50 – 201 kb if no deletion occurred. Isolates were grown from frozen on agar plates and colony PCR screening was performed as previously described [96]. To rapidly screen isolates, colony PCR was initially performed on pools of nine colonies at a time. Subsequent colony PCRs were performed on individual isolates to identify those that incorporated the non-selectable tDNA. Colony PCR was performed with Gotaq polymerase (Promega) with thermocycler conditions as follows: 1) 95°C – 2 minutes, 2) 95 °C – 1 minute, 3) 55 °C – 1 minute, 4) 72 °C – 1 minute/kb, repeat steps 2-4 25-30x, 72 °C – 10 minutes, 4 °C – hold. Products were visualized on 1.5 % agarose gels using Midori Green stain (Bulldog Bio). Finally, deletions were confirmed by Sanger sequencing. DNA was extracted with the DNeasy Blood and Tissue Kit (Qiagen) following manufacturer's protocol for Gram negative bacteria. PCR was performed using Phusion Plus polymerase (Fisher Scientific) as described above. PCR products were purified with QIAquick PCR Purification Kit (Qiagen) and sequenced by UT Genomics Core or Eurofins Scientific.

Plasmid curing

To plasmid cure the deletion strains, counterselection against the pMMB*sacBtfoX* plasmid was done as previously described [96]. In the presence of sucrose, the plasmid-encoded *sacB* gene leads to cell lethality in Gram-negative bacteria. Therefore, growth on sucrose containing plates indicates loss of the *sacB* gene. Cells were grown overnight in LB3 then serially diluted onto agar plates of LB0.1 (LB + 0.1 % NaCl) supplemented with 15 % sucrose. To confirm plasmid curing, colonies were additionally screened for kanamycin sensitivity, indicated by absence of growth in the presence of kanamycin and loss of the plasmid *ori via* PCR screening. Colonies that grew in the presence of sucrose,

were kanamycin sensitive, and had no amplification of the plasmid *ori* were considered plasmid cured.

COG analysis

Genes deleted from Δ50, Δ100, Δ183, Δ201, and Δ280 were designated into COG categories using the eggNOG annotation database with default settings [141, 142]. Genes placed into multiple COG categories were manually categorized based on KEGG Orthology and PFAM assignments.

Batch culture assays

Vibrio natriegens ATCC 14048 marked with $spec^R$ (EZ278) was used as the wildtype (WT) strain in this study [96]. Monoculture growth of plasmid cured mutants Δ50 (EZ286), Δ100 (EZ287), Δ183 (EZ288), Δ201 (EZ295), and Δ280 (EZ289) were initially compared to WT in LB3 and MHM media.

Overnight cultures were grown in LB3 at 30 °C, shaking. For growth assays in MHM, cells were pelleted and resuspended in MHM three times to prevent carry over of LB3 medium. Cells were diluted into 5 mL of fresh medium in glass culture tubes and cell growth was monitored by viable count on LB3 agar plates.

Mutant genotypes that did not grow in MHM, were additionally assayed for growth in MHM supplemented with 0.5 % casamino acids or 0.5 % tryptone following the same protocol as above.

It was determined above that MHM supplemented with tryptone permitted growth of most mutant genotypes. We wished to establish nitrogen-limited conditions for competitive growth assays but as amino acids supplied by tryptone can be used as a nitrogen source, a “Goldilocks” combination of tryptone and ammonium was needed to allow growth of mutant strains and still create nitrogen limitation.

The concentration of tryptone where nitrogen limitation is still achieved was determined. WT cells were grown overnight in MHM, pelleted, and resuspended in MHM lacking a nitrogen source (MHM-N). Cells were then diluted to 10^4 CFU/mL into 5 mL cultures of MHM (contains 400 μM ammonium sulfate), and MHM-N (contains 0 μM ammonium sulfate) supplemented with 0.5 % - 0.01 % tryptone. After 24 hours, cell densities were measured by viable plate count.

An ammonium-limiting concentration was established for MHM supplemented with 0.02 % tryptone. WT cells were prepared as described above and diluted into MHM + 0.02 % tryptone with 0 – 400 μM ammonium sulfate. Cell abundances were measured by viable plating after 24 hours.

The modified MHM recipe containing 40 μM ammonium and 0.02 % tryptone was designated MHM-C. WT and mutant cultures were grown overnight in MHM-C at 30 °C, shaking. Overnight cultures of the Δ100 strain were routinely supplemented with additional tryptone (0.5 % final w/v) and given 48 hours to grow, then pelleted and resuspended three times in MHM-C before beginning the growth assay. Cells were inoculated into 5 mL of MHM-C. Cell counts were monitored by viable plate count on LB3 agar plates and growth rates were calculated as the growth constant from the regression of cell number over time of four consecutive time points during exponential growth.

Cell diameter of WT and mutant cells was estimated with a FlowCAM imagining system (FlowCAM 8000, Yokogawa Fluid Imaging Technologies, Scarborough, ME, USA). Overnight cultures were started as described above. After seven hours of incubation, cultures were analyzed using a 20X objective. Objects between 0.6 – 3 μM were counted and mean diameter was calculated from 5000 images.

Ammonium limited chemostat culturing

WT and mutant cells were grown overnight in MHM-C, except for Δ100 which was prepared as described above. Cells were diluted to ~10^4 CFU/mL into 50 mL of fresh MHM-C. Total, WT, and mutant pool abundances were determined by viable plate count on LB3 agar plates containing no selection, + 250 μg/mL spectinomycin, and + 100 μg/mL erythromycin, respectively. Mutant genotype was indistinguishable by plate count, therefore relative abundance of mutants within the mutant pool was not resolved with this method. Culture vessels were placed on stir plates in a 30 °C incubator. Cultures were allowed to establish for seven hours, then MHM-C was continuously fed into the cultures controlled by a peristaltic pump (Watson-Marlow 323S). Headspace was aerated through a 0.2 μM filter connected to an air pump (Aqua culture WM1000). Working volume was maintained at 50 mL through continuous outflow. Sampling for viable

counts occurred first after 18 hours of continuous culturing and then every 24 hours for 35 days. Whole culture aliquots and colony isolates were frozen on days 4 ,8 ,12 ,16, 20, 24, 30, and 36. Isolates were picked with sterile toothpicks and grown in LB3 in sterile 96-well microtiter plates (Corning) for 6-8 hours, then cryopreserved at -80 °C in 10% glycerol (final v/v). Chemostat vessels were exchanged every eight days to minimize wall effects. Dilution rate and pH were monitored by periodically measuring outflow volume (mL/hr) and chekcing pH with test strips (Fisher Scientific).

Results

Assessment of genome-reduced genotypes and phenotypes

Prior laboratory studies have yielded mixed success in achieving fitness benefits of genome reduction. One aspect of these studies potentially responsible for the variation in results is the assumption of dispensable DNA [138]. Here, a targeted deletion approach was used but regions were chosen with little bias for DNA content. The only qualifying factor was avoidance of highly predicted essential genes determined previously through CRISPRi knockdown and homology to essential genes in *Vibrio cholerae* [11].

Chromosome 2 of *Vibrio natriegens* ATCC 14048 is predicted to encode only six essential genes and thus contains large regions of potentially dispensable DNA making it an ideal target for large-scale genomic reduction [11]. Genome reduced strains of *V. natriegens* created or used here possessed deleted regions of 50 kb, 100 kb, 183 kb, 201 kb, or 280 kb (Figure 4.1). Deleted DNA segments shared no or minor overlap except for Δ50 which completely overlaps with Δ100. Deleted genes (Attachment 4.1.xlsx) were assigned COG categories (Attachment 4.2.xlsx) for preliminary functional categorization. Summation of the COG categories for each mutant showed that diverse functional assignments were encompassed in the deletions and that several COG categories were shared by every mutant (Figure A4.1).

To evaluate physiological differences between WT and deletion mutants, growth in batch culture was assayed in rich, LB3 medium, and minimal, MHM medium. In LB3, all genotypes exhibited growth, albeit some differences in growth kinetics were observed. Notably, growth of Δ50 closely resembled WT. In contrast, remaining mutant genotypes

demonstrated slower initial growth, however reaching similar final cell densities to WT. This was except for Δ100, which achieved a ~100-fold lower maximum abundance (Figure 4.2A). Likewise, in MHM, Δ50 similarly resembled WT. However, Δ100, Δ183, and Δ201 completely failed to grow (Figure 4.2B).

To further characterize the growth phenotypes of the mutants unable to grow in MHM, we attempted to restore growth by adding sources of amino acids. MHM supplemented with 0.5 % casamino acids restored growth of Δ183 but not Δ100 or Δ201 (Figure A4.2A). Addition of 0.5 % tryptone restored growth of Δ183 and Δ201, however Δ100 demonstrated a ~24-hour lag period before growth began (Figure A4.2B).

Establishment of nitrogen limited conditions

The genome streamlining theory suggests that genome reduction provides a selective reproductive advantage under resource limited conditions. Here, nitrogen limitation was chosen to evaluate this theory. Nitrogen is an essential element, incorporated into nucleic acids, proteins and other biomolecules. Nitrogen is also a limiting resource in environments where naturally streamlined organisms thrive and it is suggested that streamlining selection acts to reduce cellular nitrogen quotas [143]. Therefore, we next wished to establish a "Goldilocks" combination of tryptone and ammonium to allow growth of most mutant genotypes while also establishing nitrogen-limited conditions.

WT cells were used to determine the greatest concentration of tryptone that can be added to MHM containing no additional nitrogen source (MHM-N), while still achieving nitrogen-limitation. In MHM-N growth became limited at 0.02 % tryptone. Importantly, with replete ammonium sulfate (400 μM), growth was restored, indicating cells were limited for nitrogen (Figure A4.3A).

To determine a limiting concentration of ammonium, additions of ammonium sulfate (0, 10, 20, 40, 80 , and 400 μM), were added to WT cells in MHM-N supplemented with 0.02 % tryptone. Concentrations between 0 – 40 μM ammonium sulfate limited cellular abundance (Figure A4.2B). 40 μM ammonium sulfate demonstrated a useful midpoint with slightly higher growth than no ammonium addition and limited growth compared to replete conditions (Figure A4.3B and A4.3C). MHM

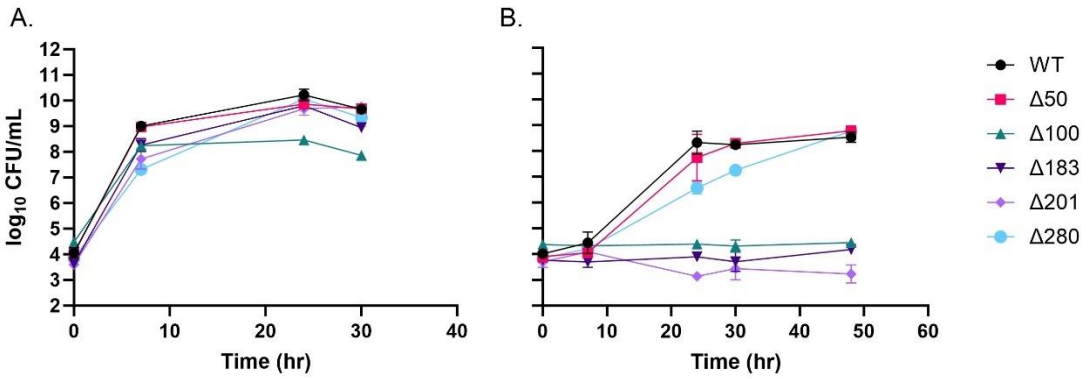

Figure 4.2 WT and deletion mutant growth curves in LB3 (A) and MHM (B). n=3; ± SD of the geometric mean.

medium with the modified tryptone (0.02 %) and ammonium (40 μM) concentrations was designated MHM-C.

Mutant physiology in ammonium-limited batch culture

WT and mutant growth in MHM-C was observed and growth rates were calculated. All mutants, except Δ100, exhibited final abundances similar to WT (Figure 4.3A). However, the growth rates of Δ183 and Δ201 were significantly lower than WT (Figure 4.3B).

As a preliminary assessment of cell size, cells were analyzed by FlowCAM. Mean cell diameters ranged from 0.92 – 1.09 μm (Table A4.1). It should be noted that this size range falls below the limit of detection (LOD = 2 μm), and microscopy is required for validation.

Competition during ammonium-limited continuous culturing

WT and mutant genotypes were co-inoculated into chemostat culturing vessels and MHM-C was fed in continuously through a peristaltic pump. Mutants were added in equal ratio and all contain the same selective marker but can be distinguished from WT which contains a different selective marker. A dilution rate of 0.33 ± 0.02 was calculated from outflow measurements. Cultures were maintained for 36 days, ~400 generations. Throughout the experiment pH strips indicated a pH of 7-8. Total, WT, and mutant populations in duplicate chemostats were tracked over time (Figure 4.4). Initially, WT and mutant populations reached similar abundances. On days 6 – 7, WT populations increased, while mutant pools declined in abundance. Between days 10 – 12 the mutant pools increased again but never overtook WT. The two populations continued to coexist with minor fluctuations and WT remained the dominant population.

Lastly, two colony morphologies were observed during chemostat culturing (Figure A4.3A); an opaque colony similar to unaged wild type, and a translucent colony. Both colony morphologies were detected on plates selective for WT or mutants suggesting the translucent colony morphotype arose in both wild type and mutant populations during N-limited growth. Importantly, PCR targeting of the *rpoS* gene indicated both morphologies were *V. natriegens* (Figure A4.3B). The translucent colonies were first observed on day three and remained present throughout the experiment.

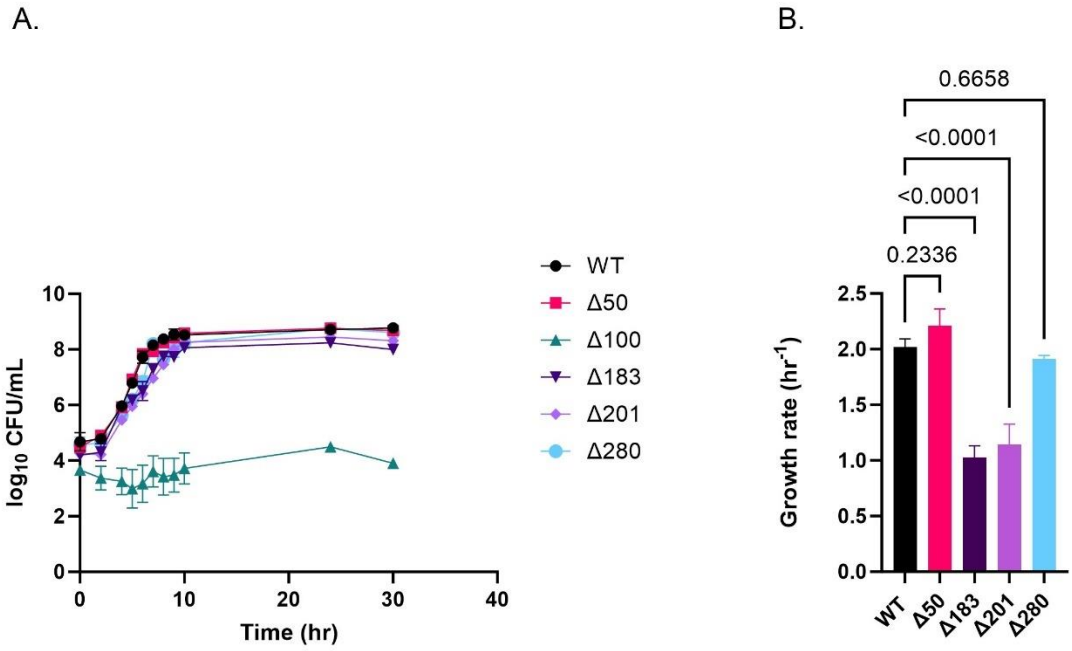

Figure 4.3(A) Monoculture growth curves and (B) growth rates of WT and deletion strains in MHM-C. n = 3; ± SD of the geometric mean, P-values calculated using a one-way ANOVA multiple comparisons test with Dunnett's correction.

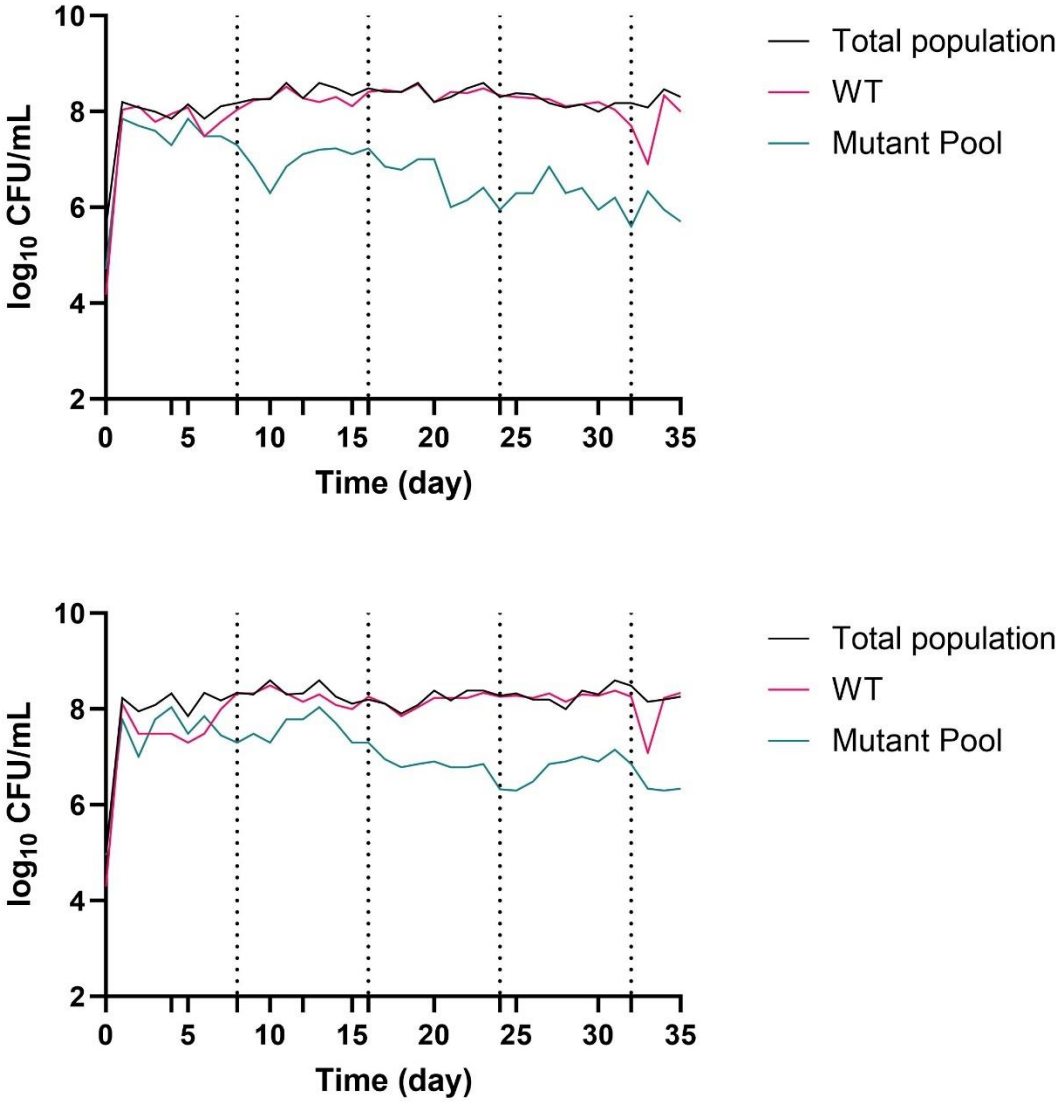

Figure 4.4 Continuous ammonium-limited co-cultures of *V. natriegens* WT and large-deletion mutants**.** Graphs represent individual replicates, top: replicate 1, bottom: replicate 2. Tick marks indicate when a new MHM-C media reservoir was attached and dotted lines denote when chemostat cultures were transferred to new vessels.

Discussion

The genome streamlining theory posits that smaller genomes provide a reproductive benefit under nutrient-limited growth [143]. Our study addressed this theory by assessing the competitive fitness of genome-reduced mutants under continuous ammonium-limited conditions. We report that WT and the mutant pool established a long-term, stable coexistence with no clear advantage of genome reduction in the conditions tested. While our results do not suggest genome loss can improve fitness during nutrient limited growth, they provoke discussion of a fundamental question in evolutionary and population ecology: how is genetic variation maintained in a community competing for the same resources? [144].

Niche-based theories such as the competitive exclusion principle postulate that two or more species occupying the same niche and space cannot coexist if competing for the same resource; a competitive advantage of one species leads the weaker competitor to extinction or a different ecological niche [145, 146]. Alternatively, but not mutually exclusive, the neutral theory of biodiversity posits that with two equal competitors, populations drift stochastically, resulting in random fluctuations of relative abundance that occur by chance rather than differences in competitive ability [147]. Additionally, understanding diversity becomes further complicated by complex trade-offs, obligatory commensalisms, interference competition, and epistasis [148, 149].

Here, we competed different genotypes of the same species assumed to initially occupy the same niche. While there were fluctuations in relative abundances, our results consistently converged on coexistence. Critically, we took measures to prevent spatial heterogeneity by continuously stirring cultures and periodically transferring cultured to new chemostat vessels to minimize influences of biofilm buildup. As such, we suspect our observations reflect true coexistence rather than a slow decline of the mutant population. One remaining explanation for the observed coexistence is evolution of niche differentiation.

Laboratory evolution has demonstrated rapid niche adaptation by the dynamic rise and fall of competing subpopulations [150, 151]. Here, we observed an increase in WT abundance and concurrent decline in the mutant population at approximately day seven.

This pattern is characteristic of a more fit subpopulation of WT cells overtaking the entire population. However, instead of being driven to extinction, a stable coexistence of the mutant pool and WT cells arose, possibly suggesting resource partitioning. Importantly, the medium MHM-C contains two nitrogen sources: ammonium and tryptone, raising the possibility for cells to utilize different nitrogen sources in this environment. Coexistence in this scenario is evocative of the resource-ratio (R*) model with two resources [146], which predicts a stable coexistence of competitors if one is a better competitor for one resource (*e.g.* ammonium) and the other is a better competitor for a second resource (*e.g.* tryptone). Notably, relative abundances of individual mutant genotypes in the mutant pool throughout the experiment are yet to be determined. Competitive exclusion would predict that the number of competing species cannot exceed the number of limiting resources [145], suggesting inter-mutant competition could lead to extinction events within the mutant pool. Consequently, an alternative interpretation of the WT takeover at day seven could be changes within the mutant population that decreased the fitness of the mutant pool similarly followed by niche differentiation.

Deletion mutants were designed to avoid essential genes located on Chromosome 2 [11]. However, inadvertently, mutants were generated that were unable to grow in minimal medium; Δ100, Δ183, and Δ201. Growth in minimal medium was restored by the addition of casamino acids and/or tryptone, suggesting these mutants were auxotrophic for one or more amino acids. Notably, Δ183 was the only mutant able to grow with casamino acid supplementation and Δ100 growth was not totally satisfied with either supplementation.

We inspected the deleted gene functions of Δ100, Δ183, and Δ201 to uncover potential auxotrophies. We note that Δ183 is lacking components of the glycine cleavage system (*gcvT, gvcH, gcvP)* and serine hydroxymethyltransferase (SHMT), responsible for catalyzing the conversion of serine and glycine. In *E.coli*, mutants defective in these enzymes became auxotrophic for serine or glycine [152, 153]. Δ201 was found to have genes deleted for thiamine (vitamin B1) biosynthesis: *thiE, thiD, thiM*. Notably, a second copy of the enzyme encoded by *thiE,* thiamine phosphatase synthase, is located on Chromosome 1. We speculate that tryptone could restore growth due to the presence of

tryptophan. Based on the KEGG PATHWAY database, tryptophan can provide NAD+ for thiamine synthesis, circumventing *thiD* and *thiM* [154]. Interestingly, we were not able to restore growth of Δ183 or Δ201 based on these predictions (data not shown), suggesting other contributing factors that are currently unknown. Finally, Δ100 which displayed weak growth under all minimal medium conditions is missing the *pdxH* gene. *E.coli* mutants lacking *pdxH* require a form of vitamin B6 known as pyridoxal [155]. A vitamin deficiency would explain the inability of tryptone and casamino acids to restore growth.

As a final observation, we noted two colony morphologies, opaque and translucent, present in both WT and mutant populations of *V. natriegens* throughout continuous culturing. Changes in opacity have been documented in many bacterial species and often reflect alterations in capsular polysaccharides and/or cell wall compositions [156]. Reversible changes in colony opacity, known as phase variation, have been reported in *Vibrio* species [157-160]. Phase variation is suggested to permit quick adaptation to environmental triggers including aeration, oxidative stress, temperature, and nutrient availability, and is mediated by genetic regulation often involving genetic rearrangements or epigenetic modification. We speculate that the observed phenotypic variants of *V. natriegens* were a response to nutrient limited conditions, though the potential reversible nature of colony opacity was not explored.

In conclusion, follow-up investigation is needed to further elaborate on the observations made in this study. Genetic diversity throughout the duration of the chemostat is relatively unknown beyond the population abundances of WT and the total mutant pool. Sequencing examination of the genotypes present throughout culturing could provide insight to the population dynamics. Monoculture chemostats would also be beneficial for comparative analysis. We report useful information of deletion mutant genotype and phenotype characteristics, but additional analysis is needed for a comprehensive understanding of growth requirements. Finally, to our knowledge this is the first report of possible phase variation in *V. natriegens* but further investigation is needed to confirm this speculation and identify a potential genetic determinant.

Acknowledgements

This work was supported by NSF OCE-2023680 to E.R.Z.

Appendix

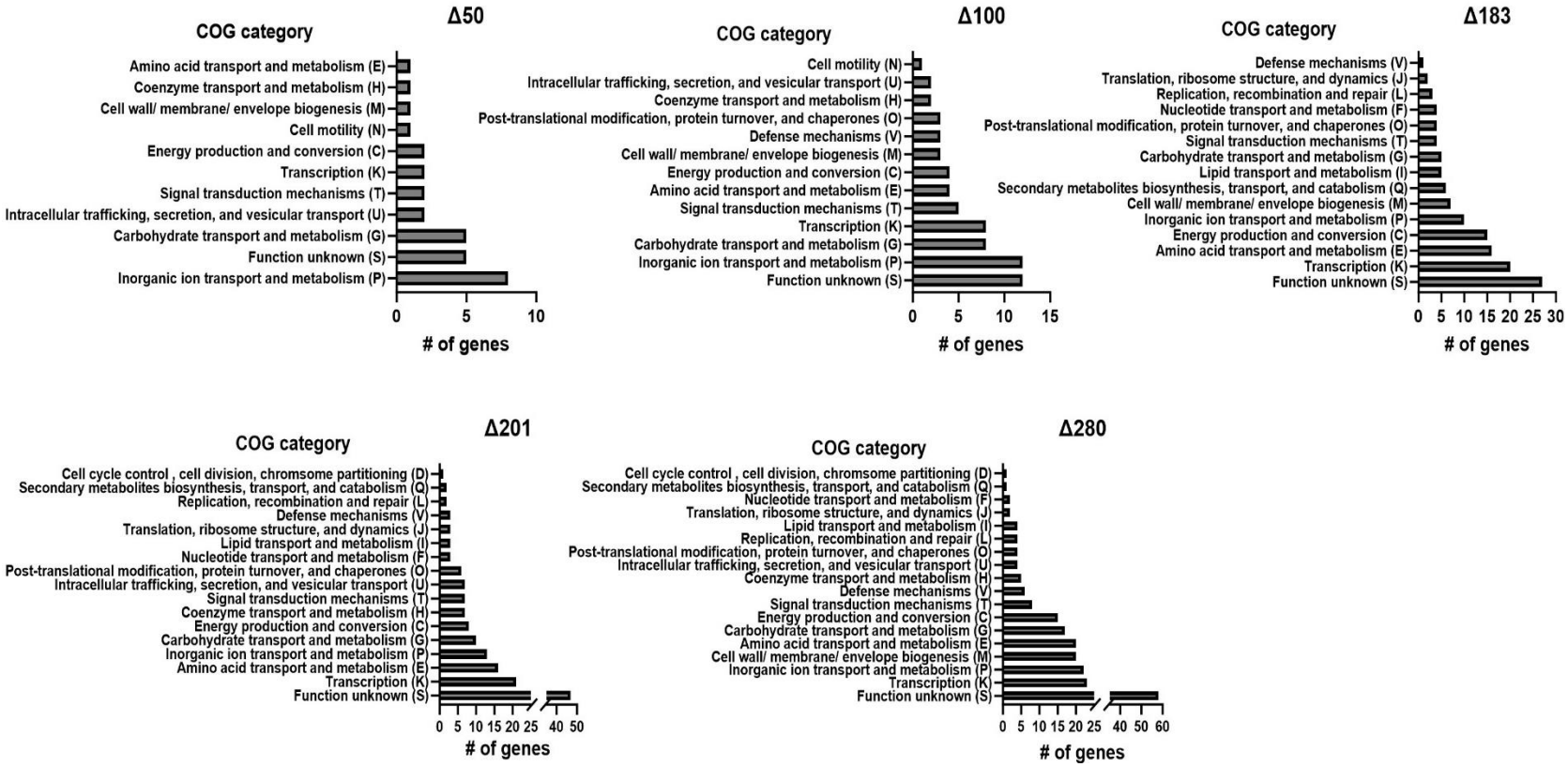

Figure A4.1 COG categories for deleted genes of each mutant.

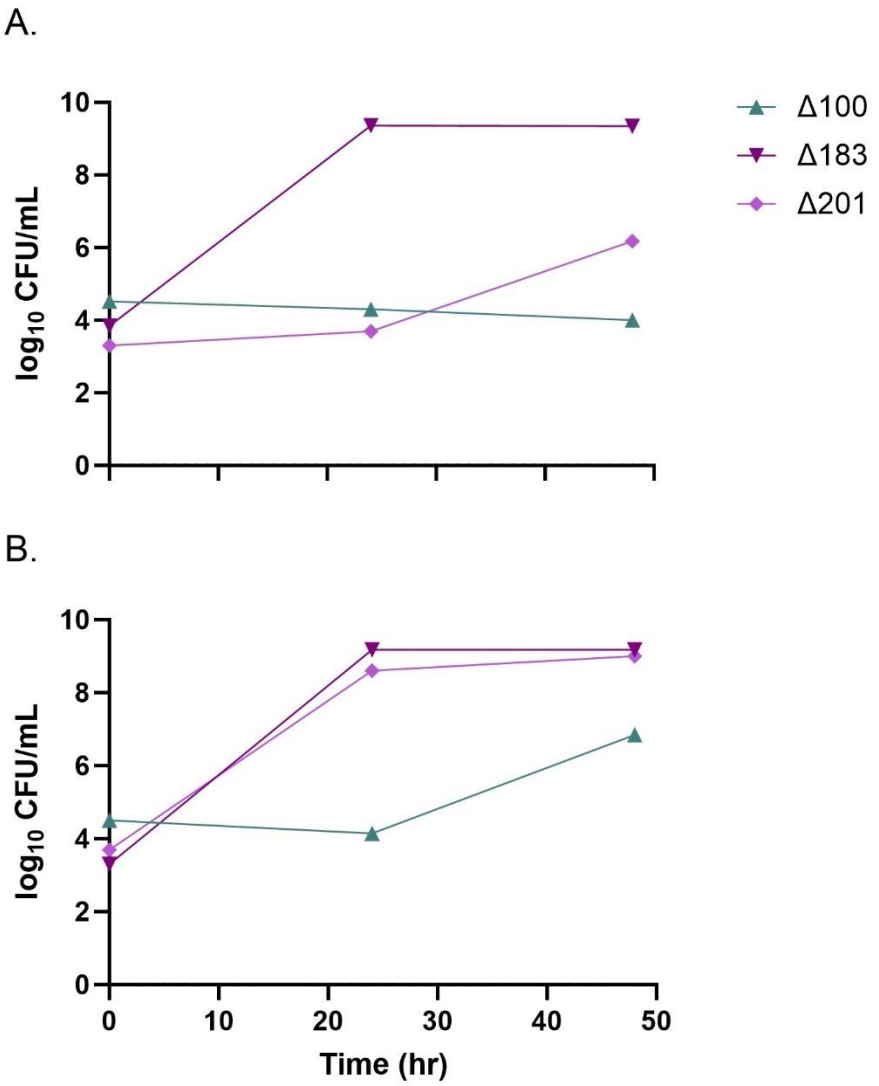

Figure A4.2(A) Growth curves in MHM + 0.5 % casamino acids and (B) MHM + 0.5 % tryptone. n = 1.

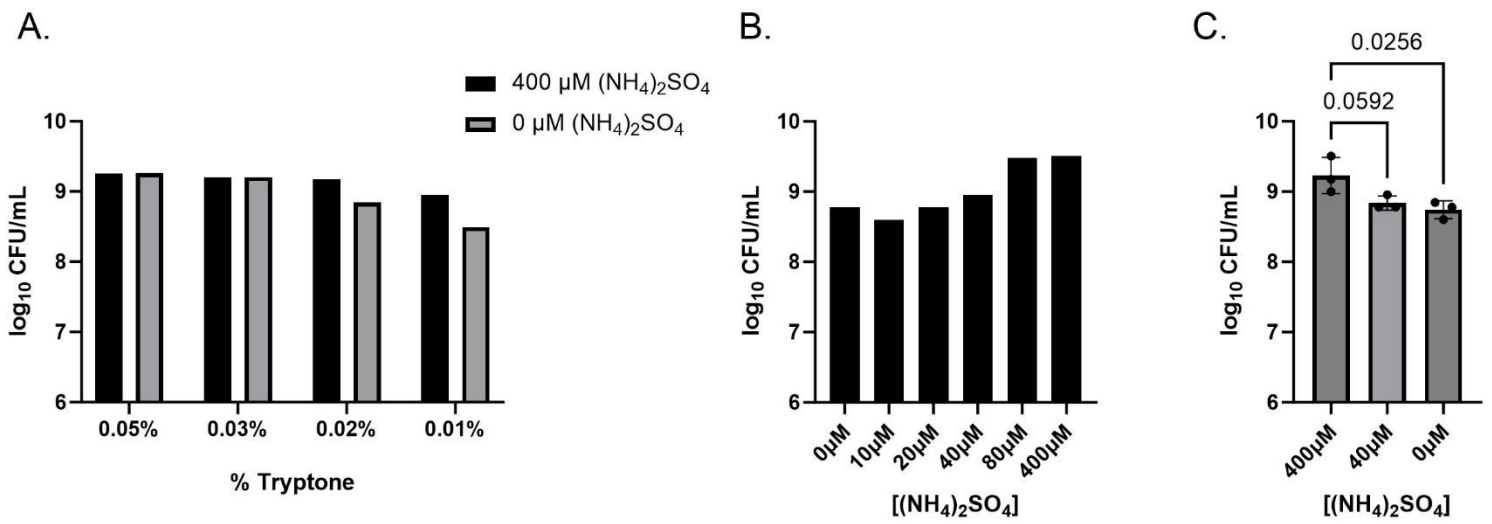

Figure A4.3(A) WT abundance after 24 hours in MHM and MHM-N with 0.01 % - 0.05 % tryptone ,(n = 1). (B) WT abundance after 24 hours in MHM + 0.02 % tryptone with 0 – 400 µM ammonium sulfate, (n = 1). (C) WT abundance after 24 hours in MHM + 0.02 % tryptone with 0, 40, and 400 µM ammonium sulfate, (n = 3; ± SD of the geometric mean). P- values calculated using a one-way ANOVA multiple comparisons test with Dunnett's correction.

Table A4.1 Cell size determined by FlowCAM (n = 5000).

Genotype	WT	Δ50	Δ183	Δ201	Δ280
Mean Diameter (µm)	0.92	0.98	1.08	1.09	0.96

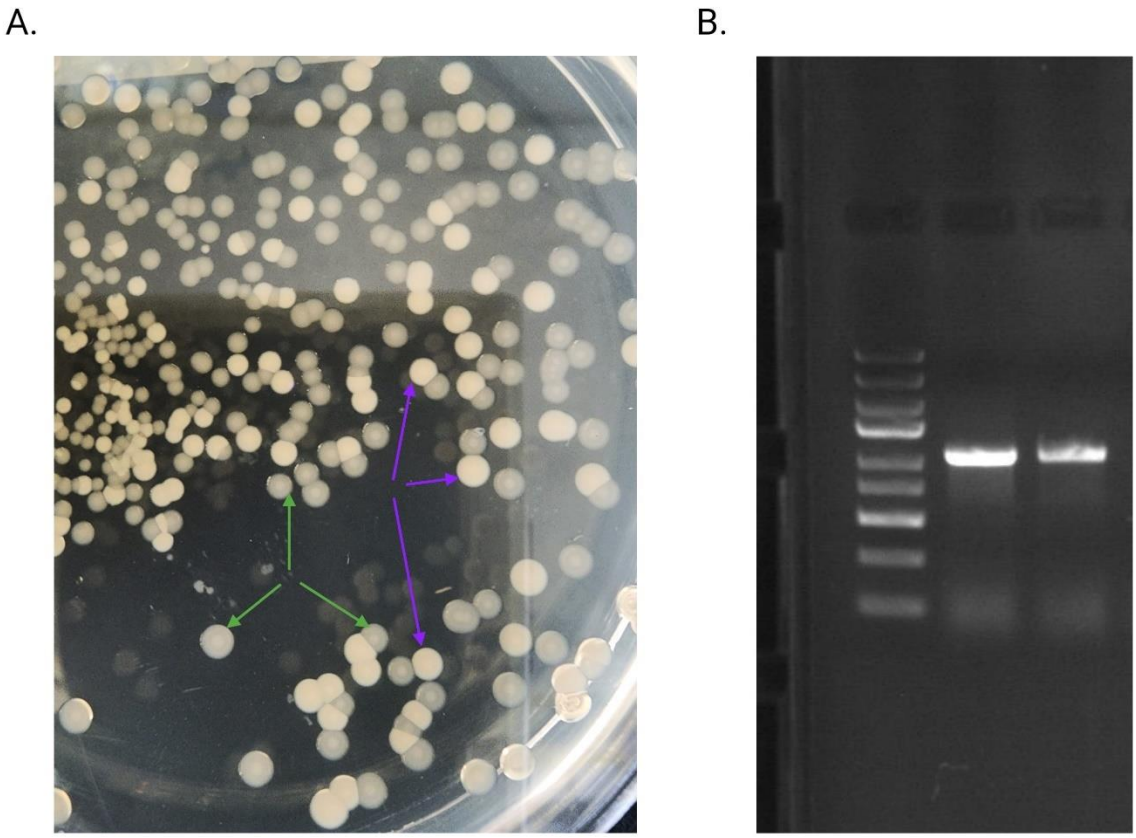

Figure A4.4(A) Green arrows indicate examples of translucent colonies and purple arrows indicate examples of opaque colonies. (B) Colony PCR targeting amplification of *V. natriegens rpoS* gene ; Column 1 – Thermo Scientific GeneRuler Express DNA Ladder, Column 2 – opaque colony, Column 3 – translucent colony. Created with BioRender.

Table A4.2 Strains used in this study.

Strain Name	**Description**	**Source**
Vibrio natriegens ATCC 14048 pMMB*sacBtfox* (EZ276)	Kan^R, sucrose sensitive	[96]
Vibrio natriegens ATCC 14048 $spec^R$ (EZ278)	Used as wildtype in this study. Chr.1 Δ1,520,008-1520031::$spec^R$	[96]
Δ50 (EZ286)	Δ1120113-1170067 [*katG3-araC*], Erm^R,	This study
Δ100 (EZ287)	Δ1120113-1219536 katG3-peptide ABC transporter substrate-binding protein], Erm^R,	This study
Δ183 (EZ288)	Δ266900-450055 [SPOR domain-containing protein CDS-*katG2*], Erm^R	This study
Δ201 (EZ295)	Δ1233268-1434447 [DUF3283 family protein CDS- eat CDS], Erm^R	This study
Δ280 (EZ289)	Δ841961-1122402 [hybrid-cluster NAD(P)-dependent oxidoreductase CDS-*katG3*], Erm^R	[96]

Table A4.3 Primer sequences used in this study. Underlined nucleotides indicate homologous regions added for SOE PCR.

Primer name	Sequence (5' to 3')	Description
KatG3F1	ATAGCCACCATCGGTTGAGA	Δ50 and Δ100 upstream arm forward primer
KatG3R1	GCTAATTCAGTTTAAGCGGCCATCTGGCTTTTTGCGTATCCAT	Δ50 and Δ100 upstream arm reverse primer
1170067F	ATGGCCGCTTAAACTGAATTAGCATACATGTCGGGCAGGAATC	Δ50 downstream arm forward primer
1173076R	GCTTGGGGTCAAGACAACAT	Δ50 downstream arm and Δ50 scar reverse primer
1119752F	GCCAGACATCCTAATGCCTTT	Δ50 and Δ100 scar forward primer
1219536F	ATGGCCGCTTAAACTGAATTAGCCGTCTTTTGAAGCCAACACC	Δ100 downstream arm forward primer
1222493R	CGAAGAAGAGGGGTTTACACTG	Δ100 downstream arm and Δ100 scar reverse primer
263889F	ATCCAAAACAGACCGCTGAA	Δ183 upstream arm forward primer
266889R	GCTAATTCAGTTTAAGCGGCCATTGTTCAAATCGTACCCGAAC	Δ183 upstream arm reverse primer
katG2F2	ATGGCCGCTTAAACTGAATTAGCGAAATGCACTTTGGTGCGTA	Δ183 downstream arm forward primer
katG2R2	CGCAGGACAACTGGAAAATA	Δ183 downstream arm reverse primer
265747F	GAGATGCTCAGCACAAGCAC	Δ183 scar forward primer
450432R	AAAGAGAGCGCTGACCTGAG	Δ183 scar reverse primer
1230198F	CGGTTCGGAGTCGAGACTAA	Δ201 upstream arm forward primer
1233268R	GCTAATTCAGTTTAAGCGGCCATTGAAGTTGGTGCGATGAGTC	Δ201 upstream arm reverse primer
1434447F	ATGGCCGCTTAAACTGAATTAGCCCTTGTGCTCCCTTTGTTGT	Δ201 downstream arm forward primer

Table A4.3 continued

1437000R	TCATACCCAAACTGAGCCCT	Δ201 downstream arm and scar reverse primer
1232892F	GTCGGGAGGGTTCACATTTC	Δ201 scar forward primer
838491F	GCTGGCACATTTTACGCATAG	Δ280 upstream arm forward primer
841961R	GCTAATTCAGTTTAAGCGGCCATTAAGAAAAACGCTGCCCTTG	Δ280 upstream arm reverse primer
katG3F2	ATGGCCGCTTAAACTGAATTAGCTCGCTAAGCTAGCATAAGCTCT	Δ280 downstream arm forward primer
katG3R2	GGATTCTGACTGGAGCAAGC	Δ280 downstream arm reverse primer
840291F	CGGCTAATCTGACCATGAAC	Δ280 scar forward primer
1122735R	GTTCCGGAGATATCGGACAA	Δ280 scar reverse primer
RpoSF	TGTCATGTCTTGCTAACTCGC	*rpoS* forward primer
RpoSR	TTGGATACCCTGCTTAAAACGC	*rpoS* reverse primer

CHAPTER FIVE

Conclusions and future directions

Summary

Vibrio natriegens has several appealing characteristics for research use as described in Chapter 1. In this dissertation, I developed genetic techniques for *V. natriegens* and implemented these techniques in the remaining research chapters. The genetic developments made in Chapter 2 were solutions to several caveats of current techniques that we wanted to mitigate for this work. I developed an intergenic location for selectable marker insertion and provided protocols for plasmid curing, rapid mutant screening, chromosomal gene complementation, and large-scale genomic deletions. In Chapter 3 I demonstrated the peroxide degradation function of three catalase genes and showed the involvement of regulatory genes *oxyR* and *rpoS* in *V. natriegens* oxidative stress response. In Chapter 4, I empirically examined the genome streamlining hypothesis through a resource-limited, continuous-culturing competition assay with originally constructed genome-reduced mutants. In Chapter 5, I will discuss relevant ambiguities from the research chapters and suggest some future avenues of exploration.

General considerations for the future of *Vibrio natriegens* research

The literature review and primary research presented in this dissertation aimed to highlight and begin resolving unknowns in the field of *V. natiregens* research. Interest in *V. natriegens* has grown over the past decade and implementation into novel applications has rapidly emerged. To aid advancement, others have indicated a need to develop a systems level understanding of *V. natriegens* by relating its genome, transcriptome, proteome, metabolome, and regulatory mechanisms [29]. Pertaining to this, one knowledge gap that created a challenge during this dissertation work was a lacking understanding of diversity across *V. natriegens* strains.

Our current understanding of *V. natriegens* relies on a few laboratory isolates. Some strain variations have previously been reported (growth rate, low-salt tolerance, genome size)[6], and in Chapter 3, I shed light on variations in *rpoS* sequence and function. To contextualize these differences, and potentially reveal others, a broader genotypic and phenotypic comparative analysis would be useful. Additionally, this could be strengthened by the inclusion of new environmental isolates.

This initiative could provide several benefits to the *V. natriegens* community. First, the documentation of differences between laboratory strains. As I noted in my *rpoS* analysis, even strains regarded as the same were found to have genetic differences demonstrated to impact function. This is perhaps unsurprising given that *rpoS* is a common mutational target in domesticated strains of bacteria [120]. A comprehensive comparison of laboratory and new isolates may also reveal other common genetic targets or phenotypes of laboratory domestication in *V. natriegens*. Domestication has been reported in *Escherichia coli, Staphylococcus aureus, Bacillus subtilis,* and other pathogenic and biotechnologically relevant species [161-163]. Some targets included structural, morphological, and resource utilization adaptations. Although the heightened interest in *V. natriegens* is relatively new, it has been in culture since the late 1950's. I hypothesize that similar signs of domestication could be detected in *V. natriegens*. It would be valuable to have *a priori* understanding of strain differences and domestication in *V. natriegens* for academic and industrial applications alike.

Comparison of laboratory strains and new isolates could also provide insight into other useful characteristics of *V. natriegens,* for instance, fast growth rate. Researchers have aimed to understand the mechanisms that permit fast growth in *V. natriegens* mainly through genomic comparisons to other model organisms such as *E. coli* and *V. cholerae* [17, 22]. Growth rate variations have been reported across *V. natriegens* strains and a recent isolation of fast-growing *Vibrio* species obtained isolates faster than *V. natriegens* ATCC 14048 [6, 7]. A follow up to these studies with more isolates, genomic comparison, and genetic analysis could improve our understanding of fast growth.

Finally, comparative analysis could be used to investigate natural transformation ability. Despite *V. natriegens* having the genetic potential for natural competency, it has been challenging to induce natural transformation in the lab, necessitating the methods discussed and used throughout this thesis [32, 33, 96]. For this discussion, it is noteworthy to again recall our finding of *rpoS* mutations in Chapter 3. It has been shown that *rpoS* is involved in natural competency of *V. cholerae* through the regulation of chitinases [30, 164]. Potentially, the difficulty in achieving natural competency for *V. natriegens* has been unknown mutations in *rpoS.* A current objective stemming from this

thesis is to test natural competency and chitin utilization in *V. natriegens* possessing the proposed "wildtype" *rpoS* sequence from Chapter 3. Alternatively, through a comparative analysis, isolates with inducible natural competency could be found and possibly *transform* our understanding of natural transformation. More generally, it is also important to consider that *rpoS* is a global regulator and mutations in *rpoS* can have pleiotropic effects. In the effort of a systems level understanding of *V. natriegens,* comparative analyses could reveal differences that improve our organismal understanding.

On understanding *Vibrio natriegens'* oxidative stress response

In Chapter 3, I utilized a gene knockout approach to investigate the functions of three *katG* genes in *V. natriegens.* I also demonstrated the involvement of regulatory genes, *oxyR* and *rpoS,* in *V. natriegens* oxidative stress response. This genetic approach was particularly appealing to investigate the *katG* genes in isolation and to generate a triple knockout to serve as a no-catalase control. However, my analysis ultimately required some speculation about gene regulation and additional peroxide degradation/protection mechanisms which should inspire future research.

Further work could be done to investigate mechanisms of oxidative stress protection beyond the *katG* genes. For example, I observed that *V. natriegens* cultures displayed a tolerance to hydrogen peroxide during exponential growth that could not be attributed to peroxide degradation. One possible explanation is that the cells were employing DNA and protein repair and/or protection mechanisms rather than relying on active degradation. Second, even the triple *katG* knockout exhibited hydrogen peroxide degradation following cell growth on acetate. This is hypothesized to have been carried out by peroxidase enzymes. These hypotheses could be explored with further genetic knockout experiments, although, another useful endeavor may be to combine genetics with expression analysis to efficiently assess several genes potentially involved in *V. natriegens* oxidative stress response. One suggestion would be to perform temporal transcriptomics analysis of *V. natriegens* with and without hydrogen peroxide exposure to identify genes involved in the oxidative stress response during different growth phases.

Genes predicted to have a role in protection from oxidative stress could be verified with genetic knockouts.

Follow up should also be considered for understanding the regulatory mechanisms governing oxidative stress response in *V. natriegens*. I demonstrated that *oxyR* and *rpoS* are involved in protection against hydrogen peroxide and I suggested that *rpoS* regulates two of the three *katG* genes in *V. natriegens*. *In silico* analysis was also used to predict additional genes that may be part of the *oxyR* regulon. To verify the role of *oxyR* and *rpoS* on *katG* expression, and any other gene of interest, qRT-PCR could be performed with wildtype and knockout *oxyR* and *rpoS* strains. This would allow quantification of changes in target gene expression and provide more information about regulatory control.

As a final consideration, expression analysis could also be beneficial for determining if phenotypic differences observed in solo *katG* strains were attributed to differences in gene expression or enzyme activity. For example, during extended stationary phase hydrogen peroxide exposure, *katG3* was determined to contribute the least to peroxide degradation. An open question is whether *katG3* is expressed less than the other *katG* genes during this condition or if the enzyme is functionally different.

Future work could also expand on the complexity of culturing conditions to investigate *V. natriegens* oxidative stress response in a coculture or community setting. I hypothesize that planktonic cultures of *V. natriegens* could provide cross protection to catalase negative species, as has been observed with other catalase positive heterotrophs [101]. Another interesting study could be to investigate if the ability to detoxify oxidative stress impacts biofilm community interactions. This could include exploring whether ability to detoxify oxidative stress impacts *V. natriegens'* capacity to form biofilms on ecologically relevant surfaces like seagrasses, or if multispecies biofilm assemblages are affected by *V. natriegens* oxidative stress response. Perhaps there is a role for *V. natriegens* oxidative stress response in community interactions that would additionally provide an evolutionary insight.

Lessons from *Vibrio natriegens* genome reduction and continuous culturing

In Chapter 4, an ammonium limited continuous culturing system was used to compete genome-reduced strains of *V. natriegens* against the parental genotype. As a test to the genome streamlining theory, the goal of this work was to investigate whether genome reduced mutants had a competitive fitness advantage over the parental strain during prolonged nutrient limited growth. My results demonstrated no clear advantage of genome reduction under the conditions tested.

To comprehensively interpret competition outcomes, a few follow up experiments should be performed. First, monoculture experiments would provide a useful comparison of growth dynamics to aid in understanding what observations were possibly driven by competition and evolution. Second, determination of the mutant genotypes during competition would assist with interpretations of competitive interactions and outcomes. Currently, multiplex PCR is being performed on mutant isolates to achieve this.

One limitation faced was the difficulty in determining the nutritional requirements of some of the mutant strains that could not grow in minimal medium. This information would help with interpretations and could be used for future experimental setups. As a final consideration for the experimental design, the biofilm mitigation strategy could be addressed. Chemostat vessel exchanges seemed to be effective in reducing buildup on the glassware. However, as bottle cap fixtures were retained throughout these exchanges, buildup became visible on the outside of plastic tubing that contacted the cultures and within the tubing used to extract samples. A simple modification would be to include exchanges of the cap fixtures in future studies.

Future work holds many possibilities. One follow up to this work could be to investigate adaptive changes in wildtype and mutant isolates from the continuous culture. A simple experiment would be to compete evolved isolates against their parental genotype under the same chemostat conditions to look for a competitive advantage of the evolved strain. Genome sequencing could also be used to identify specific mutations. An interesting question may be how mutations compared between wildtype and deletion mutants, in other words, did genome reduction change the trajectory of evolution? Other considerations for additional studies may include varying experimental conditions or

using different approaches to create mutants. Experimental design for this work is challenging due to our limited understanding of the bacterial genome and evolutionary events that have led to naturally streamlined organisms. This is highlighted by the many genome reduction studies that report unexpected fitness outcomes. Although this suggests it is complicated to design a rational approach, it is crucial to determine what effects experimental setups have on evolutionary outcomes to work towards understanding underlying mechanisms of evolution.

REFERENCES

1. Payne, W.J., *Studies on Bacterial Utilization of Uronic Acids III. Induction of Oxidative Enzymes in a Marine Isolate.* Journal of bacteriology, 1958. **76**(3): p. 301-307.
2. Payne, W.J., Eagon, R. G., Williams, A. K., *Some observations on the physiology of Pseudomonas natriegens nov. spec.* Antonie van Leeuwenhoek, 1961. **27**: p. 121–128.
3. Baumann, P., L. Baumann, and M. Mandel, *Taxonomy of marine bacteria: the genus Beneckea.* Journal of Bacteriology, 1971. **107**(1): p. 268-294.
4. Austin, B., Zachary, A., Colwell, R.R., *Recognition of Beneckea natriegens (Payne et al.) Baumann et al. as a Member of the Genus Vibrio, as Previously Proposed by Webb and Payne.* International journal of systematic and evolutionary microbiology, 1978. **28**(2): p. 315-317.
5. Eagon, R.G., *Pseudomonas natriegens, a marine bacterium with a generation time of less than 10 minutes.* Journal of bacteriology, 1962. **83**(4): p. 736-737.
6. Weinstock, M.T., et al., *Vibrio natriegens as a fast-growing host for molecular biology.* Nature methods, 2016. **13**(10): p. 849-851.
7. Peng, Y., et al., *Next-generation microbial workhorses: comparative genomic analysis of fast-growing vibrio strains reveals their biotechnological potential.* Biotechnology Journal, 2020. **15**(5): p. 1900499.
8. Maida, I., et al., *Draft Genome Sequence of the Fast-Growing Bacterium Vibrio natriegens Strain DSMZ 759.* Genome announcements, 2013. **1**(4).
9. Lee, H.H., et al., *Vibrio natriegens , a new genomic powerhouse.* bioRxiv, 2016.
10. Wang, Z., et al., *Draft genome sequence of the fast-growing marine bacterium Vibrio natriegens strain ATCC 14048.* Genome announcements, 2013. **1**(4): p. 10.1128/genomea. 00589-13.
11. Lee, H.H., et al., *Functional genomics of the rapidly replicating bacterium Vibrio natriegens by CRISPRi.* Nature microbiology, 2019. **4**(7): p. 1105-1113.
12. Li, T., S. Menegatti, and N. Crook, *Breakdown of polyethylene therepthalate microplastics under saltwater conditions using engineered Vibrio natriegens.* AIChE Journal, 2023. **69**(12): p. e18228.
13. Gong, Z., et al., *Identification of Emerging Industrial Biotechnology Chassis Vibrio natriegens as a Novel High Salt-Tolerant and Feedstock Flexibility Electroactive Microorganism for Microbial Fuel Cell.* Microorganisms, 2023. **11**(2): p. 490.
14. Ellis, G.A., et al., *Exploiting the Feedstock Flexibility of the Emergent Synthetic Biology Chassis Vibrio natriegens for Engineered Natural Product Production.* Marine Drugs, 2019. **17**(12).
15. Tian, J., et al., *Discovery and remodeling of Vibrio natriegens as a microbial platform for efficient formic acid biorefinery.* Nature Communications, 2023. **14**(1): p. 7758.
16. Örencik, C., et al., *An analysis and optimization of growth condition requirements of the fastgrowing bacterium Vibrio natriegens.* BioRxiv, 2019.

17. Hoffart, E., et al., *High Substrate Uptake Rates Empower Vibrio natriegens as Production Host for Industrial Biotechnology.* Applied and environmental microbiology, 2017. **83**(22).
18. Schulze, C., et al., *Investigation of exopolysaccharide formation and its impact on anaerobic succinate production with Vibrio natriegens.* Microbial Biotechnology, 2024. **17**(1): p. e14277.
19. Thiele, I., et al., *High-cell-density fed-batch cultivations of Vibrio natriegens.* Biotechnol Lett, 2021. **43**(9): p. 1723-1733.
20. Coyer, J.A., et al., *N2 fixation in marine heterotrophic bacteria: dynamics of environmental and molecular regulation.* Proceedings of the National Academy of Sciences, 1996. **93**(8): p. 3575-3580.
21. Nissen, H., Heldal, M., Norland., S. , *Growth, elemental composition, and formation of polyphosphate bodies in Vibrio natriegens cultures shifted from phosphate-limited to phosphate-pulsed media.* Canadian Journal of Microbiology, 1987. **33**: p. 583-588.
22. Long, C.P., et al., *Metabolism of the fast-growing bacterium Vibrio natriegens elucidated by 13C metabolic flux analysis.* Metabolic engineering, 2017. **44**: p. 191-197.
23. Coppens, L., et al., *Vibrio natriegens genome-scale modeling reveals insights into halophilic adaptations and resource allocation.* Molecular Systems Biology, 2023. **19**(4): p. e10523.
24. Pfeifer, E., et al., *Generation of a prophage-free variant of the fast-growing bacterium Vibrio natriegens.* Applied and environmental microbiology, 2019. **85**(17): p. e00853-19.
25. Blattner, F.R., Plunkett, G. III., Bloch, C.A., Perna, N.T., Burland, V., Riley, M., Collado-Vides, J., Glasner, J.D., Rode, C.K., Mayhew, G.W., Gregor, J., Davis, N.W., Kirkpatrick, H.A., Goeden, M.A., Rose, D.J., Mau, B., Shao, Y., *The Complete Genome Sequence of Escherichia coli K-12.* Science, 1997. **277**: p. 1453-1462.
26. Aiyar, S.E., T. Gaal, and R.L. Gourse, *rRNA promoter activity in the fast-growing bacterium Vibrio natriegens.* Journal of bacteriology, 2002. **184**(5): p. 1349-58.
27. Tschirhart, T., et al., *Synthetic Biology Tools for the Fast-Growing Marine Bacterium Vibrio natriegens.* ACS synthetic biology, 2019. **8**(9): p. 2069-2079.
28. Hoff, J., et al., *Vibrio natriegens: an ultrafast-growing marine bacterium as emerging synthetic biology chassis.* Environmental microbiology, 2020. **22**(10): p. 4394-4408.
29. Thoma, F. and B. Blombach, *Metabolic engineering of Vibrio natriegens.* Essays in Biochemistry, 2021. **65**(2): p. 381-392.
30. Meibom, K.L., et al., *Chitin induces natural competence in Vibrio cholerae.* Science, 2005. **310**(5755): p. 1824-1827.
31. Shin, J., K. Rychel, and B.O. Palsson, *Systems biology of competency in Vibrio natriegens is revealed by applying novel data analytics to the transcriptome.* Cell Reports, 2023. **42**(6).

32. Dalia, T.N., et al., *Multiplex Genome Editing by Natural Transformation (MuGENT) for Synthetic Biology in Vibrio natriegens.* ACS synthetic biology, 2017. **6**(9): p. 1650-1655.
33. Specht, D.A., et al., *Efficient natural plasmid transformation of Vibrio natriegens enables zero-capital molecular biology.* PNAS nexus, 2024. **3**(2): p. pgad444.
34. Zhang, Y., et al., *Systems metabolic engineering of Vibrio natriegens for the production of 1, 3-propanediol.* Metabolic Engineering, 2021. **65**: p. 52-65.
35. Yin, M., et al., *Changes in Vibrio natriegens growth under simulated microgravity.* Frontiers in microbiology, 2020. **11**: p. 2040.
36. Wang, S., et al., *Transcriptomic responses of the fast-growing bacterium Vibrio natriegens during cold-induced loss of culturability.* Applied Microbiology and Biotechnology, 2023. **107**(9): p. 3009-3019.
37. Wang, Z., et al., *Melanin produced by the fast-growing marine bacterium Vibrio natriegens through heterologous biosynthesis: characterization and application.* Applied and environmental microbiology, 2020. **86**(5): p. e02749-19.
38. Chimalapati, S., et al., *Natural Transformation in Vibrio parahaemolyticus: a Rapid Method To Create Genetic Deletions.* Journal of bacteriology, 2018. **200**(15): p. e00032-18.
39. Lloyd, C.J., et al., *Natural Transformation in a Classical-Biotype Vibrio cholerae Strain.* Applied and Environmental Microbiology, 2021. **87**(10): p. e00060-21.
40. Dalia, T.N., et al., *Enhancing multiplex genome editing by natural transformation (MuGENT) via inactivation of ssDNA exonucleases.* Nucleic acids research, 2017. **45**(12): p. 7527-7537.
41. Zheng, M., & Storz, G., *Redox Sensing by Prokaryotic Transcription Factors.* Biochemical pharmacology, 2000. **59**(1): p. 1-6.
42. De Souza Silva, O. and M. Blokesch, *Genetic manipulation of Vibrio cholerae by combining natural transformation with FLP recombination.* Plasmid, 2010. **64**(3): p. 186-195.
43. Saltikov, C.W. and D.K. Newman, *Genetic identification of a respiratory arsenate reductase. Proceedings of the National Academy of Sciences of the United States of America*, 2003. **100**(19): p. 10983-10988.
44. Calfee, B.C., Glasgo, L.D., Zinser E.R., *Prochlorococcus Exudate Stimulates Heterotrophic Bacterial Competition with Rival Phytoplankton for Available Nitrogen.* MBio, 2022. **13**(1): p. e02571-21.
45. Morris, J.J., & Zinser, E. R., *Continuous hydrogen peroxide production by organic buffers in phytoplankton culture media.* Journal of phycology, 2013. **49**(6): p. 1223-1228.
46. Moore, L.R., Coe, A., Zinser, E. R., Saito, M. A., Sullivan, M. B., Lindell, D., Frois-Moniz, K., Waterbury, J., & Chisholm, S. W, *Culturing the marine cyanobacterium Prochlorococcus.* Limnology and Oceanography: Methods, 2007. **5**(10): p. 353-362.
47. Blokesch, M. and G.K. Schoolnik, *The extracellular nuclease Dns and its role in natural transformation of Vibrio cholerae.* Journal of bacteriology, 2008. **190**(21): p. 7232-7240.

48. Zhang, Y., Sun, Q., Liu, Y., Cen, X., Liu, D., & Chen, Z. , *Development of a plasmid stabilization system in Vibrio natriegens for the high production of 1,3-propanediol and 3-hydroxypropionate.* Bioresources and Bioprocessing, 2021. **8**: p. 1-11.
49. Christman, M.F., et al., *Positive control of a regulon for defenses against oxidative stress and some heat-shock proteins in Salmonella typhimurium.* Cell, 1985. **41**(3): p. 753-762.
50. Greenberg, J.T. and B. Demple, *Overproduction of peroxide-scavenging enzymes in Escherichia coli suppresses spontaneous mutagenesis and sensitivity to redox-cycling agents in oxyR-mutants.* The EMBO Journal, 1988. **7**(8): p. 2611-2617.
51. Kong, I.S., et al., *Role of catalase and oxyR in the viable but nonculturable state of Vibrio vulnificus.* FEMS Microbiology Ecology, 2004. **50**(3): p. 133-42.
52. Dalia, A.B., E. McDonough, and A. Camilli, *Multiplex genome editing by natural transformation. Proceedings of the National Academy of Sciences of the United States of America*, 2014. **111**(24): p. 8937-42.
53. Stukenberg, D., et al., *The Marburg Collection: A Golden Gate DNA Assembly Framework for Synthetic Biology Applications in Vibrio natriegens.* ACS synthetic biology, 2021. **10**(8): p. 1904-1919.
54. Lyell, N.L., et al., *Effective mutagenesis of Vibrio fischeri by using hyperactive mini-Tn 5 derivatives.* Applied and environmental microbiology, 2008. **74**(22): p. 7059-7063.
55. Storz, G., L.A. Tartaglia, and B.N. Ames, *The oxyR regulon.* Antonie Van Leeuwenhoek, 1990. **58**: p. 157-161.
56. Lieder, S., et al., *Genome reduction boosts heterologous gene expression in Pseudomonas putida.* Microbial cell factories, 2015. **14**: p. 23.
57. Mizoguchi, H., et al., *Superpositioning of deletions promotes growth of Escherichia coli with a reduced genome.* DNA research : an international journal for rapid publication of reports on genes and genomes, 2008. **15**(5): p. 277-84.
58. Park, M.K., et al., *Enhancing recombinant protein production with an Escherichia coli host strain lacking insertion sequences.* Applied microbiology and biotechnology, 2014. **98**: p. 6701-6713.
59. Morimoto, T., et al., *Enhanced recombinant protein productivity by genome reduction in Bacillus subtilis.* DNA research, 2008. **15**(2): p. 73-81.
60. Po´sfai, G., Guy Plunkett III, Tama´s Fehe´r, David Frisch, Gunther M. Keil, Kinga Umenhoffer, Vitaliy Kolisnychenko Buffy Stahl, Shamik S. Sharma, Monika de Arruda, Valerie Burland, Sarah W. Harcum, Frederick R. Blattner, *Emergent Properties of Reduced-Genome Escherichia coli.* Science, 2006. **312**: p. 1044-1046.
61. Choe, D., et al., *Minimal genome: Worthwhile or worthless efforts toward being smaller?* Biotechnology journal, 2016. **11**(2): p. 199-211.
62. Ma, S., et al., *Bacterial genome reduction for optimal chassis of synthetic biology: a review*. Critical Reviews in Biotechnology, 2023: p. 1-14.
63. LeBlanc, N. and T.C. Charles, *Bacterial genome reductions: Tools, applications, and challenges.* Frontiers in Genome Editing, 2022. **4**: p. 957289.

64. Kurokawa, M. and B.W. Ying, *Experimental Challenges for Reduced Genomes: The Cell Model Escherichia coli.* Microorganisms, 2019. **8**(1): p. 3.
65. Csörgő, B., et al., *A compact Cascade–Cas3 system for targeted genome engineering.* Nature methods, 2020. **17**(12): p. 1183-1190.
66. Larrimore, K.E. and G. Rancati, *The conditional nature of gene essentiality.* Current Opinion in Genetics & Development, 2019. **58**: p. 55-61.
67. Hashimoto, M., et al., *Cell size and nucleoid organization of engineered Escherichia coli cells with a reduced genome.* Molecular microbiology, 2005. **55**(1): p. 137-49.
68. Fei, F., et al., *Effects of synthetic large-scale genome reduction on metabolism and metabolic preferences in a nutritionally complex environment.* Metabolomics, 2016. **12**: p. 1-14.
69. Blomfield, I., et al., *Allelic exchange in Escherichia coli using the Bacillus subtilis sacB gene and a temperature-sensitive pSC101 replicon.* Molecular microbiology, 1991. **5**(6): p. 1447-1457.
70. Logue, C.-A., I.R. Peak, and I.R. Beacham, *Facile construction of unmarked deletion mutants in Burkholderia pseudomallei using sacB counter-selection in sucrose-resistant and sucrose-sensitive isolates.* Journal of microbiological methods, 2009. **76**(3): p. 320-323.
71. Kunst, F. and G. Rapoport, *Salt stress is an environmental signal affecting degradative enzyme synthesis in Bacillus subtilis.* Journal of bacteriology, 1995. **177**(9): p. 2403-2407.
72. Webb, C. and W. Payne, *Influence of Na+ on synthesis of macromolecules by a marine bacterium.* Applied Microbiology, 1971. **21**(6): p. 1080-1088.
73. Khademian, M. and J.A. Imlay, *How Microbes Evolved to Tolerate Oxygen.* Trends in Microbiology, 2021. **29**(5): p. 428-440.
74. Fasnacht, M. and N. Polacek, *Oxidative stress in bacteria and the central dogma of molecular biology.* Frontiers in Molecular Biosciences, 2021. **8**: p. 671037.
75. Imlay, J.A., *Where in the world do bacteria experience oxidative stress?* Environmental microbiology, 2019. **21**(2): p. 521-530.
76. Imlay, J.A., *Cellular defenses against superoxide and hydrogen peroxide.* Annual review of biochemistry, 2008. **77**: p. 755-776.
77. Latour, J.-M., *Manganese, the stress reliever.* Metallomics, 2015. **7**(1): p. 25-28.
78. Sedoud, A., et al., *The cyanobacterial photoactive orange carotenoid protein is an excellent singlet oxygen quencher.* The Plant Cell, 2014. **26**(4): p. 1781-1791.
79. Manchester, L.C., et al., *Melatonin: an ancient molecule that makes oxygen metabolically tolerable.* Journal of pineal research, 2015. **59**(4): p. 403-419.
80. Mishra, S. and J. Imlay, *Why do bacteria use so many enzymes to scavenge hydrogen peroxide?* Archives of biochemistry and biophysics, 2012. **525**(2): p. 145-60.
81. Sen, A. and J.A. Imlay, *How Microbes Defend Themselves From Incoming Hydrogen Peroxide.* Frontiers in immunology, 2021. **12**: p. 667343.

82. Imlay, J.A., *The molecular mechanisms and physiological consequences of oxidative stress: lessons from a model bacterium.* Nature Reviews Microbiology, 2013. **11**(7): p. 443-454.
83. Loewen, P., *Probing the structure of catalase HPII of Escherichia coli—a review.* Gene, 1996. **179**(1): p. 39-44.
84. Schellhorn, H., *Regulation of hydroperoxidase (catalase) expression in Escherichia coli.* FEMS microbiology letters, 1995. **131**(2): p. 113-119.
85. Tartaglia, L.A., G. Storz, and B.N. Ames, *Identification and molecular analysis of oxyR-regulated promoters important for the bacterial adaptation to oxidative stress.* Journal of molecular biology, 1989. **210**(4): p. 709-719.
86. Loewen, P.C. and B.L. Triggs, *Genetic Mapping of katF, a Locus That with katE Affects the Synthesis of a Second Catalase Species in Escherichia coli.* Journal of bacteriology, 1984. **160**(2): p. 668-675.
87. Ivanova, A., et al., *Role of rpoS (katF) in oxyR-independent regulation of hydroperoxidase I in Escherichia coli.* Molecular microbiology, 1994. **12**(4): p. 571-578.
88. Wang, H., et al., *Catalases promote resistance of oxidative stress in Vibrio cholerae.* PLoS One, 2012. **7**(12): p. e53383.
89. Wang, H.W., et al., *Roles of alkyl hydroperoxide reductase subunit C (AhpC) in viable but nonculturable Vibrio parahaemolyticus.* Applied and environmental microbiology, 2013. **79**(12): p. 3734-43.
90. Vattanaviboon, P. and S. Mongkolsuk, *Unusual adaptive, cross protection responses and growth phase resistance against peroxide killing in a bacterial shrimp pathogen, Vibrio harveyi.* FEMS microbiology letters, 2001. **200**(1): p. 111-116.
91. Lin, L.-C., et al., *Differential expression of catalases in Vibrio parahaemolyticus under various stress conditions.* Research in microbiology, 2015. **166**(8): p. 601-608.
92. Yu, S.C., et al., *Protective roles of katG-homologous genes against extrinsic peroxides in Vibrio parahaemolyticus.* FEMS microbiology letters, 2016. **363**(6): p. fnw038.
93. Chen, C.-L., et al., *Functions of VPA1418 and VPA0305 Catalase Genes in Growth of Vibrio parahaemolyticus under Oxidative Stress.* Applied and environmental microbiology, 2016. **82**(6): p. 1859-1867.
94. Yang, Y., L. Zhou, and X. Luo, *Non-redundant expression of the two katG genes in Vibrio parahaemolyticus V110.* Journal of basic microbiology, 2019. **59**(5): p. 535-541.
95. Anand, A., et al., *OxyR Is a Convergent Target for Mutations Acquired during Adaptation to Oxidative Stress-Prone Metabolic States.* Molecular biology and evolution, 2020. **37**(3): p. 660-667.
96. Glasgo, L.D., K.L. Lukasiak, and E.R. Zinser, *Expanding the capabilities of MuGENT for large-scale genetic engineering of the fastest-replicating species, Vibrio natriegens.* Microbiology Spectrum, 2024: p. e03964-23.

97. Ma, L., et al., *Degradation of hydrogen peroxide at the ocean's surface: the influence of the microbial community on the realized thermal niche of Prochlorococcus.* The ISME journal, 2018. **12**(2): p. 473-484.
98. Berube, P.M., et al., *Physiology and evolution of nitrate acquisition in Prochlorococcus.* The ISME journal, 2015. **9**(5): p. 1195-1207.
99. Laurenceau, R., et al., *Toward a genetic system in the marine cyanobacterium Prochlorococcus.* Access microbiology, 2020. **2**(4): p. e000107.
100. Berczynski, P., et al., *Radical-scavenging activity of penicillin G, ampicillin, oxacillin, and dicloxacillin.* Luminescence, 2017. **32**(3): p. 434-442.
101. Morris, J.J., et al., *Dependence of the cyanobacterium Prochlorococcus on hydrogen peroxide scavenging microbes for growth at the ocean's surface.* PLoS One, 2011. **6**(2): p. e16805.
102. Merritt, J.H., D.E. Kadouri, and G.A. O'Toole, *Growing and analyzing static biofilms.* Current protocols in microbiology, 2011. **22**(1): p. 1B-1.
103. O'Leary, N.A., et al., *Reference sequence (RefSeq) database at NCBI: current status, taxonomic expansion, and functional annotation.* Nucleic Acids Research, 2016. **44**(D1): p. D733-D745.
104. Fu, L., et al., *CD-HIT: accelerated for clustering the next-generation sequencing data.* Bioinformatics, 2012. **28**(23): p. 3150-3152.
105. Katoh, K., et al., *MAFFT: a novel method for rapid multiple sequence alignment based on fast Fourier transform.* Nucleic Acids Research, 2002. **30**(14): p. 3059-3066.
106. Capella-Gutiérrez, S., J.M. Silla-Martínez, and T. Gabaldón, *trimAl: a tool for automated alignment trimming in large-scale phylogenetic analyses.* Bioinformatics, 2009. **25**(15): p. 1972-1973.
107. Nguyen, L.T., Schmidt, H. A., von Haeseler, A., & Minh, B. Q, *IQ-TREE: a fast and effective stochastic algorithm for estimating maximum-likelihood phylogenies.* Molecular biology and evolution, 2015. **32**(1): p. 268-274.
108. Letunic, I. and P. Bork, *Interactive Tree Of Life (iTOL) v5: an online tool for phylogenetic tree display and annotation.* Nucleic Acids Research, 2021. **49**(W1): p. W293-W296.
109. Thompson, J.R. and M.F. Polz, *Dynamics of Vibrio Populations and Their Role in Environmental Nutrient Cycling.* The biology of vibrios, 2006: p. 190-203.
110. Morris, J.J., A.L. Rose, and Z. Lu, *Reactive oxygen species in the world ocean and their impacts on marine ecosystems.* Redox Biology, 2022. **52**: p. 102285.
111. Yuan, F., et al., *The Richness and Diversity of Catalases in Bacteria.* Frontier in microbiology, 2021. **12**: p. 645477.
112. Lange, R., and and R. Hengge-Aronis, *Identification of a central regulator of stationary-phase gene expression in Escherichia coli.* Molecular microbiology, 1991. **5**(1): p. 49-59.
113. Proenca, A.M., et al., *Cell aging preserves cellular immortality in the presence of lethal levels of damage.* PLoS biology, 2019. **17**(5): p. e3000266.

114. Gupta, A. and J.A. Imlay, *Escherichia coli induces DNA repair enzymes to protect itself from low-grade hydrogen peroxide stress.* Molecular microbiology, 2022. **117**(4): p. 754-769.
115. Münch, R., et al., *Virtual Footprint and PRODORIC: an integrative framework for regulon prediction in prokaryotes.* Bioinformatics, 2005. **21**(22): p. 4187-4189.
116. Solovyev, V., and Salamov A., *Automatic Annotation of Microbial Genomes and Metagenomic Sequences.* Metagenomics and its applications in agriculture, biomedicine and environmental studies, 2011: p. 61-78.
117. Papenfort, K., et al., *Differential RNA-seq of Vibrio cholerae identifies the VqmR small RNA as a regulator of biofilm formation.* Proceedings of the National Academy of Sciences, 2015. **112**(7): p. E766-E775.
118. Zambrano, M.M., et al., *Microbial competition: Escherichia coli mutants that take over stationary phase cultures.* Science, 1993. **259**(5102): p. 1757-1760.
119. Snyder, E., D.M. Gordon, and D.M. Stoebel, *Escherichia coli lacking RpoS Are Rare in Natural Populations of Non-Pathogens.* G3: Genes| Genomes| Genetics, 2012. **2**(11): p. 1341-1344.
120. Bleibtreu, A., et al., *The rpoS Gene Is Predominantly Inactivated During Laboratory Storage and Undergoes Source-Sink Evolution in Escherichia coli Species.* Journal of bacteriology, 2014. **196**(24): p. 4276-4284.
121. Singh, R., et al., *Comparative study of catalase-peroxidases (KatGs).* Archives of biochemistry and biophysics, 2008. **471**(2): p. 207-14.
122. Martinez-Gutierrez, C.A. and F.O. Aylward, *Genome size distributions in bacteria and archaea are strongly linked to evolutionary history at broad phylogenetic scales.* PLoS Genetics, 2022. **18**(5): p. e1010220.
123. Batut, B., et al., *Reductive genome evolution at both ends of the bacterial population size spectrum.* Nature Reviews Microbiology, 2014. **12**(12): p. 841-50.
124. Mira A., O.H., Moran NA.,, *Deltional bias and the evolution of bacterial genomes.* TRENDS in Genetics, 2001. **17**(10): p. 589-596.
125. Moran, N.A., *Microbial Minimalism: Genome Reduction in Bacterial Pathogens.* Cell, 2002. **108**(5): p. 583-586.
126. Novichkov, P.S., et al., *Trends in prokaryotic evolution revealed by comparison of closely related bacterial and archaeal genomes.* Journal of bacteriology, 2009. **191**(1): p. 65-73.
127. Grote, J., et al., *Streamlining and core genome conservation among highly divergent members of the SAR11 clade.* MBio, 2012. **3**(5).
128. Dufresne, A., Laurence Garczarek and Frédéric Partensky, *Accelerated evolution associated with genome reduction in a free-living prokaryote.* Genome Biology, 2005. **6**(2).
129. Morris, J.J., R.E. Lenski, and E.R. Zinser, *The Black Queen Hypothesis: evolution of dependencies through adaptive gene loss.* MBio, 2012. **3**(2).
130. Giovannoni, S.J., et al., *Genome Streamlining in a Cosmopolitan Oceanic Bacterium.* Science, 2005. **309**(5738): p. 1242-1245.

131. Sun, Z. and J.L. Blanchard, *Strong genome-wide selection early in the evolution of Prochlorococcus resulted in a reduced genome through the loss of a large number of small effect genes.* PLoS One, 2014. **9**(3): p. e88837.
132. Yu, B.J., et al., *Minimization of the Escherichia coli genome using a Tn5-targeted Cre/loxP excision system.* Nature biotechnology, 2002. **20**(10): p. 1018-23.
133. Kolisnychenko, V., et al., *Engineering a reduced Escherichia coli genome.* Genome research, 2002. **12**(4): p. 640-7.
134. Goryshin, I.Y., et al., *Chromosomal Deletion Formation System Based on Tn5 Double Transposition: Use for Making Minimal Genomes and Essential Gene Analysis.* Genome research, 2003. **13**(4): p. 644-653.
135. Komatsu, M., et al., *Genome-minimized Streptomyces host for the heterologous expression of secondary metabolism.* Proceedings of the National Academy of Sciences, 2010. **107**(6): p. 2646-2651.
136. Karcagi, I., et al., *Indispensability of Horizontally Transferred Genes and Its Impact on Bacterial Genome Streamlining.* Molecular biology and evolution, 2016. **33**(5): p. 1257-69.
137. Choe, D., et al., *Adaptive laboratory evolution of a genome-reduced Escherichia coli.* Nature communications, 2019. **10**(1): p. 935.
138. Vernyik, V., et al., *Exploring the fitness benefits of genome reduction in Escherichia coli by a selection-driven approach.* Scientific reports, 2020. **10**(1): p. 7345.
139. Ying, B.W. and K. Yama, *Gene Expression Order Attributed to Genome Reduction and the Steady Cellular State in Escherichia coli.* Frontiers in microbiology, 2018. **9**: p. 2255.
140. Gresham, D. and J. Hong, *The functional basis of adaptive evolution in chemostats.* FEMS microbiology reviews, 2015. **39**(1): p. 2-16.
141. Cantalapiedra, C.P., et al., *eggNOG-mapper v2: functional annotation, orthology assignments, and domain prediction at the metagenomic scale.* Molecular biology and evolution, 2021. **38**(12): p. 5825-5829.
142. Huerta-Cepas, J., et al., *eggNOG 5.0: a hierarchical, functionally and phylogenetically annotated orthology resource based on 5090 organisms and 2502 viruses.* Nucleic acids research, 2019. **47**(D1): p. D309-D314.
143. Giovannoni, S.J., J. Cameron Thrash, and B. Temperton, *Implications of streamlining theory for microbial ecology.* ISME J, 2014. **8**(8): p. 1553-65.
144. Hutchinson, G.E., *The Paradox of the Plankton.* The American Naturalist, 1961. **95**(882): p. 137-145.
145. Hardin, G., *The Competitive Exclusion Principle: an idea that took a century to be born has implications in ecology, economics, and genetics.* Science, 1960. **131**(3409): p. 1292-1297.
146. Tilman, D., *Resource competition and community structure*. 1982: Princeton university press.
147. Hubbell, S.P., *The unified neutral theory of biodiversity and biogeography* 2011: Princeton University Press.

148. Maharjan, R.P. and T. Ferenci, *Epistatic interactions determine the mutational pathways and coexistence of lineages in clonal Escherichia coli populations.* Evolution, 2013. **67**(9): p. 2762-2768.
149. Degermendzhi, A., *Coexistence of microbial populations and autostabilization of regulating factors in continuous culture: theory and experiments.* Aquatic ecology, 2010. **44**: p. 541-560.
150. Blount, Z.D., et al., *Genomic analysis of a key innovation in an experimental Escherichia coli population.* Nature, 2012. **489**(7417): p. 513-518.
151. Maharjan, R.P., et al., *Simple phenotypic sweeps hide complex genetic changes in populations.* Genome Biology and Evolution, 2015. **7**(2): p. 531-544.
152. Plamann, M.D., W.D. Rapp, and G.V. Stauffer, *Escherichia coli K12 mutants defective in the glycine cleavage enzyme system.* Molecular and General Genetics MGG, 1983. **192**: p. 15-20.
153. Pizer, L.I., *Glycine synthesis and metabolism in Escherichia coli.* Journal of bacteriology, 1965. **89**(4): p. 1145-1150.
154. Kanehisa, M. and S. Goto, *KEGG: Kyoto Encyclopedia of Genes and Genomes.* Nucleic acids research, 2000. **28**(1): p. 27-30.
155. Shimizu, S. and W.B. Dempsey, *Genetic map position of the pdxH gene in Escherichia coli.* Journal of Bacteriology, 1976. **127**(3): p. 1593-1594.
156. Van Der Woude, M.W. and A.J. Bäumler, *Phase and antigenic variation in bacteria.* Clinical microbiology reviews, 2004. **17**(3): p. 581-611.
157. Chang, C., X. Jin, and H. Chaoqun, *Phenotypic and genetic differences between opaque and translucent colonies of Vibrio alginolyticus.* Biofouling, 2009. **25**(6): p. 525-531.
158. Hilton, T., et al., *Capsular polysaccharide phase variation in Vibrio vulnificus.* Applied and Environmental Microbiology, 2006. **72**(11): p. 6986-6993.
159. Chatzidaki-Livanis, M., M.K. Jones, and A.C. Wright, *Genetic variation in the Vibrio vulnificus group 1 capsular polysaccharide operon.* Journal of bacteriology, 2006. **188**(5): p. 1987-1998.
160. Beyhan, S. and F.H. Yildiz, *Smooth to rugose phase variation in Vibrio cholerae can be mediated by a single nucleotide change that targets c-di-GMP signalling pathway.* Molecular microbiology, 2007. **63**(4): p. 995-1007.
161. Eydallin, G., et al., *The nature of laboratory domestication changes in freshly isolated Escherichia coli strains.* Environmental Microbiology, 2014. **16**(3): p. 813-828.
162. Somerville, G.A., et al., *In vitro serial passage of Staphylococcus aureus: changes in physiology, virulence factor production, and agr nucleotide sequence.* Journal of bacteriology, 2002. **184**(5): p. 1430-1437.
163. Kearns, D.B. and R. Losick, *Swarming motility in undomesticated Bacillus subtilis.* Molecular microbiology, 2003. **49**(3): p. 581-590.
164. Dalia, A.B., *RpoS is required for natural transformation of Vibrio cholerae through regulation of chitinases.* Environmental Microbiology, 2016. **18**(11): p. 3758-3767.

VITA

Liz Glasgo was born and raised in southwest Ohio. In 2016, she obtained a Bachelor of Science degree in Microbiology from Bowling Green State University in Bowling Green, Ohio. Liz then moved to Knoxville, Tennessee in 2018 to pursue a Doctor of Philosophy in Microbiology at the University of Tennessee. Maybe Liz yearns for the north or maybe the cold, flatlands of Ohio never truly let anyone leave. Either way, after graduation, Liz will return to the Motherland to continue her career in microbiology research.